INFORMATION TO USERS

This manuscript has been reproduced from the microfilm master. UMI films the text directly from the original or copy submitted. Thus, some thesis and dissertation copies are in typewriter face, while others may be from any type of computer printer.

The quality of this reproduction is dependent upon the quality of the copy submitted. Broken or indistinct print, colored or poor quality illustrations and photographs, print bleedthrough, substandard margins, and improper alignment can adversely affect reproduction.

In the unlikely event that the author did not send UMI a complete manuscript and there are missing pages, these will be noted. Also, if unauthorized copyright material had to be removed, a note will indicate the deletion.

Oversize materials (e.g., maps, drawings, charts) are reproduced by sectioning the original, beginning at the upper left-hand corner and continuing from left to right in equal sections with small overlaps.

ProQuest Information and Learning
300 North Zeeb Road, Ann Arbor, MI 48106-1346 USA
800-521-0600

EFFECTS OF UNCOUPLING PROTEIN-2 OVER-EXPRESSION ON THE CYCLIC ADENOSINE MONOPHOSPHATE SIGNALING PATHWAY OF GLUCOSE-STIMULATED INSULIN SECRETION

A Thesis

Submitted to the Graduate Faculty

in Partial Fulfilment of the Requirements

for the Degree of

Master of Science

in the Department of Anatomy and Physiology

Faculty of Veterinary Medicine

University of Prince Edward Island

Timothy S. McQuaid

Charlottetown, P. E. I.

March, 2002

CONDITIONS OF USE OF THE THESIS

SIGNATURE PAGES

iii-iv

REMOVED

Abstract

Insulin is a peptide hormone that promotes the removal of glucose from the blood and its storage or metabolism in muscle, liver and adipose cells. Obesity and type 2 diabetes mellitus are two of the largest health concerns facing society today and both metabolic disorders involve abnormalities in the relative level of insulin secretion from pancreatic β-cells. Elucidating the factors that control insulin secretion is vital to the development of effective therapies to counteract abnormal secretion. Uncoupling proteins (UCPs) uncouple electron transport from oxidative phosphorylation and attenuate the production ATP, a key messenger in the insulin secretory cascade. One member of the UCP family, UCP-2, is expressed in pancreatic islets and its over-expression leads to a decrease in both ATP production and glucose-stimulated insulin secretion (GSIS). While many ATP-dependent pathways exist which may be affected, the generation of cAMP and its ability to potentiate GSIS is the focus of this study.

Transient transfection of a UCP-2 containing plasmid vector (pUCP-2) into a clonal β-cell line (βTC6-f7) was used as a model of UCP-2 over-expression and all results were verified in intact islets infected with a UCP-2 containing adenovirus construct (AdUCP-2). The cell line model was validated by measuring ATP and GSIS in UCP-2 transfected cells. Forskolin, an adenylyl cyclase activator, was used to elevate cAMP levels. Insulin secretion was also measured and related to the concentration of cAMP under each condition.

Transfection of a plasmid carrying an enhanced green fluorescent protein (EGFP) gene did not alter insulin secretion as compared to untransfected βTC6-f7 cells. GSIS was significantly attenuated in pUCP-2 transfected βTC6-f7 cells exposed to 11 mM and 22 mM glucose as compared to untransfected controls. ATP production was also attenuated in pUCP-2 transfected βTC6-f7 cells, though to a lesser extent than in AdUCP-2 infected islets. Interestingly, AdUCP-2 infected βTC6-f7 cells had a reduction in ATP similar to that of AdUCP-2 infected islets.

Generation of cAMP in response to glucose was not affected by UCP-2 over-expression in either pUCP-2 transfected βTC6-f7 cells or AdUCP-2 infected islets. Forskolin induced a concentration-dependent rise in cAMP (up to a three-fold increase) in islets only (both AdUCP-2 infected and control). In βTC6-f7 cells exposed to 2.8 mM glucose, forskolin (> 0.1 μM) was able to increase insulin secretion from control βTC6-f7 cells only. In intact islets exposed to 2.8 mM glucose, insulin secretion was increased in both AdUCP-2 infected islets and control islets, though secretion from control islets was significantly greater than that of AdUCP-2 infected islets in the presence of 10 μM forskolin. With exposure to 11 mM glucose, forskolin (> 0.1 μM) was able to restore insulin secretion in pUCP-2 transfected βTC6-f7 cells to that of control cell, which was unaffected by forskolin. This pattern of secretion was also observed in intact islets exposed to 11 mM glucose. Efforts to directly quantify UCP-2 expression in each model using immunoblotting were unsuccessful. RT-PCR amplification of UCP-2 mRNA did show a 2.5-3 fold induction in pUCP-2 transfected and AdUCP-2 infected βTC6-f7 cells.

Using EGFP expression as a marker of UCP-2 expression, AdUCP-2/EGFP infected βTC6-f7 cells appeared to have a higher efficiency of gene transfer than pEGFP transfected βTC6-f7 cells.

In conclusion, transient transfection of pUCP-2 is a convenient and valid model in which to study the effects of UCP-2 over-expression on the ATP-dependent pathways of GSIS. Neither basal nor stimulated generation of cAMP is affected by UCP-2 over-expression nor is cAMP's ability to potentiate GSIS. Forskolin was able to restore insulin secretion in UCP-2 over-expressing cells and islets, an effect which is independent of elevations in cAMP. This could possibly be mediated by alterations in K^+ channel activity, which is also a key factor in GSIS, but further experiments are needed to test this hypothesis.

Acknowledgments

I wish to thank my supervisory committee members: Drs Tarek Saleh, Sherri Ihle, Sean Brosnan (MUN) and Susan Dohoo, as well as my supervisor Dr. Catherine Chan for their guidance and support. Also, technical support from Monique Saleh and Dr. Molly Kibenge, collaboration from Dr. Michael Wheeler and colleagues at the University of Toronto and for general assistance from faculty, staff and students of the Department of Anatomy and Physiology. Project funding was provided by the Canadian Diabetes Association, while personal stipend was funded in part by the Department of Anatomy and Physiology and an NSERC post-graduate fellowship. I would finally like to thank my family and wife Sarah for their endless patience and support throughout the project.

Table of Contents

List of Figures

List of Tables

List of Abbreviations

Abbreviation	Term
AC	Adenylyl cyclase
ACC	Acetyl CoA carboxylase
ADP	Adenosine diphosphate
AdUCP-2	Uncoupling protein-2 adenovirus
AdUCP-2/EGFP	Uncoupling protein-2/enhanced green fluorescent protein adenovirus
ANOVA	Analysis of Variance
ATP	Adenosine triphosphate
AVC	Atlantic Veterinary College
BAT	Brown adipose tissue
BMI	Body mass index
bp	Base pairs
°C	Degrees celsius
Ca^{2+}	Calcium ion
$[Ca^{2+}]_i$	Intracellular calcium concentration
cAMP	Cyclic adenosine monophosphate
CCCP	Carbonyl cyanide *m*-chlorophenylhydrazone
Ci	Curie
CO_2	Carbon dioxide
CoA	Co-enzyme A
CoQ	Co-enzyme Q
CPM	Counts per minute
DAG	Diacyl glycerol
DEPC	Diethyl pyrocarbonate
DMEM	Dulbecco's modified Eagle's medium
DMSO	Dimethyl sulfoxide
DNA	Deoxyribonucleic acid
EDTA	Ethylenediaminetetra-acetic acid
EGFP	Enhanced green fluorescent protein
ER	Endoplasmic reticulum
$FADH_2$	Reduced flavin adenine dinucleotide
FBS	Fetal bovine serum
FFA	Free fatty acid
g	Grams
GDP	Guanosine diphosphate
GIP	Gastric inhibitory polypeptide

GLP-1	Glucagon-like peptide-1
GLUT-χ	Glucose transporter-χ
GSIS	Glucose-stimulated insulin secretion
GTP	Guanosine triphosphate
h	Hours
HBSS	Hanks' balanced saline solution
HBSS*	Hanks' balanced saline solution with 0.2% BSA
HCl	Hydrochloric acid
HEPES	N- {2-Hydroxyethyl}piperazine-N-{2-ethanesulfonic acid}
HLA	Human leukocyte antigen
HNFχ1	Hepatic nuclear factorχ1
IBMX	Isobutylmethylxanthine
IMM	Inner mitochondrial membrane
IP_3	Inositol triphosphate
^{125}I	Iodine isotope-125
K^+	Potassium ion
kbp	Kilobase pairs
kDa	Kilodalton
K_m	Michaelis-Menton constant
KRB	Krebs ringer buffer
L	Liters
LC-CoA	Long chain acyl CoA
m	Meter
M	Molar
$MgCl_2$	Magnesium chloride
min	Minutes
MODYχ	Maturity onset diabetes of the young
MOI	Multiplicity of infection
mRNA	Messenger ribonucleic acid
MW	Molecular weight
Na^+	Sodium ion
Na_2PO_4	Sodium phosphate
NaCl	Sodium chloride
NADH	Reduced nicotinic adenine dinucleotide
NSB	Non-specific binding
^{32}P	Phosphorus isotope-32
PBS	Phosphate buffered saline
PDE	Phosphodiesterase
pfu	Plaque forming units
PKA	Protein kinase A
PKC	Protein kinase C

PLC	Phospholipase C
PP	Pancreatic polypeptide
PPAR-χ	Peroxisome proliferator-activated receptor-χ
pEGFP	Enhanced green fluorescent protein plasmid
pUCP-2	Uncoupling protein-2 plasmid
RER	Rough endoplasmic reticulum
RIA	Radioimmunoassay
RNA	Ribonucleic acid
ROS	Reactive oxygen species
rpm	Revolutions per minute
RT-PCR	Reverse transcriptase-polymerase chain reaction
s	Seconds
SDS-PAGE	Sodium dodecyl sulfate-polyacrylamide gel electrophoresis
SEM	Standard error of the mean
SNARE	Soluble N-ethylmaleimide sensitive fusion protein
SRP	Signal recognition particle
SUL	Sulphonylurea
TC	Total count
TNF-α	Tumor necrosis factor-α
t-SNARE	Plasma membrane associated SNARE
v-SNARE	Vesicle associated SNARE
Tween 20	Polyoxyethylenesorbitan monolaureate
UCP-χ	Uncoupling protein-χ
WAT	White adipose tissue
ZDF	Zucker diabetic fatty

1. INTRODUCTION

1.1 The Discovery of Insulin

In 1889, von Mering and Minkowski found that a complete pancreatectomy would induce severe hyperglycemia in dogs (1). It had been previously established by Langerhans in 1869 that the pancreas contained small, highly innervated islands of cells scattered amongst the rest of the acinar tissue. Ligation of the main pancreatic duct disrupted digestive processes, but did not cause hyperglycemia (1). From this, it was concluded that some internal pancreatic secretion from these "islands" (now known as the islets of Langerhans) was responsible for controlling carbohydrate metabolism.

Though it was postulated that pancreatic islets contained a hypoglycemic agent, early preparations of pancreatic extracts were quite crude and had very inconsistent and sometimes even fatal effects. The problem lay in isolating the pure internal secretory products given the experimental methods of that day. Through ingenious foresight and experimental design, one Dr. Frederick Banting was able to isolate the islets exclusively. An avid reader of the medical journals, Banting stumbled across an article one day that struck a chord. A unique case was presented in which a blockage of the main pancreatic duct by a calcification had caused the acinar tissue to degenerate, while the islets remained unaffected. Having just given a lecture on pancreatic physiology to a group of local medical students, lightning was about to strike (2).

> "About two in the morning after the lecture and the article had been chasing each other through my mind for some time, the idea occurred to me that by the experimental ligation of the duct and the

> subsequent degeneration of a portion of the pancreas, that one might obtain the internal secretion free from the external secretion. I got up and wrote down the idea." (3)

Upon discussion of this idea with Dr. J. J. R. MacLeod, a world renowned expert in carbohydrate metabolism, both the feasibility and potential of the work was questioned. However, MacLeod would provide Banting with the appropriate facilities should he wish to conduct the experiments, though he was not optimistic of their results. With the help of a graduate student named Charles Best and biochemist James Collip, Banting was able to isolate the elusive internal extract from the islets. This extract did indeed prove successful in treating diabetic animals as outlined in an excerpt from their paper published in the *Journal of Laboratory and Clinical Medicine*; February, 1922.

> "In the course of our experiments we have administered over seventy-five doses of extract from degenerated pancreatic tissue to ten different diabetic animals. Since the extract has always produced a reduction of the percentage sugar of the blood and the sugar excreted in the urine, we feel justified in stating that this extract contains the internal secretion of the pancreas." (4)

This internal secretion now bears the name "insulin" and represents one of the most fundamental breakthroughs in the history of medicine. For this, Banting and MacLeod shared the Noble prize for physiology or medicine in 1923. Over 75 years later, a complete understanding of this "insulin", its synthesis, secretion and actions, remains elusive.

1.2 Anatomy and Organization of the Pancreas

Located near the upper portion of the abdomen in close association with the duodenum, the pancreas is divided into two parts: exocrine and endocrine. The exocrine pancreas consists of acinar cells which secrete important digestive enzymes ("pancreatic juice") into the duodenum via the main and accessory pancreatic ducts (5). The endocrine pancreas consists of the islets of Langerhans, clusters of hormone secreting cells which are dispersed throughout the acinar tissue. Endocrine secretions are collected in the venous blood supply from the islets and circulated throughout the body (6). Individual islets vary significantly in size and make up 1 - 4 % of the total pancreatic volume (6).

Unlike the exocrine pancreas, which consists of acinar cells and connective tissue, four main types of endocrine cells are located within the islet. These can be distinguished morphologically (i.e. by size and granule appearance) and by immunostaining techniques. The islet cells include α-cells, β-cells, δ-cells and PP-cells (7). The organization of these cells is conserved in all islets and is reflective of the function of each. Insulin producing β-cells are the most abundant cell type, making up 60 - 80% of islet cells. These cells are found at the core of the islet and the insulin that they secrete promotes removal of glucose from the blood (7). PP-cells and α-cells each make up 15 - 20% of islet cell content and produce pancreatic polypeptide (PP) and glucagon, respectively. Glucagon has a counter action to that of insulin in that it increases blood glucose concentrations, while PP functions to regulate exocrine secretions and gall bladder function (7). The δ-cells represent 5 - 10% of islet cells and generate somatostatin, which serves as a regulatory hormone and inhibits many secretory and proliferative processes throughout the body (8), including insulin and

glucagon secretion (7). These latter three cell types are found exclusively within the periphery of the islet (mantle) and for organizational purposes may simply be referred to as non-β-cell types (6).

Often thought of as micro organs, islets are highly vascularized and are innervated by sympathetic and parasympathetic nerve fibers. Depending on its size, one to three afferent arterioles enter the islet through a discontinuity in the non-β-cell mantle. These arterioles branch into capillary networks within the islet core, with the endocrine cells aggregated around the blood vessels in a "rosette" pattern. At an undefined point within the islet, the transition from arteriole (afferent) to venule (efferent) takes place. The venules pass laterally through the inner side of the islet mantle before connecting to the main collecting venule which runs along the outer surface of the islet. Products secreted by the islet cells are collected in these blood vessels and transported to the rest of the body (Figure1.1) (7). Thus, the physical organization of the islet is key to the regulatory actions that the secretory products have on different cell types. Somatostatin (inhibitory) and glucagon (stimulatory) have effects on insulin secretion from β-cells, while insulin inhibits α- and δ- cell secretions (7). Given the vascular orientation discussed above, it is proposed that blood flow is from β-cell to α-cell to δ-cell within the islet. Non-β-cells are immediately exposed to high concentrations of β-cell secretions after a stimulus (e.g. rise in blood glucose), which inhibits glucagon or somatostatin secretion. While non-β-cell secretions may diffuse through the interstitial fluid to adjacent cells (paracrine effect), they must enter the general circulatory system and be returned to the islet via the afferent arterioles to have any major influence on the majority of the β-cells which are located in the islet core (6).

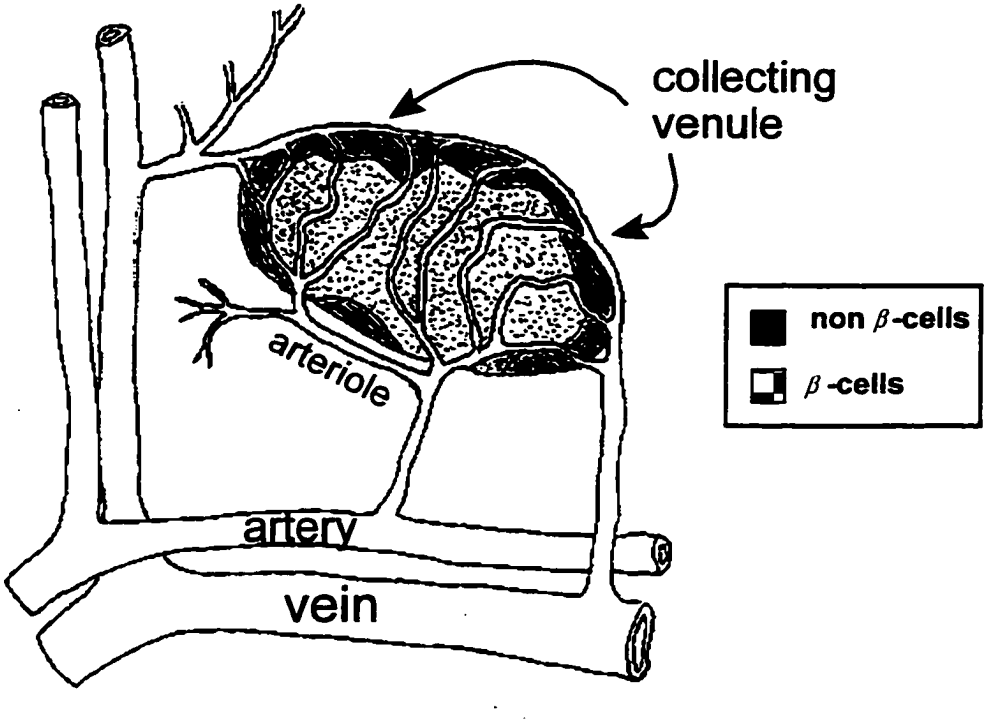

Figure 1.1 Microvasculature of the islet. (Taken from ref. (7))

Intra-islet communication pathways have also been described which have an influence on secretory events. Gap junctions between both common and mixed cell types in islets allow for the transmission of ions, small molecules, nucleotides and even electrical impulses. Direct hormone transport across these junctions is not seen and thus they represent pathways through which only signaling events are shared. The existence of tight junctions *in vivo* has been debated, but most reports indicate that they are relatively rare in islets. Also, islets show a significant heterogeneity in terms of glucose sensitivity, size and cell composition (7). Because of this, the question has been raised as to whether physical location of the islet within the pancreas, as well as even the β-cell within the islet, may influence its function.

1.3 Metabolic Effects of Insulin

Insulin has many physiological effects, including regulation of carbohydrate, lipid and protein metabolism, as well as supporting cell growth and division (1). Its implications in metabolic processes are well characterized and represent its most significant role. The primary target tissues of insulin with significant expression of insulin receptors are liver, muscle and adipose tissue. These receptors are mobile within the plasma membrane and can be subject to clustering in the presence of an insulin stimulus (9). Receptor binding sets forth a complex series of events which promotes the uptake and storage of fuels within the target cells.

The insulin receptor consists of two different subunits, α and β, with each functional receptor containing a pair of these units. The α subunit, located on the extracellular side of

the membrane, contains the insulin binding site. The β subunit has a membrane-spanning segment and an intracellular domain. Adjacent subunits are bound together by disulfide bonds (Figure 1.2). Upon insulin binding to the α subunit, the β subunit undergoes autophosphorylation at tyrosine residues using ATP as a phosphate donor (i.e. the insulin binding to the receptor mediates its own phosphorylation). This autophosphorylation gives the receptor tyrosine kinase activity which in turn promotes phosphorylation of other proteins. This series of post-binding events mediates the effects of insulin binding on the target cell (10). Binding of insulin also regulates its own actions through a negative feedback loop which decreases both the level of expression and insulin affinity of unoccupied receptors on the membrane surface (11). After post-binding events have occurred, the receptor/protein complex is internalized by endocytosis at a "coated pit" (1). While the insulin is degraded within fused lysosomes, the receptors may be degraded as well or recycled back to the membrane surface (12).

Insulin's action on its target tissues results in a net increase of glucose uptake and storage. Glucose requires a transport protein to cross the cell membrane. There are five separate isoforms of glucose transporters which are expressed preferentially in different tissues and whose activities depends on insulin to varying degrees (13). For example, in most target tissues insulin receptor binding results in the mobilization of glucose transporter-4 (GLUT-4) to the membrane surface and increases the net transport of glucose from the blood into the cell. These transporters are localized in a pool of intracellular vesicles which translocate to the plasma membrane surface where they fuse and transporters are incorporated into the plasma membrane (Figure 1.3). When the insulin stimulus subsides,

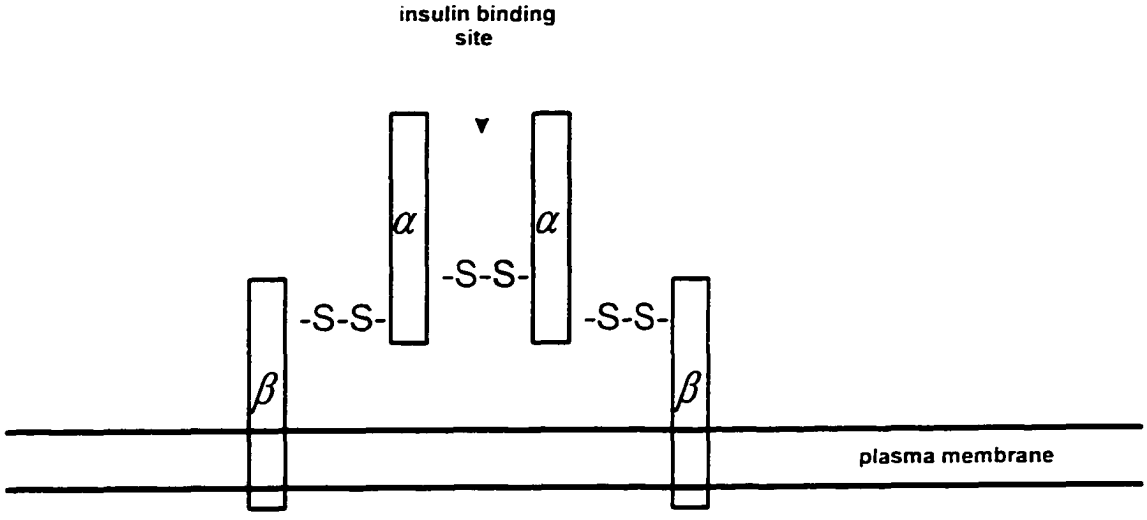

Figure 1.2 Subunit arrangement and interactions of the insulin receptor. (Taken from ref. (10))

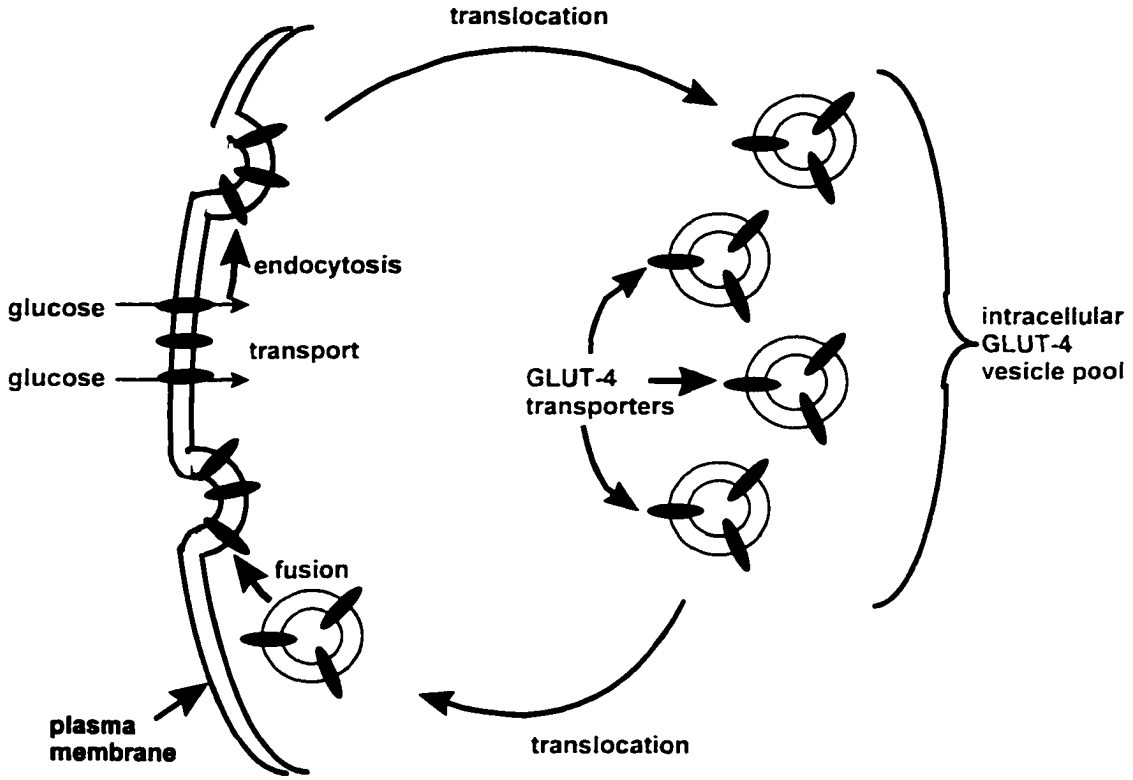

Figure 1.3. Translocation of GLUT-4 transporters in target cells in response to insulin receptor binding. (Taken from ref. (12))

the transporters are recycled back into the intracellular storage pool (12). In contrast, GLUT-1 transporters located in brain cells are constitutively expressed on the cell surface and are thus insensitive to insulin (13).

Insulin receptor binding also causes alterations in the activity of certain enzymes. Enzymes involved in glucose consuming pathways (glycolysis, glycogen synthesis, etc.) are influenced by both direct activation and increased synthesis (transcription and translation). Glucose producing pathways (gluconeogenesis, glycogen breakdown, etc.) are attenuated by inactivation of key enzymes which they employ (12). The most prominent effects of insulin are on carbohydrate metabolism, but lipid and protein metabolism are also influenced.

1.3.1 Effects on Glucose Metabolism

Insulin binding increases glucose utilization by its target cells. One pathway through which it achieves this is by increasing glucose storage as glycogen in muscle and liver, and as triglycerides in adipose tissue and liver. Both glycogen synthase (storage) and glycogen phosphorylase (breakdown) exist in activated and inactivated forms depending on their phosphorylation state (1). For clarity, we will briefly look at the overall scheme for glucose regulation. Glucagon, the principle hormone involved in augmenting blood glucose, binds to its receptor on target tissues and activates adenylyl cyclase which increases cAMP. A cAMP-dependent protein kinase (PKA) is then activated which phosphorylates both glycogen synthase and glycogen phosphorylase. This action inhibits the former and activates the latter, resulting in a net glycogen breakdown and a rise in blood glucose concentrations. Conversely, insulin binding serves to decrease cAMP levels and allow protein phosphatases

to dephosphorylate the enzymes promoting glycogen synthesis. Thus, the glucagon/insulin balance is in a constant state of flux that is determined by blood glucose concentrations. Insulin does not, however, lower baseline cAMP levels and only exerts this action on glucagon stimulated cells (1). Insulin binding also increases the activity of glycolytic enzymes such as hexokinase and pyruvate dehydrogenase to speed up glucose metabolism (14). The liver's ability to synthesize glucose through gluconeogenesis requires additional actions to control blood glucose concentrations. Glucagon binding causes PKA-induced phosphorylation of pyruvate kinase and fructose-2,6-bisphosphatase. The net effect is the inhibition of the glycolytic pathway and the enhancement of the gluconeogenic pathway, resulting in an increase in blood glucose concentration (1;14). When insulin binding lowers the concentrations of cAMP these effects are reversed and glucose is consumed. A list of important glycolytic and glycogenic enzymes as well as the effects of insulin and glucagon on each is given in Table 1.1 (14).

1.3.2 Effects on Lipid Metabolism

Adipocytes and hepatocytes can also store glucose in the form of triglycerides, representing another pathway of glucose consumption. As discussed previously, insulin binding increases the glycolytic rate and pyruvate dehydrogenase is activated to metabolize the pyruvate produced (1). This generates acetyl CoA which can then be fed into lipogenic pathways to synthesize fatty acids. Glycolytic intermediates serve as a source of glycerol and the fatty acids are esterfied to form triglycerides. Insulin also stimulates

Enzyme	Activity increased by	Pathway involved in
glycogen synthase	insulin	glycogenesis
phosphorylase kinase	glucagon	glycogenolysis
glucokinase	insulin	glycolysis
glucose-6-phosphatase	glucagon	gluconeogenesis
phosphofructokinase	insulin	glycolysis
fructose-1,6-bisphosphatase	glucagon	gluconeogenesis
pyruvate dehydrogenase	insulin	glucose oxidation
pyruvate carboxylase	glucagon	gluconeogenesis

Table 1.1 Enzymes of glucose metabolism influenced by insulin and glucagon receptor binding.

lipogenesis by activating acetyl CoA carboxylase (a key enzyme in acetyl CoA polymerization and fatty acid synthesis) and inhibiting triacylglycerol lipase (the primary lipolytic enzyme), again through lowering of cAMP and PKA activity (1).

Insulin can also participate in lipolytic events that aid in the uptake of fats into other tissues. Triacylglycerol may be transported through the body in the form of lipoproteins, but can not enter a cell without first being broken down to fatty acids and glycerol. The enzyme lipoprotein lipase, found on the outer surface of endothelial cells and hepatocytes, performs this task and its activity is increased directly by insulin. In addition, insulin can activate 3-hydroxy-3-methyl glutaryl CoA reductase, which is a key enzyme involved in cholesterol synthesis (1).

1.3.3 Effects on Protein Metabolism

Given the ability of insulin to stimulate cell division (1), one might postulate that insulin must be able to stimulate protein synthesis as well. Insulin binding has been shown to increase amino acid uptake as well as influencing the phosphorylation state and transcription of enzymes involved in protein metabolism. This latter effect may be due to increased phosphorylation of protein S6 in the 40S ribosomal subunit, which increases mRNA binding to the ribosome and enhances translation (1). Albumin is one such protein whose gene expression is positively influenced at the transcriptional concentration by insulin in certain tissues (15). Skeletal muscle from diabetic rats shows a decreased rate of mRNA translation to protein, a defect which can be corrected by insulin treatment. A reduction in ribosome number due to increased degradation can be seen in diabetic animals following

insulin withdrawal (15).

1.4 Metabolic Abnormalities Associated with Insulin

Now that we have seen the multitude of effects insulin has on metabolic processes, we can begin to understand its contribution to the pathology of certain diseases. Two major metabolic disorders associated with insulin related abnormalities are diabetes mellitus and obesity.

1.4.1 Diabetes Mellitus

By definition, diabetes mellitus is a condition which is characterized by chronic hyperglycemia. It may cause a number of complications, including cardiovascular and renal disease, blindness, neuropathy and peripheral vascular disorders (16). In Canada, it is estimated that this disease affects 1.2 - 1.4 million people over the age of twelve (~5% of the population) and costs the Canadian health care system over a billion dollars annually (17). The general pathogenesis underlying this disorder is a lack of insulin action on target tissues. Exactly how this comes about can be quite different for individual cases of diabetes mellitus. Most cases fall into two categories: Insulin-Dependent Diabetes Mellitus (type 1) and Non-Insulin-Dependent Diabetes Mellitus (type 2). As discussed later, the latter exhibits an immense diversity within its own classification.

Type 1 diabetes is characterized by an autoimmune destruction and eventual complete loss of the pancreatic β-cells, requiring exogenous insulin therapy to maintain blood glucose homeostasis (18). This disorder typically occurs early in life (before or during adolescence)

and thus is also referred to as juvenile-onset diabetes mellitus. The development of symptoms and progression of the disorder is usually quite rapid. Although certain genetic links (relating particularly to characteristics of human lymphoctye antigen (HLA) expression) have been shown to confer a susceptibility to type 1 diabetes, environmental influences also play a significant role. Studies on monozygotic twins show only a 40% concordance of the disorder between pairs, indicating that additional factors are also present (18). Although type 1 diabetes is perhaps better known to the lay public, it represents only about 10% of all cases of diabetes in humans (19).

Type 2 diabetes is responsible for the majority of diabetes cases in humans (17). Often diagnosed after the age of 40 (and hence referred to as adult-onset diabetes mellitus), patients with type 2 diabetes exhibit impaired insulin action and/or secretion, resulting in hyperglycemia. While the severity of the insulin impairment can vary significantly, most cases can be controlled by diet and oral hypoglycemic agents without the need for direct insulin replacement (20). Type 2 diabetes has a much slower progression and symptoms can be present for years prior to diagnosis. Impaired glucose tolerance without fasting hyperglycemia (i.e the patient remains normoglycemic under conditions of moderate to low glucose intake, but fails to respond adequately to a large glucose challenge) can be traced back to early stages of the disorder (11). Though the exact causes of type 2 diabetes are not clear, there are several key risk factors and indicators of a pre-diabetic state. For example, the strongest risk factor for type 2 diabetes (aside from age) is obesity. Not only is obesity seen in 60% of patients with type 2 diabetes, but the severity of the diabetic condition correlates with the duration and, to a lesser extent, the degree of obesity in the patient (16).

Even the anatomical distribution of the fat mass may be an important factor in the development of type 2 diabetes. Excessive fat in the upper body (android obesity), particularly in visceral deposits within the body cavity which surround the internal organs, is linked to increased incidence of this disorder (21).

The pathogenesis of type 2 diabetes is complex. Many factors have been proposed that contribute to its progression and explain its strong link to obesity. Given the multifactorial nature of glycemic control, any alteration in the pathways of insulin secretion or action represents a possible mechanism by which diabetes may occur. One significant area of debate focuses on the contribution of genetic vs. environmental influences to the development of the disease. Identical twin studies show over 90% concordance for the disease, along with a significantly higher prevalence (42%) in first degree relatives of these diabetic twin pairs (20). Also, distinct ethnic subgroups have also been identified which have unusually high or low prevalence of type 2 diabetes (eg: Pima Indians, >30% (20); native Nauruan Islanders, 25% (16); Mainland China, <2% (11)). There is little argument that type 2 diabetes has a significant genetic component, but its pattern of inheritance does not fit any classical Mendelian pattern and thus it is difficult to track through pedigree analysis (19). Evidence for the contribution of environmental factors is strong as well. Obesity has already been mentioned as the most prevalent trait in type 2 diabetics, but diet, age and concentration of exercise/activity are other important determinants (20). The current theory of pathogenesis suggests genetic predispositions underlie the development of type 2 diabetes, with environmental factors influencing the actual onset and progression of the disease. Another central question involves the roles of *relative* insulin deficiency and insulin resistance in the

pathogenesis of type 2 diabetes. Insulin deficiency can be caused by a partial loss in β-cell mass or a dysfunction in the secretory process. Lower absolute concentrations of circulating insulin do not necessarily reflect a deficient state as deficiency is *relative* to the amount of glucose present in the blood (i.e. Deficiency is any case where insufficient insulin is secreted to maintain normoglycemia in the patient). Insulin resistance refers to the inability of the secreted insulin to remove glucose from the blood. This may arise due to a variety of abnormalities including defective insulin molecules or receptors, as well as alterations in post-receptor binding events. Some degree of insulin resistance is present in the majority of type 2 diabetics, both lean and obese, and virtually all patients exhibit a *relative* insulin deficiency (11). After countless studies, the current hypothesis is that the disease is a result of a combination of both factors. However, it is evident that the contribution of each is different in unique cases of type 2 diabetes and this may vary at different stages of the disease (11).

1.4.2 Obesity

Though the definition of obesity varies from source to source, it is generally agreed that an individual with a body mass index (BMI = weight (kg)/height $(m)^2$) of greater than 25 is above the acceptable weight range. An individual with a BMI of more than 27 is universally classified as overweight (17). Obesity has become a significant health concern, particularly in the Western hemisphere, and the problem continues to escalate. A National Statistics survey indicated that obesity is more prevalent in males than females between the ages of 18-64 (35% and 23%, respectively, given a BMI >27). More importantly, a similar

survey of people aged 35-64 revealed that in subjects who had diabetes, almost 60% were overweight (BMI >27) compared to only 32% of those that did not have diabetes (17).

The development of obesity is also under both environmental (e.g. diet, physical activity) and genetic (metabolic abnormalities) influences. The balance of fuel intake and expenditure determines the degree of storage necessary and thus influences overall fat mass. Given the extensive number of factors which contribute to food intake, absorption and metabolism, there is a diverse array of possible metabolic alterations that could contribute to obesity. Several animal models of genetic obesity exist, which include the *fa/fa* (Zucker fatty) rat and the *ob/ob* mouse (*n.b.* the Zucker "lean" rat refers to that which expresses normal leptin receptors and is designated as +/+). The underlying genetic defects in both examples cause a disruption in food intake regulation which is normally under the control of the hormone leptin. The *ob/ob* mouse lacks the functional hormone itself, while the *fa/fa* rat produces non-functional leptin receptors. Both models exhibit insulin resistance but are able to compensate for the resistance by increasing insulin output (hyperinsulinemia) and thus do not develop a diabetic phenotype (9). Diabetic variations of the Zucker fatty rat (Zucker Diabetic Fatty (ZDF) rat) and the *ob/ob* mouse (*db/db* mouse) are also found. In the ZDF rat, it has long been known that the genetic variation responsible for the diabetic phenotype is independent of the *fa* gene (22). Recently, an autosomal recessive defect in β-cell gene expression has been identified which may be responsible for preventing the compensatory hyperinsulinemia (23). The *db/db* mouse carries a mutation in the leptin receptor analogous to that in the *fa/fa* rat (giving it the same obese phenotype as the *ob/ob* mouse), but it also becomes diabetic for reasons not yet determined (24).

The action of insulin on adipocytes was discussed earlier and illustrates how alterations in its secretion may affect fat mass. As a storage hormone, insulin increases fatty acid synthesis and storage of triglycerides in fat cells. Unlike muscle cells, which have a limited capacity for glycogen storage, fat cells may increase their fat storage capacity enormously if needed. An empty adipocyte has the potential to increase its fat mass by 100 times. Fat cells may also be formed by *de novo* adipogenesis if the existing storage capacity has been filled, further increasing the overall storage capacity of adipose tissue (25). Thus, hyperinsulinemia results in increased fat storage. Existing hyperinsulinemia can be exacerbated by an increase in food intake, which stimulates further increases in insulin secretion. Insulin resistance can also contribute to the development of obesity. The degree of resistance can vary between target tissues (muscle, adipose and liver), and imbalances in insulin action can cause obesity and fatty liver. For example, muscle represents the largest source for glucose uptake in the body. Insulin resistance in muscle will attenuate overall glucose uptake. This is compensated for by adipocytes and hepatocytes which will store excess glucose as fats. It has been shown that muscle and liver become resistant before and/or to a greater degree than adipose tissue (26). Adding to this, the failure of muscle cells to remove glucose will cause hyperglycemia because adipose tissue is less efficient than muscle in lowering blood glucose (13). The hyperglycemia will continue to stimulate β-cell secretion and contribute to hyperinsulinemia. Of note, pharmacological treatment of diabetics using phenformin or somatostatin analogues, both of which diminish insulin secretion, does lead to a decrease in body weight and suggests that insulin secretion is an effective therapeutic target for obesity in some cases (27).

1.4.3 Diabetes-Obesity Link

The exact relationship between diabetes and obesity is still under intense investigation. Though several postulated mechanisms appear valid, no universal link has yet been determined. Increases in plasma free fatty acids (FFAs) (as seen in obesity) can diminish insulin action (28;29) and are also detrimental to β-cell function. Islet hyperplasia and decreased sensitivity to glucose are common consequences of chronic FFA elevation (30;31). The actions of tumor necrosis factor-α (TNF-α) and leptin (both secreted by adipose cells) may also represent key pathways through which obesity may induce diabetes. TNF-α can cause hyperlipidemia and inhibit insulin-induced glucose uptake in fat and muscle, hence contributing to insulin resistance (32). Leptin is another current focus of research in the field of obesity and diabetes given its regulatory function on food intake (21) and insulin secretion (33). Leptin receptors have been found on pancreatic β-cells and there is speculation that an "adipoinsular axis" exists that represents a feedback loop between adipose tissue and the pancreas. Insulin promotes fat storage, which in turn increases leptin secretion to subsequently inhibit further insulin release (33). The heterogeneity of both diabetes and obesity makes it unlikely that the correction of any one single factor in their respective pathogeneses will result in total resolution of the disease. Thus, each small piece of information will be important in solving the complete puzzle.

1.5 Insulin: Structure & Synthesis

The human insulin gene, residing on chromosome 11, is 1430 base pairs long and contains three distinct exons that code for the entire preprohormone. Non-coding regions at

the 5' and 3' ends of the transcribed mRNA contain a transcriptional promoter (TATAAA) and a polyadenylation site (AATAAA), respectively. The preproinsulin initially translated consists of Pre, A, B, and C (connecting peptide) regions (Figure 1.4a). The Pre region contains a 24 amino acid, hydrophobic signal peptide which directs the translation process to the rough endoplasmic reticulum (RER). Such signal peptides allow cytoplasmic and secretory proteins to be sorted as well as permitting secretory proteins to cross membrane barriers (34).

Initial translation begins on cytoplasmic ribosomes until the signal peptide is uncoded. A signal recognition particle (SRP) binds to the signal peptide and ribosome, halting translation. The ribosome/RNA complex is translocated to the RER membrane. Upon binding to the SRP receptor, translation continues and the growing peptide is inserted into the RER lumen. Once there, the signal peptide is enzymatically removed and the prohormone (proinsulin) is transported to the Golgi complex. In the Golgi, the proinsulin is packaged into secretory granules along with proteolytic enzymes that will remove the 35 amino acid connecting peptide (C-peptide), leaving the biologically active hormone. The C-peptide ensures proper folding of the hormone, but must be removed to have an active insulin molecule (34). The processed insulin is then composed of two chains (A & B) held together by disulphide bonds (Figure 1.4b). Amino acid sequences among most mammalian insulin molecules are highly conserved (>92%) and most of the substitutions that have been observed are at biologically inactive sites (34).

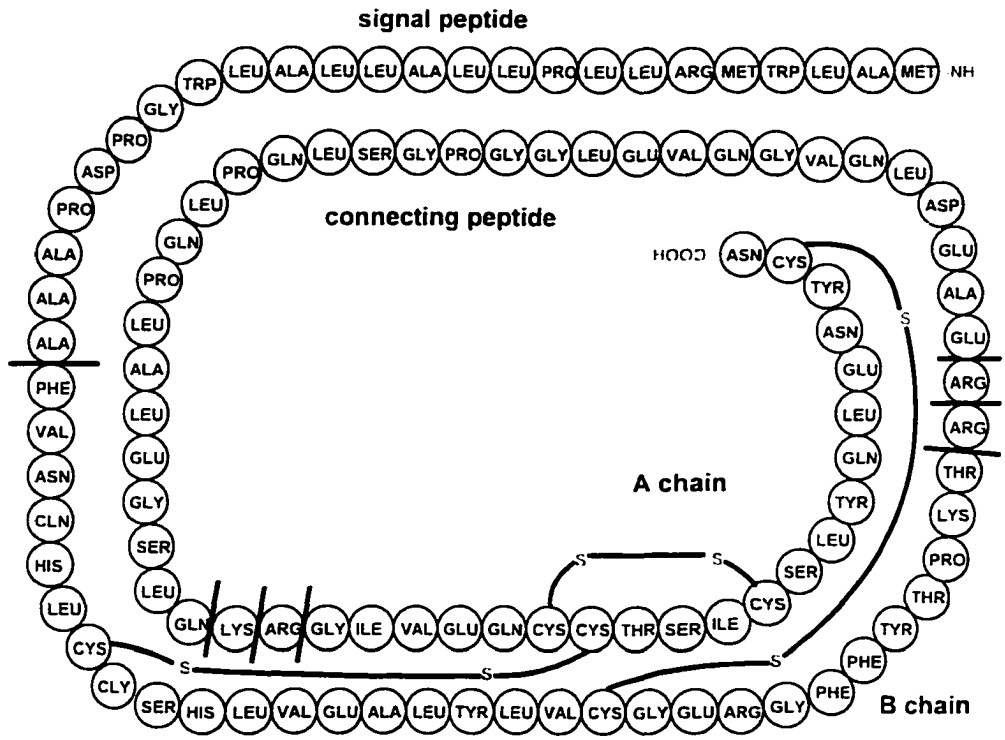

Figure 1.4a. Structure of human preproinsulin. Straight lines represent sites of cleavage during processing by endopeptidases. (Taken from ref. (34))

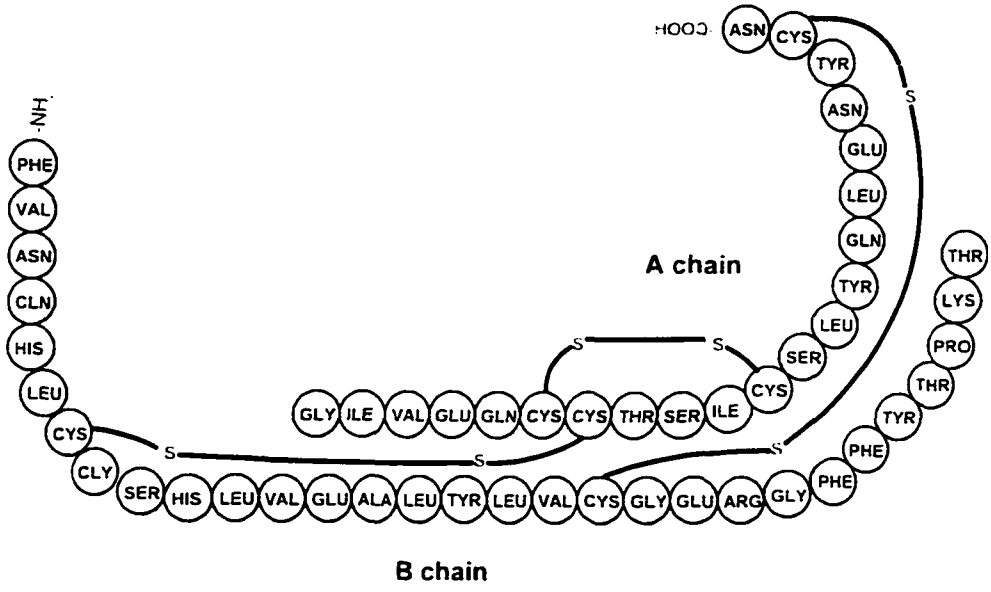

Figure 1.4b. Structure of human insulin. (Taken from ref. (34))

The proteolytic events that occur within the granule are collectively referred to as maturation. Under the electron microscope, different stages of granule maturation can be seen. Mature granules have a very dense core with a light surrounding halo, while immature granules are less dense with no halo (Figure 1.5). Fully mature granules usually contain 90 - 95% mature insulin, 5 - 10% proinsulin, connecting peptide (approximately the same amount as mature insulin) and the proteolytic enzymes, all of which are released upon secretion. C-peptide is eventually degraded in the blood stream. The proteolytic enzymes are inactive at physiological pH (35). Once released from the granule, they pose no threat to other proteins and are also degraded. Excessive stimulation of the β-cell (e.g. hyperglycemia) can lead to exhaustion of mature granule reserves and secretion of immature granules may occur. These granules contain predominantly inactive proinsulin which will not resolve hyperglycemia.

Glucose is the major stimulus for both insulin synthesis and secretion. It increases both transcription and translation of insulin mRNA. Translation effects are prominent during short term stimulation, but chronic glucose exposure results in significant increases in insulin mRNA production (36). The regulation is thought to be mediated by the metabolism of glucose, given the intimate association between insulin biosynthesis and glucokinase activity (a key enzyme in glycolysis) (37). As well, mannoheptulose (an inhibitor of glucose metabolism) also inhibits glucose stimulated insulin biosynthesis (38). The maturation process is another site at which regulation of synthesis may occur, as glucose has been shown to decrease the half-life ($t_{1/2}$) of proinsulin by up to 50% (34). Glucose also has a dose-dependent stabilizing effect on insulin mRNA (possibly mediated by cAMP), preventing its degradation and further increasing biosynthesis (39). It is noteworthy that

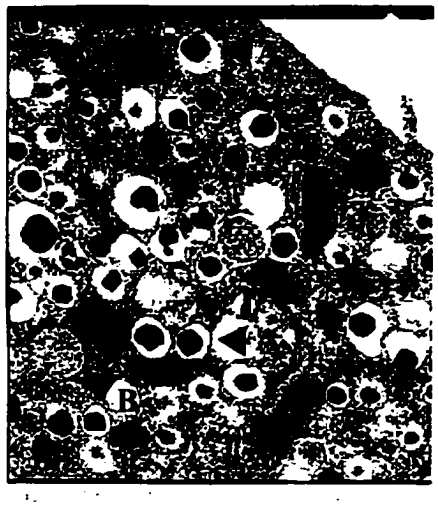

Figure 1.5. Electron micrograph (16 000 x) of a rat β-cell showing mature (A) and immature (B) insulin granules. (DW Wadowska, Dr. GM Wright and Dr. CB Chan, unpublished data)

virtually all compounds that can elicit insulin secretion (except sulphonylureas) can also stimulate its synthesis, indicating that there are likely many redundant pathways involving several possible second messengers (1).

1.6 Insulin Secretion

The process of insulin secretion has been the focus of intense research efforts for over fifty years. Amazingly, a complete understanding of the series of events from stimulation to secretion remains elusive. The difficulty lies in the complexity of the stimulus, primarily the metabolism of glucose and other nutrients. These processes themselves are quite diverse and produce a wide array of metabolites, which have an even larger repertoire of effects. Although there does appear to be a primary sequence of events which takes place under normal circumstances, common functions can occur through several different pathways, indicating that there is some degree of redundancy. The following discussion will attempt to highlight the key events that have been elucidated and important considerations which have yet to be addressed.

Insulin is secreted through both constitutive and regulated pathways. The former represents only a minor contribution and is often termed basal or unstimulated secretion. Upon stimulation, regulated insulin release is biphasic. There is an initial sharp rise in insulin output within the first 5 minutes after stimulation which falls back to about half maximum after ten minutes (Figure 1.6). A more gradual increase is then observed which persists at a given level, dependent on the strength and duration of the stimulus (35;40). The two phases of insulin release are thought to be due to the existence of two distinct storage

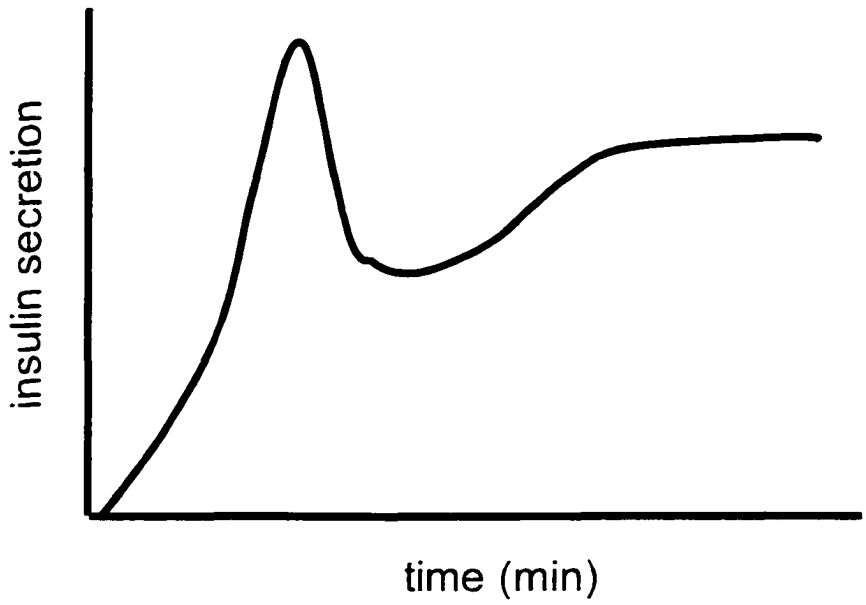

Figure 1.6. Biphasic pattern of insulin secretion in response to glucose. (Taken from ref. (40))

pools of mature granules. The first pool lies near the periphery of the inner face of the plasma membrane. Since these granules have already undergone most of the necessary trafficking and priming events, they can be released rapidly upon stimulation (41). The second insulin pool is thought to be a larger, more distal pool stored in the cytoplasm. These granules are not readily available upon stimulation and require several additional events before being secreted. This would explain the delayed and more sluggish response to stimulation observed in the second phase of insulin secretion. This second phase has been shown to be dependent on insulin biosynthesis, thus refilling of the cytoplasmic pool during persistent stimulation is thought to be a limiting factor (40). Taken together, we can see that insulin secretion is pulsatile, rather than linear. Of these two phases, the first phase represents 75% or more of the total insulin secreted during the stimulation (42). Thus, any alteration in events critical to this initial phase will significantly affect the level of insulin secretion and disrupt glycemic control. This is evident in that loss of the first phase of insulin secretion is seen in many type 2 diabetics (43). The sequence of events involved in the exocytosis of substances from cells is highly conserved throughout most organisms (44). In general, exocytosis requires ATP, calcium and various proteins (collectively called the exocytotic machinery) which regulate the exocytotic events. Secretory vesicles leave the Golgi and are coated with clathrin to prevent random fusion to other membrane surfaces. When secretion is stimulated, this clathrin coat is removed and the vesicle is translocated or "recruited" to the inner face of the plasma membrane (44). This translocation requires the actions of both microtubule/kinesin and actin/myosin systems (45). Microtubules and actin filaments make up a large part of the cytoskeleton. Tubulin and actin exist in the cytosol as

monomers which polymerize into microtubules and microfilaments, respectively, upon stimulation (46). Glucose has been shown to induce these polymerizations in an ATP-dependent, but not calcium-dependent, manner (46). Microtubules are thought to direct granules from the cytosolic pool towards the plasma membrane first, while microfilaments, located closer to the inner face of the plasma membrane, transport the granules the rest of the way. Kinesin (microtubule) and myosin (microfilament) serve as the motor proteins in this translocation, using ATP as the energy source. The mechanism of translocation can be envisioned as the secretory granule "walking" along the microtubule or microfilament (Figure 1.7). Phosphorylation is thought to play a role in promoting granule translocation. Various kinases, some of which are cAMP-dependent (e.g. PKA) (47) or Ca^{2+}-dependent (e.g. CaM II kinase, myosin light chain kinase) (47:48), have been shown to influence granule motility, possibly by acting on (49) key exocytotic proteins (50).

Once the granule reaches the inner face of the plasma membrane, it must "dock". This process is thought to involve the formation of a soluble N-ethylmaleimide sensitive fusion protein receptor (SNARE) complex. Each secretory vesicle membrane contains a v-SNARE unique to the granule type. A complimentary t-SNARE is located on the inner face of the plasma membrane. Along with a few other regulatory proteins and ATP, the two complimentary SNAREs bind to initiate "docking" (Figure 1.8) (50;51). Once docked, a series of ATP-dependent "priming" events occur prior to calcium induced fusion with the plasma membrane. The vesicle's contents are emptied into the extracellular space to subsequently diffuse into capillaries and enter the blood stream (50). This model illustrates how a pool of "docked" and "primed" insulin granules can be quickly released by a sharp

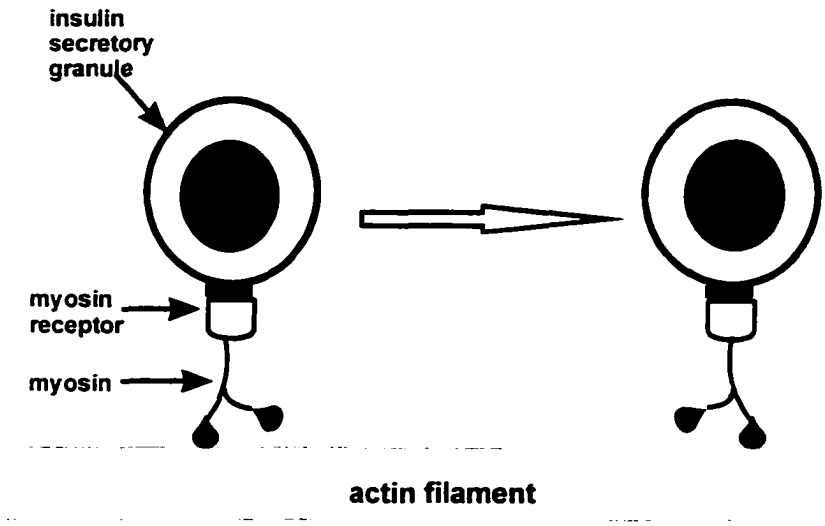

Figure 1.7. Actin-myosin mediated translocation of an insulin secretory granule. (Taken from ref. (52))

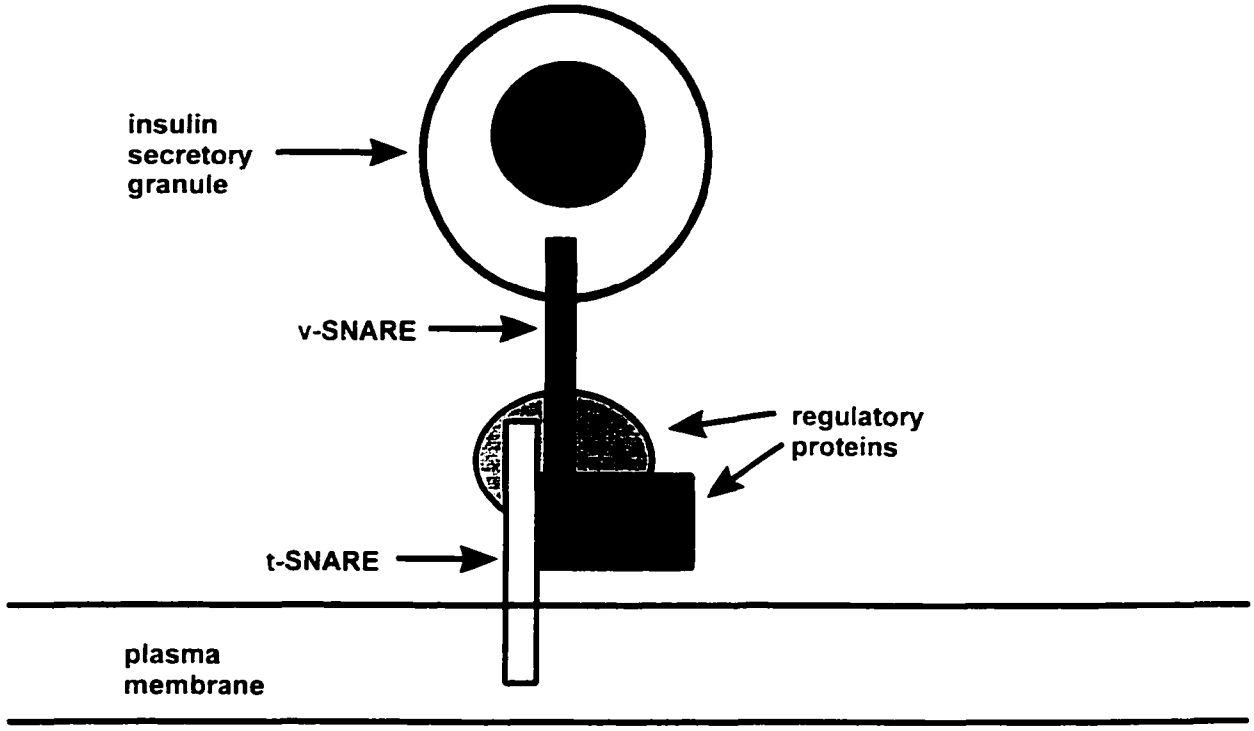

Figure 1.8. Components and postulated arrangement of the SNARE complex mediating granule docking and fusion to the β-cell plasma membrane. (Taken from ref. (51))

rise in intracellular calcium. Now that we see the general events at work in exocytosis we can look more closely at its stimulation as it pertains to the insulin secreting pancreatic β-cell. β-cells respond to subtle changes in blood glucose concentrations that induce insulin secretion. Glucose enters the β-cell through a glucose transporter protein (GLUT-2) in a facilitative manner down a concentration gradient (13). The acute glucose sensitivity of the β-cell is directly related to the high K_m of GLUT-2, making it well suited for its role in this system (i.e. glucose transport is not a rate limiting step in the secretion process in normal islet cells) (13). It has, however, been speculated that some diabetic conditions may be a result of impaired function of this transporter (53). GLUT-2 is also highly expressed in liver, kidney and intestinal cells, where rapid glucose transport is important (13). Once inside the β-cell, glucose stimulates the release of insulin through the generation of metabolic products, the most important of which is ATP. Glucokinase, the enzyme responsible for phosphorylating intracellular glucose in the β-cell, also has a high K_m and is often thought of as the glucose sensor or "glucostat" of the β-cell. Although both glucokinase and hexokinase catalyze the same reaction, the K_m of glucokinase is much higher (>8 mM, glucokinase vs. 0.1 mM, hexokinase). Hence, it is much better suited to respond to physiological glucose concentrations. Defective glucokinase can also be responsible for an impaired β-cell response to glucose (1).

The mechanism of insulin release is generally accepted to be as follows: Metabolism of glucose through glycolysis and the Krebs' cycle generates ATP from substrate and oxidative phosphorylation. This causes an increase in the ATP/ADP ratio within the cell and subsequent closure of ATP-sensitive potassium channels (K^+_{ATP}) on the plasma membrane.

Potassium is unable to leave the cell and the resulting membrane depolarization opens voltage sensitive Ca^{2+} channels. Influx mediates the rise in $[Ca^{2+}]_i$ needed to activate the insulin secretion process. The prominent species involved in the insulin secretory cascade and how their actions contribute to insulin secretion will now be reviewed.

1.6.1 Glucose Metabolism in the β-cell and the Generation of ATP

The complete metabolism of glucose to carbon dioxide and water proceeds through three principle pathways: glycolysis, the Krebs' cycle and oxidative phosphorylation. Glycolysis begins with the ATP-dependent phosphorylation of glucose by glucokinase, which prevents glucose from leaving the cell. The phosphorylated glucose is then broken down into two pyruvate molecules by a series of enzyme catalyzed reactions known as glycolysis (see Appendix A, Figure A.1). Overall, two molecules of ATP are consumed, but four are produced through substrate level phosporylation. In the absence of oxygen (anaerobic respiration), pyruvate is converted to lactate by lactate dehydrogenase which re-oxidizes the reduced nicotinic adenine dinucleotide (NADH) so that glycolysis may continue (54). When oxygen is present, the pyruvate produced from glycolysis is then transported to the mitochondria where it is oxidized to acetyl CoA by pyruvate dehydrogenase, generating another molecule of NADH. Acetyl CoA then undergoes further oxidation by Krebs' cycle enzymes and generates two more NADH molecules as well as one reduced flavin adenine dinucleotide ($FADH_2$) molecule per molecule of acetyl CoA (see Appendix A, Figure A.2) (55). The reduced co-factors generated from glycolysis and the Kreb's cycle (10 NADH and 2 $FADH_2$ per molecule of glucose) donate their electrons to redox proteins known as

cytochromes, which are located in the inner mitochondrial membrane (IMM). Cytochromes contain iron atoms which can be converted to different redox states (e.g. Fe(II)⟶Fe(III)) and are arranged in four "complexes" which collectively make up the electron transport chain, ending with the reduction of molecular oxygen to water (see Appendix A, Figure A.3). The flow of electrons down the chain is driven by the release of free energy from each redox reaction, which drives proton pumping into the inter membrane space at complexes I, III and IV. A proton gradient builds up across the inner membrane which stores the free energy. A protein complex located in the inner membrane known as the ATP synthase complex allows the favorable diffusion of protons back to the matrix, with the free energy released driving the phosphorylation of ADP to ATP. This pathway is known as oxidative phosphorylation and produces theoretically 34 molecules of ATP for every molecule of glucose metabolized (56).

1.6.2 Importance of ATP in Insulin Secretion

In addition to its role in inducing membrane depolarization required for calcium influx, ATP has several other vital roles in the secretion process. The enzyme adenylyl cyclase catalyzes the conversion of ATP to cyclic adenosine monophosphate (cAMP), an important second messenger involved in potentiating insulin secretion (57). Thus, the raw supply of ATP will determine the amount of cAMP produced. ATP also provides the driving force for the myosin-actin and kinesin-microtubule systems responsible for movement of secretory vesicles from the Golgi apparatus to the plasma membrane (45). Exocytosis events alluded to earlier also require ATP to occur. Lastly, many key phosphorylation reactions are

essential for secretion and ATP serves as a major phosphate donor for these reactions (58). In fact, as more becomes known about the secretory machinery and how it is controlled by phosphorylation, this role for ATP appears to be more prominent than once thought. Takahashi et al. (1999) found that phosphorylation (via cAMP-dependent PKA) and not hydrolysis was the main pathway through which ATP increased insulin secretion at steps distal to calcium influx (58). ATP hydrolysis is still important in "priming" events, but is likely maximally effective at lower concentrations (59). Glycolytic pathways consume over 90% of the glucose taken up by pancreatic β-cells (60). Production of ATP by glucose oxidation represents the most significant contribution by glucose to insulin secretion. In β-cells, 98% of this ATP is thought to be generated from oxidative phosphorylation (61). Defects in mitochondrial metabolism can be responsible for diabetes mellitus and so-called "mitochondrial diabetes" accounts for 1-2 % of all cases in humans (62).

1.6.3 The ATP-Sensitive K^+ Channel (K^+_{ATP})

Potassium is the most abundant intracellular cation and is the primary determinant of the β-cell resting potential (approximately -70 mV) (63). The β-cell K^+_{ATP} channel is ligand-gated: open when ADP is bound and closed when ATP is bound (Figure 1.9). Therefore, when the ATP/ADP ratio increases, more of these channels close. As potassium is trapped inside the cell, the membrane potential becomes increasingly positive and voltage-gated calcium channels begin to open at about -40 mV. The resulting calcium influx is fundamental to secretion as will be discussed later. Defects in K^+_{ATP} channel closure can lead to deficient insulin secretion and diabetes (64). An important clinical implication of this

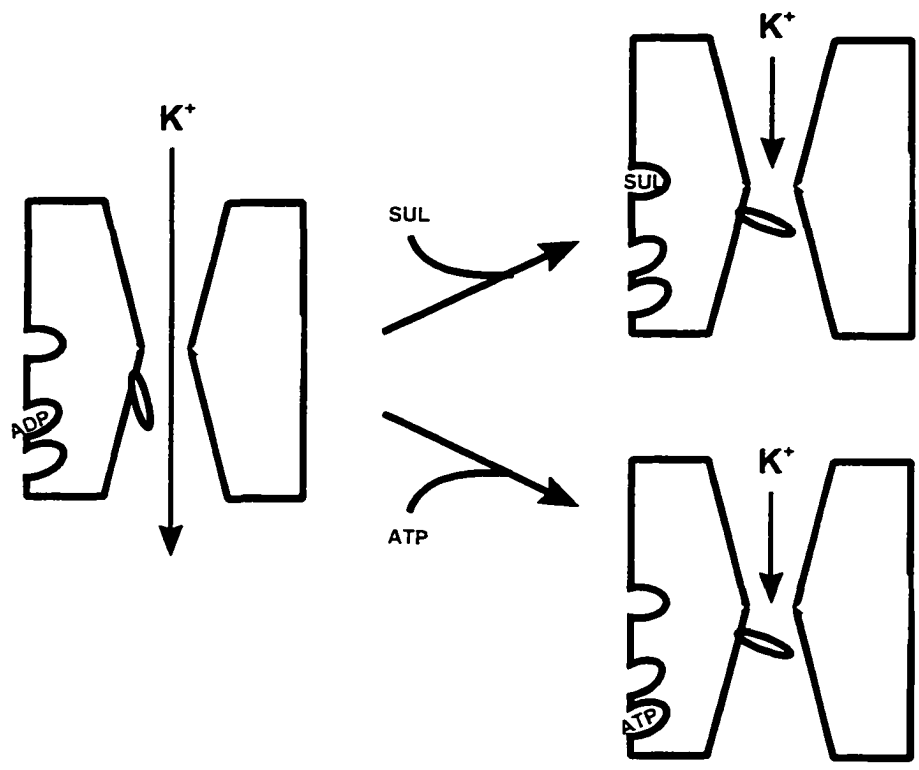

Figure 1.9. Schematic representation of the β-cell K^+_{ATP} channel. ATP, ADP and sulphonylurea (SUL) binding sites are indicated. (Taken from ref. (63))

channel is the existence of another distinct gating site. Sulphonylureas are commonly used oral hypoglycemic drugs, that bind to a distinct sulphonylurea site that also closes the K^+_{ATP} channel, thus stimulating calcium influx and insulin secretion (refer back to Figure 1.9, page 36) (63).

The existence of glucose effects independent of the K^+_{ATP} channel has been proposed for some time. This other pathway does not affect intracellular calcium, but rather serves to potentiate the Ca^{2+}-induced release of insulin (i.e. more insulin is secreted at a given concentration of intracellular calcium) (65). Hence, it acts in synergism with the K^+_{ATP}-dependent pathway. The K^+_{ATP}-independent pathway is dependent on glucose metabolism, as mannoheptulose (an inhibitor of glycolysis) blocks this pathway (65). Though such a pathway has been demonstrated, its physiological role is speculative. No concentration-response between glucose and K^+_{ATP}-independent insulin release is observed, although agents that increase cAMP concentrations are effective in increasing release at high glucose concentrations (>16 mM). These effects may be mediated by PKA and PKC given that this type of secretion can be elicited upon their activation (10), and their activities can be influenced by cAMP (57).

1.6.4 Intracellular Calcium

A rise in intracellular calcium concentration is fundamental for insulin release from the stimulated β-cell (57;66;67). In fact, oscillations in insulin secretion mirror oscillations in glucose metabolism and calcium influx (48). Calcium concentrations inside the unstimulated β-cell are kept below 100 nM by the actions of Ca^{2+} ATPase pumps, the

Na^+/Ca^{2+} antiport, calcium buffering by intracellular storage organelles (endoplasmic reticulum (ER) and mitochondria) and soluble calcium binding proteins in the cytoplasm (e.g. calmodulin). Extracellular Ca^{2+} is approximately 10,000 fold higher, usually in the mM range (40). This large gradient allows for rapid influx of calcium following membrane depolarization and opening of voltage-gated calcium channels. While β-cells express L-, P/Q- and N-type calcium channels, voltage-gated L-type channels are the major site of the Ca^{2+} influx (67). Liberation of calcium from intracellular stores also helps increase intracellular calcium. However, this process is thought to potentiate secretion through increases in granule mobility and refilling of the readily releasable pool (57;66). Many insulin secretagogues (e.g. nutrients, drugs, hormones, etc.) function by promoting a rise in intracellular calcium through various mechanisms. Agents that promote (e.g. sulphonylureas) or inhibit (e.g. the Ca^{2+} channel blocker nifedipine) calcium influx cause a profound increase or decrease in insulin secretion, respectively. As well, removal of extracellular calcium markedly reduces insulin secretion (66).

Calcium appears to have several important roles in the exocytotic process. It is primarily involved in granule fusion. Calcium directly interacts with the regulatory protein synaptotagmin to mediate SNARE complex rearrangement and membrane fusion(68). Influx of extracellular calcium appears to mediate these reactions for the most part. Granule trafficking is another important event which appears to be calcium-dependent. It is speculated that calcium released from intracellular stores mediates granule movement, which is attenuated by calcium chelating agents (e.g. EDTA) (66). Phosphorylation of secretory proteins such as myosin light chains by Ca^{2+}-dependent protein kinases likely mediates this

effect (48). Trafficking events are still observed, albeit at a lower rate, under non-stimulatory conditions in the β-cell (i.e. at resting $[Ca^{2+}]_i$). This may indicate that they require a lower concentration and/or are under the influence of other mediators. Taken together, these observations support the aforementioned hypothesis of two distinct intracellular pools of calcium working together in the overall secretion process. Influx results in immediate high $[Ca^{2+}]_i$ near the inner surface of the plasma membrane where it is required for the fusion events. Liberation from intracellular stores creates a lesser, more generalized increase in $[Ca^{2+}]_i$ which promotes the movement of granules stored throughout the cytoplasm. Calcium also binds to a soluble protein called calmodulin. The complex formed has many actions which include activation of kinases (CaM kinases) which can catalyze phosphorylation of key exocytotic proteins (67).

Calcium may even be able to regulate itself through modulation of the ATP/ADP ratio, the factor primarily responsible for its influx. It has been shown that rises in $[Ca^{2+}]_i$ decrease ATP concentrations, and therefore the ATP/ADP ratio, in pancreatic islets. Subsequent re-opening of the K^+_{ATP} channels would restore membrane potential and prevent further calcium influx. This effect could be mediated by increased ATP consumption by Ca^{2+}ATPase pumps attempting to restore calcium homeostasis (69). Calcium extrusion is also mediated by the Ca^{2+}/Na^+ exchanger which would promote sodium entry. The Na^+/K^+ ATPase would then become active and also represent an ATP consuming process (57).

Calcium appears to be the principle messenger for glucose stimulated insulin secretion to occur. Secretion can, however, be induced under conditions where extracellular calcium is removed and intracellular stores are depleted by activators of protein kinases A

and C (70). Although this would not occur physiologically, it does indicate that phosphorylation reactions may also be important to calcium's role in the secretory cascade. This messenger alone, however, does not account for all insulin that is secreted and other mediators that significantly potentiate the process are necessary for adequate secretion of insulin (70). One of the most prominent potentiators of insulin secretion is cAMP.

1.6.5 cAMP

Cyclic adenosine monophosphate (cAMP) is generated from ATP by the action of the enzyme adenylyl cyclase (AC). This enzyme has nine identified isoforms and is subject to regulation by guanosine triphosphate binding (G)-proteins (both inhibitory and stimulatory), various drugs (e.g. forskolin) and the Ca^{2+}/calmodulin complex. Subtypes V and VI represent the majority of AC isoforms in human and rat islets, although expression of AC III (71) and AC IX (72) has also been reported. AC activity can be altered both positively and negatively by G-protein linked effects, while stimulation by protein kinase C (PKC) phosphorylation has been demonstrated for AC V (72). Both AC V and AC VI are also inhibited by the Ca^{2+}/calmodulin complex *in vitro*, with a negative feedback loop existing between calcium influx and cAMP generation. This inhibition can be overcome by the actions of G-proteins and the adenylyl cyclase activating drug forskolin (72). Of note, AC VI is only inhibited under conditions of Ca^{2+} influx and not through liberation of Ca^{2+} from intracellular stores (73). It may be speculated that the potentiating action of cAMP on insulin secretion occurs during granule trafficking, given the model of Ca^{2+} action proposed earlier. In contrast to this, glucose is only able to increase cAMP in the presence of extracellular

calcium (57). Thus, the exact relationship between Ca^{2+} and cAMP remains unclear. Phosphodiesterase (PDE) enzymes represent the main degradation pathway of cAMP and thus play a significant role in regulation of cAMP levels and its signaling capabilities. PDEs are subject to regulation by Ca^{2+} and phosphorylation state (72). The PDE inhibitor isobutylmethylxanthine (IBMX) augments glucose stimulated insulin secretion likely by decreasing cAMP turnover.

Cyclic AMP is a potentiator of insulin secretion rather than an initiator (63). This is evident in that it is only effective at increasing insulin secretion at stimulatory and not basal glucose concentrations (57). Though both the first and second phases of insulin secretion are affected by cAMP, the latter represents about 80% of the total cAMP effect (74). Activation of PKA is the principle mechanism of cAMP action in the secretion process. A negative feedback loop exist between the two, as PKA inhibits AC V and VI subtypes (71). PKA has a wide range of substrates and phosphorylation of exocytotic proteins, particularly those involved in granule trafficking, is a likely mechanism of its action. This would accelerate refilling of the primary granule pool located at the plasma membrane and represent a pathway for potentiating the second phase of insulin secretion. It could also explain the increase in β-cell sensitivity to fixed calcium concentrations observed when cAMP is elevated (57;75). These granule mobilization events require ATP and hence glucose metabolism (76).

Agents that elevate cAMP also increase $[Ca^{2+}]_i$ by reducing the inactivation time of L-type calcium channels (77). This provides one pathway through which cAMP may augment the first-phase insulin response to glucose. As well, mobilization of calcium from

intracellular stores has also been reported in response to elevations in cAMP. This effect is PKA-dependent and may be due to increasing sensitivity of inositol trisphosphate (IP_3) receptors on the rough endoplasmic reticulum (RER) through phosphorylation (78). Interestingly, cAMP has also been shown to reduce $[Ca^{2+}]_i$ by increasing its uptake into thapsigargin-sensitive intracellular stores (79). This process is ATP-dependent and is postulated to occur via activation by PKA phosphorylation of Ca^{2+} ATPase pumps in the RER membrane. Thus, it is possible that cAMP functions in a dual capacity to finely control $[Ca^{2+}]_i$ such that it is adequate for maximal stimulation of exocytosis but does not progress to cytotoxic levels (79).

Phosphorylation of ion channels is another possible target for PKA, though its contribution remains to be established. PKA-independent effects on exocytosis are also speculated. A role for cAMP in distal steps of exocytosis has recently been proposed with the identification of cAMP binding to Rab interacting molecules (Rim) 1 and 2, two important proteins involved in regulating vesicle fusion (80). Finally, cyclic nucleotide-gated ion channels have been described in certain neural cells which conduct Ca^{2+}, Na^+ and K^+ (72). No such channels have yet been identified in islet cells, but should they exist, could represent an additional secondary pathway of cAMP action.

1.6.6 Lipid Based Signaling

Since the primary events that trigger insulin secretion are dependent on ATP formation, it would seem logical that metabolism of any fuel molecule to generate ATP could function as a signal for secretion. Although β-cells oxidize fatty acids for energy to sustain

themselves, the slow rate of free fatty acid (FFA) transport into the cell limits their ability to elicit the rapid rise in ATP needed for first-phase secretion. Glucose, on the other hand, readily enters the β-cell through the high capacity GLUT-2 transporter when a concentration gradient exists (13). ATP derived from fatty acid oxidation contributes to basal or non-stimulated insulin secretion. Therefore, high levels of FFAs in the blood will induce basal hyperinsulinemia.

Lipid based molecules can, however, play a role in the amplification of signaling in glucose-stimulated insulin secretion (GSIS). The classical second messengers diacylglycerol (DAG) and inositol trisphosphate (IP_3), both derived from inositol phosphate hydrolysis by phospholipase C (PLC), are two such molecules. DAG is an activator of PKC, which could mediate important phosphorylation reactions, while IP_3 serves to liberate calcium from intracellular stores, raising the $[Ca^{2+}]_i$ (81). Glucose has been shown to activate PLC (82), raising the question of the potential importance of these messengers. *In vitro* studies have shown no detectable change in DAG following glucose stimulation, though artificially increasing it through the use of acetylcholine significantly amplifies the insulin response to glucose. Surprisingly, IP_3 levels are increased by glucose stimulation, which would seem odd given that DAG and IP_3 are produced in a 1:1 ratio from the hydrolysis reaction. The explanation for this is that DAG is already abundant under non-stimulated conditions (~200 μM) while IP_3 is present at very low levels (< 1 μM) (81). The glucose-induced IP_3 elevation is only about 1μM, a change not detectable for DAG given its high basal level. Why not disregard DAG altogether, given that IP_3 is also produced and has been shown to effectively enhance insulin secretion on its own? The reason is because agents which increase DAG

concentration also potentiate the insulin response (82). It would appear that in glucose-induced insulin secretion, IP_3 is the main player, while secretion induced by muscarinic agonists could involve both IP_3 and DAG (81).

Two other important lipid related molecules are also proposed to play key roles in insulin secretion (53;83). Malonyl CoA, formed from acetyl CoA by acetyl CoA carboxylase (ACC), and long chain acyl CoA (LC-CoA) esters from FFA breakdown play important roles in fuel switching in the mitochondria. The acetyl CoA required for malonyl CoA synthesis could theoretically come from fatty acid breakdown, but in the β-cell it is thought to be primarily derived from glucose (84). Citrate is one of the primary precursors, being converted to acetyl CoA by citrate lysase (53). Malonyl CoA inhibits the oxidation of LC-CoAs in the mitochondria, thus causing a shift toward glucose oxidation and increasing the β-cell sensitivity to glucose. In normal islets, ACC activity is high and fatty acid synthase activity is very low (85). This ensures that although a significant amount of malonyl CoA is produced, it serves to regulate fatty acid oxidation rather than stimulate fatty acid synthesis. LC-CoA also appears to play a role in the signaling pathway given the positive correlation between cytosolic LC-CoA and secretion (37). It is conceivable that LC-CoA (source of acyl chains) acts together with glucose (a source of glycerol) to generate a rise in DAG, potentially contributing to the signaling pathway (86). Other effects of LC-CoA that could contribute to insulin secretion include activation of certain PKC isoforms (87) and acylation of G-proteins (88).

It is important not to confuse the beneficial effects of fatty acid derived LC-CoA with the detrimental effects of high FFAs in the β-cell. At low FFA levels, the increased glucose

transport allows glucose concentration in the β-cell to be high enough that it can produce enough malonyl CoA to inhibit LC-CoA, and ultimately FFA oxidation in the mitochondria. This is the basis of the β-cell's role in being a glucose sensor and permits it to respond to changing blood glucose concentrations. When FFAs become too high, this effect is overwhelmed and the β-cell loses glucose sensitivity. Recall that decreased β-cell glucose sensitivity is seen in most cases of type 2 diabetes; therefore, this model may provide a possible link between obesity (high FFAs) and diabetes. A family of ligand-activated transcription factors known as the peroxisome proliferator-activated receptors (PPARs) have recently been implicated in this reduction of sensitivity. PPARs bind long chain fatty acids as well as other specific agonists and mediate the induction of various fatty acid oxidizing enzymes, thus reducing the fat content of target cells(89). This subsequently reduces the levels of circulating FFAs and fat content within islets. The potential importance of PPARs is evident in that the antidiabetic thiazolidinedione drugs are ligands for PPAR-γ and are thought to increase β-cell sensitivity (89).

1.6.7 Hormonal and Neural Regulation of Insulin Secretion

Several hormones and neurotransmitters also function in the regulation of insulin secretion. Most do so through receptor mediated alterations in levels and/or sensitivity of the key messengers mentioned earlier. G-proteins are thought to provide the link between receptor binding and intracellular effects in many of these cases. G-proteins contain three subunits (α, β and γ) and function by cycling between GDP- and GTP-bound states. This alters subunit interactions which can influence an array of intracellular components either

positively or negatively (Figure 1.10) (67).

Glucagon (90), glucagon-like peptide-1 (GLP-1) (90), and gastric inhibitory polypeptide (GIP) (91) are among the better described insulinotropic hormones. Secretion of glucagon from pancreatic α-cells is in response to low blood glucose, while GIP and GLP-1 secretion is elicited from the intestine after a meal. All three hormones function through G-protein linked activation of adenylyl cyclase to increase cAMP formation and potentiate insulin secretion. This is a physiologically desirable effect given the stimulus and actions of each (90;91). When these conditions cause blood glucose to rise, insulin is needed to promote uptake.

Neural control over insulin secretion is regulatory as opposed to stimulatory. Actions of the sympathetic nervous system serve primarily to attenuate secretion in response to glucose (92;93). These inhibitory actions are attributed to α_2-adrenergic receptor activation (e.g. norepinephrine) (94). The actions of this sympathetic neurotransmitter are again mediated primarily through G-protein manipulation of adenylyl cyclase activity and thus cAMP levels (95). The parasympathetic system stimulates insulin secretion through cholinergic receptor agonists, primarily acetylcholine (92). Acetylcholine's action involves an increase in calcium release from intracellular stores mediated by an elevation in IP_3 levels (96). Opposing neurotransmitters may even influence the secretion of their counterparts as part of their inhibitory or potentiating effects. For example, it has been shown that acetylcholine can inhibit norepinephrine release from nerve terminals and vice-versa (92).

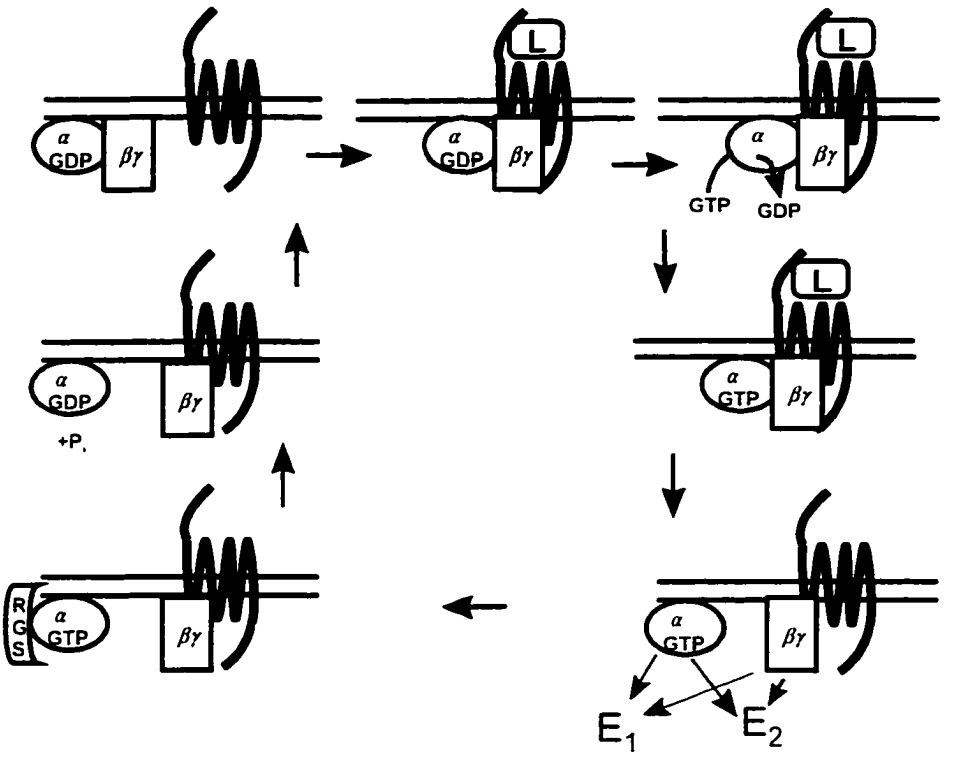

Figure 1.10. Heterotrimeric G-protein cycle. Upon ligand (L) binding to a G-protein coupled receptor, GTP replaces GDP on the α-subunit. This causes dissociation of the α and βγ subunits where each exert an effect on target enzymes (E_1 & E_2). A Regulator of G-protein Signaling (RGS) stimulates GTPase activity of the α-subunit, hydrolyzing GTP to GDP + P_i. The release of P_i drives the reassociation of the subunits back to their original configuration. (Taken from ref. (67))

Control of insulin secretion by the autonomic nervous system is physiologically significant. Under conditions of stress and physical activity where blood glucose concentrations must be high, there is increased activity of the sympathetic nervous system and subsequent inhibition of insulin release. In fact, plasma norepinephrine levels are directly proportional to workload intensity during exercise (93). The relationship between sympathetic and parasympathetic control is complex. Campfield and Smith (1983) found that certain concentrations of acetylcholine, which *alone* caused a significant increase in insulin output, could be completely inhibited by a norepinephrine concentration which *alone* caused an attenuation of much lower proportion. Further increasing the acetylcholine concentration eventually overcame this blockade (92). Thus, the contribution of the sympathetic nervous system appears to be dominant, perhaps due to differences in receptor number or binding affinity for each on the β-cell.

1.7 Uncoupling of Oxidative Phosphorylation

As discussed in section 1.6.1 (page 33), metabolism of fuel molecules (e.g. glucose, fatty acids) generates ATP from oxidative phosphorylation. The end result is the reduction of molecular oxygen (O_2) to form water; thus measuring O_2 consumption (also termed mitochondrial respiration) gives an indication of the activity of the electron transport system. Electron transport and oxidative phosphorylation are not perfectly coupled processes (i.e. less ATP is generated than predicted given the amount of electron transport) (97;98). This imbalance is referred to as uncoupling and is a result of protons being translocated back to the matrix independently of the ATP synthase complex. The free energy from this favorable

diffusion is released as heat. The degree of uncoupling varies between tissues, but can account for as much as 25 % (liver) or even 50% (heart) of oxygen consumption by cells (99). A family of IMM proteins has been shown to catalyze dissipation of the proton gradient in the absence of ATP synthesis. As such, they have been dubbed the uncoupling proteins (UCPs).

1.7.1 UCP-1

Although the thermogenic role of brown adipose tissue (BAT) had been known for 40 years, it was not until 1978 that the actual component responsible for its action, a 32 kDa mitochondrial protein, was identified (100). Named UCP-1, this first member of the UCP family is expressed exclusively in BAT and plays a vital role in the thermogenic response to cold in rodents, hibernating animals and newborn mammals. UCP-1 catalyzes a proton leak in BAT mitochondria and its expression is upregulated by cold exposure or treatment with norepinephrine, the sympathetic transmitter released in response to cold exposure. Of note, its activity can be inhibited by purine nucleotides such as ADP, ATP, GDP and GTP (100).

UCP-1's mechanism of action is still debated, but the most accepted hypothesis is that it involves fatty acid cycling. In this model, the protein itself acts as a fatty acid anion channel that transports the anion across the IMM into the inter membrane space. After becoming protonated in this acidic environment, the neutral fatty acid then diffuses back through the IMM to the matrix, taking the proton with it. Under the basic conditions of the matrix the fatty acid deprotonates to complete the cycle, the net result being the transport of a proton back to the matrix (101). The concept of fatty acid cycling is supported by the

dependence of UCP-1 expression and activity on levels of FFAs (99). The anion transporter is thought to be a channel rather than a carrier based on the kinetics of ion translocation and the proposed tertiary structure of UCP-1. Analysis of its amino acid sequence reveals six hydrophobic transmembrane segments joined by polar loops, a signature feature of ion channels (98).

With the actual protein identified, researchers then began to study possible physiological actions of UCP-1, other than thermogenesis. The process of uncoupling leads to inefficient production of ATP and requires cells to metabolize more fuels in order to maintain an adequate supply of ATP. By increasing the metabolic rate, could UCP-1 play a role in the regulation of body weight? In support of this theory, the BAT of the genetically obese *fa/fa* rat, *ob/ob* and *db/db* mouse models show an impaired thermogenic response to cold exposure and have reduced UCP-1 activity (102). However, the development of the UCP-1 knockout mouse by Enerbeck et al. (1997) addressed this question with a resounding "no". The UCP-1 knockout mice failed to develop obesity as predicted (103). Also, adult mammals (other than rodents) possess insignificant amounts of BAT and thus it would have little contribution to their overall metabolic rate.

1.7.2 UCP-2 and UCP-3

Though UCP-1 had not provided all the answers, researchers now had a better understanding of the uncoupling process. Uncoupling had long been observed in other tissues and in 1997 two new members of the UCP family were discovered. In mice and humans, UCP-2 and UCP-3 bear 55% and 57% amino acid sequence homology respectively

to UCP-1, with 73% homology to each other (104). While UCP-3 expression is confined primarily to skeletal muscle (with a small amount in BAT), UCP-2 is expressed ubiquitously. High levels of UCP-2 mRNA can be found in white adipose tissue (WAT), intestine, lung, heart, kidney and tissues of immunological function such as spleen and thymus where lymphocytes are abundant (98;102). Other tissues with significant UCP-2 expression include skeletal muscle (98), pancreatic islets (105;106) and BAT (98). In fact, it was later hypothesized that the failure of UCP-1 knockout mice to become obese may have been due to a five-fold increase in UCP-2 expression observed in their BAT (103).

Given their high degree of amino acid sequence homology, UCP-2 and UCP-3 are thought to behave similarly to UCP-1. UCP-1 facilitates proton transport when expressed in yeast and reconstituted liposomes (107). This effect is seen in both UCP-2 and UCP-3, which also increase O_2 consumption in yeast (108). In cell culture systems, mitochondrial membrane potential and growth rates are reduced by increasing UCP-2 and UCP-3 expression (108;109). Though functionally similar, there are some differences in the regulation of expression/activity and possible physiological roles of these new UCPs. Tissue specific differences in regulation have also been observed. In BAT, fasting over a 24-48 hour period down-regulates UCP-3 while UCP-2 is unaffected. In skeletal muscle, however, both are strongly up-regulated (110;111). Fasting also upregulates UCP-2 in WAT (98). Though cold exposure serves to up-regulate UCP-1, it has no effect on expression of either UCP-2 or UCP-3 (98;102;112). Clearly much more information is required in order to fully characterize the regulatory characteristics of these UCPs. Extrapolation of results between different UCPs and even between different tissues may not be reliable.

The widespread expression of UCP-2 makes it the most interesting and potentially important focus of study within the UCP family. Its effect of decreasing metabolic efficiency may have several physiological consequences in the many tissues where it resides. For these reasons, it will be discussed in greater detail.

1.7.3 The *ucp-2* Gene

The *ucp-2* gene maps to human chromosome 11, mouse chromosome 7 (108) and rat chromosome 1 (113). In mice, this region has been shown to be strongly associated with obesity, hyperinsulinemia and diabetes (108). The *ucp-2* gene shows a high degree of conservation over different species (97) and it lies only 7-8 kb downstream from the *ucp-3* gene (100). The close association between the two tends to confound genetic analysis of polymorphisms and their relation to phenotype. The transcribed human UCP-2 mRNA consists of 8 exons, of which the first two are not translated. The *ucp-1* and *ucp-3* genes have six translated exons, but lack any pre-translation exons (98). No function of the two pre-translation exons has yet been determined (100). The promoter region of the *ucp-2* gene lacks the signature TATA or CAAT boxes seen in the *ucp-1* promoter, but is rich in G-C pairs. Several key regulatory elements for factors such as cAMP response binding protein, glucocorticoid receptors and PPARs are evident in the promoter (114).

Analysis of genetic variations in the *ucp-2* gene in relation to metabolic disorders such as diabetes have yielded minimal results to date. Substitution of alanine for valine at amino acid 55 increases metabolic efficiency and decreases fat oxidation in Caucasian subjects, suggesting a possible disruption in uncoupling activity by this mutation (115).

However, no association with obesity or insulin resistance was found (116). A 45 bp insertion/deletion in exon 8 of the human *ucp-2* gene has been found to be associated with weight gain and lower levels of circulating leptin, but not glucose intolerance in South Indian patients. These results were not observed in British subjects (117). Walder et al. (1998) studied the genetic variances described above in Pima Indians, a unique population that shows a high prevalence of both obesity and type 2 diabetes. Both polymorphisms were associated with decreased resting metabolic rate, but only subjects > 45 years of age that were homozygous for the exon 8 variant had higher BMIs (118).

1.7.4 Regulation of UCP-2 Expression

The majority of studies to elucidate the physiological role(s) of UCP-2 have focused on factors and pathological conditions affecting its expression, rather than the genetic analysis previously discussed. Reliable α-UCP-2 antibodies have only recently been developed and tested, thus most of the studies have looked at levels of UCP-2 mRNA as a measure of its expression. Skeletal muscle and adipose tissue have been most extensively investigated because of their large contribution to energy stores and energy expenditure. Immune based tissues like the spleen and thymus have also recently come to the forefront of UCP-2 research in terms of response to infection (e.g. fever, oxidative processes of macrophages). Pancreatic islets are another potentially important area of research due to their dependence on ATP for insulin secretion.

As mentioned earlier, skeletal muscle predominantly expresses UCP-3, with lesser amounts of UCP-2 found. The expression of both UCPs appears to be positively correlated

with % body fat and UCP-3 expression actually increases as a function of % body fat (119). Type 2 diabetic patients tend to show 2-3 fold higher levels of UCP-2 and UCP-3 mRNA in skeletal muscle and adipose tissues, with no difference observed between insulin-sensitive and insulin-resistant diabetics within that group. This effect is independent of obesity given that BMI and % body fat were consistent between diabetic and control groups (119). Other studies have shown the induction of skeletal muscle UCP-2 and UCP-3 mRNA by a high fat diet (120) and starvation (110), both of which result in elevations of FFAs. However, starvation does not lead to increased UCP-2 or UCP-3 mRNA in type 2 diabetic patients, though pre-fasting levels are still higher than those in non-diabetic controls (121). Taken together, these studies indicate that up-regulation of UCPs in skeletal muscle may be an adaptive response to increased levels of FFAs. Failure of *adequate* induction may be responsible for the development of chronic obesity. Evidence supporting this idea was found by Nordfors et al. (1998) where they showed obese subjects had 28% lower skeletal muscle UCP-2 mRNA levels than controls (122).

As in skeletal muscle, conditions that lead to elevations in FFAs induce an increase in UCP-2 mRNA in adipocytes (112). This UCP-2 mRNA is also positively correlated to BMI (123). In addition, key factors governing fatty acid metabolism in adipocytes have been shown to be associated with UCP-2 expression (98;124). PPAR binding enhances the transcription of enzymes involved in fatty acid oxidation. PPAR-γ agonists in particular have been shown to increase UCP-2 mRNA in adipocytes (124). Leptin, a hormone which controls food intake and regulates energy stores, increases UCP-2 mRNA about 6 fold in adipocytes (98). Leptin has no effect on UCP-2 mRNA in the genetically obese *fa/fa* rat, as

would be expected given its defective leptin signaling pathway (106) The *ob/ob* mouse has increased UCP-2 mRNA in both skeletal muscle and adipose tissue compared to wild-type controls under normal conditions (125). Strains of mice like the A/J and KsJ, which are resistant to obesity induced by high fat diet, have higher adipose UCP-2 mRNA than obesity prone mice (e.g. C57BL/6J), suggesting that obesity prone mice fail to adequately induce UCP-2 in adipose tissue when FFAs are elevated (98;108).

Regulation of reactive oxygen species (ROS) production has recently become a focus in UCP-2 research. The generation of ROS is directly proportional to the proton gradient across the IMM. Proton pumping by the electron transport chain complexes is slowed down by back pressure as this gradient increases. The consequence of this is an increase in the half-life of reduced CoQ (CoQ •) (see Appendix A, Figure A.3). CoQ • is involved in production of superoxide anion (O_2^-), and subsequently H_2O_2, from the action of superoxide dismutase (98). Thus, increased uncoupling relieves the back pressure and allows the electron transport chain to flow freely, reducing CoQ • and ROS production. The consequences of this action can be both beneficial and detrimental. On the positive side, uncoupling can protect cells from oxidative damage due to excess substrate, as seen with hyperglycemia or hyperlipidemia. Indeed, increased UCP-2 expression is observed in hepatocytes of the *ob/ob* mouse (126) and has been shown to decrease apoptosis in animals with fatty liver (127). However, decreasing the oxidant capacity of immune cells such as macrophages which rely on ROS to kill invading microorganisms increases susceptibility to infection (128). Also, the thermogenic properties of uncoupling may be involved in the fever response that accompanies infection. Faggioni et al. (1998) found that UCP-2 mRNA is

increased in liver (28 fold), muscle (5 fold) and adipose tissue (5 fold) by bacterial lipopolysaccharide administration (129).

1.7.5 Possible Physiological Roles of UCP-2

Given our current knowledge of UCP-2 expression and action, a few well defined aspects of these potential physiological roles can be seen. Firstly, conditions in which high levels of FFAs are present increase UCP-2 expression in normal animals. Agents which promote β-oxidation where fatty acids are broken down (e.g. leptin, PPARs) also upregulate UCP-2. Therefore, it seems evident that UCP-2 serves to increase and/or favor fatty acid metabolism. With regards to its contribution to body weight, UCP-2 is up-regulated in response to an obese state. However, it may not be the most influential determinant of body weight given that UCP-2 knockout mice fail (128) to become obese (130). UCP-3 has much higher expression in skeletal muscle, the site of much of the body's energy expenditure. Interestingly, UCP-3 knockout mice do not develop obesity either and show no change in the expression of UCP-1 or UCP-2 (131). The exact compensatory mechanisms preventing the obese phenotype remain to be determined. It is conceivable that in patients who have a defective UCP (be it UCP-1, UCP-2 or UCP-3), attenuations in compensatory mechanisms (e.g. alternative UCP up-regulation) may partially underlie the onset of obesity. Secondly, UCP-2's effects on ROS generation have been reported (128;132;133). Importantly, UCP-2 knockout mice are more resistant to *Toxoplasma gondii* infection and their macrophages have an 80% higher oxidant capacity (128). Susceptibility to hyperglycemic or hyperlipidemic damage of tissues and age-related oxidative stress in UCP-2 knockout mice

remain to be determined.

1.7.6 UCP-2 in Pancreatic Islets

Pancreatic islets express detectable levels of UCP-2 (105;106). Its regulation is similar to that in other tissues and can vary in different pathological conditions. Elevations in FFAs (134) and leptin (106) induce increases in UCP-2 mRNA in islets and clonal β-cells. However, leptin is unable to upregulate UCP-2 in *fa/fa* rat islets due to dysfunctional leptin receptors (106). PPAR-γ agonists such as troglitazone can also elevate UCP-2 (135). The common denominator for all these factors is increased fatty acid oxidation. In fact, PPAR-γ agonist effects may represent the mechanism of FFA-induced increases in UCP-2 since fatty acids bind PPARs to stimulate the transcription of enzymes involved in their metabolism (112).

Uncoupling leads to inefficient production of ATP. Glucose-stimulated insulin secretion (GSIS) from pancreatic β-cells depends on the generation of ATP from glucose metabolism. Thus, increased uncoupling in β-cells would lead to diminished insulin secretion in response to glucose. Indeed, Chan et al. found that inducing UCP-2 over-expression in isolated Zucker lean (+/+) rat islets led to a substantial reduction in ATP (136) and severe blunting of GSIS (105;136). In INS-1 clonal β-cells, oleate-induced up-regulation of UCP-2 also led to a decrease in the glucose-induced rise of the ATP:ADP ratio and insulin secretion (134). In contrast to this, Wang et al. (1999) found that over-expression of UCP-2 in isolated ZDF islets improved glucose sensitivity and insulin secretion (137). However, ZDF islets have a 15-17 fold higher fat content and decreased islet UCP-2 mRNA compared with Zucker

lean islets (135). This apparent beneficial effect of UCP-2 in islets may be due to increased fatty acid oxidation which would lower islet fat levels and the basal ATP:ADP ratio, thereby improving β-cell sensitivity and function. Recall that FFAs contribute to basal but not stimulated insulin secretion. When basal FFAs and ATP:ADP ratio are high, then the stimulatory effect of glucose is lessened (137).

Evidence is beginning to show that UCP-2 may be a factor in decreased glucose sensitivity in β-cells of diabetic patients. For example, the *db/db* mouse (a genetic model of obesity-induced type 2 diabetes) (138) and the *ob/ob* mouse (a genetic model of obesity which exhibits moderate hyperglycemia but not overt diabetes) (130) have increased pancreatic UCP-2 expression. The ZDF rat has lower islet UCP-2 expression, but is hyperinsulinemic (135). Hepatic nuclear factors 1α and 4α (HNF1α and HNF4α) are found in islets (and other tissues) and regulate the expression of many genes involved in fuel metabolism (139;140). Mutations of HNF4α and HNF1α have been shown to be the underlying defects in the development of two forms of diabetes known as maturity onset diabetes of the young, subtypes 1 and 3 (MODY1 and MODY3) (139;141). Although there is no reduction in β-cell mass, these forms of diabetes are characterized by a substantial loss of GSIS with ~30% of patients requiring insulin therapy (139). Interestingly, increases in the expression of either HNF results in increased islet UCP-2 expression with consequent reductions in ATP, membrane depolarization and GSIS (139;140). Taken together, these findings are all consistent with a negative effect of UCP-2 on insulin secretion.

Perhaps the most convincing data on UCP-2's role in regulating GSIS come from studies involving UCP-2 knockout (-/-) mice. These UCP-2 -/- mice had approximately 3 fold

higher plasma insulin concentrations, without any change in insulin sensitivity, in both the stimulated (fed) and unstimulated (fasting) state, indicating an increased glucose responsiveness in the islets. ATP levels were also higher in UCP-2 -/- mouse islets. Glucose clearance was increased in UCP-2 -/- mice, which had lower fed state blood glucose concentrations and responded much more acutely to glucose challenge (130). Cross breeding the UCP-2 -/- mice with control UCP-2 +/+ mice allowed for generation of heterozygote (UCP-2 +/-) mice which displayed intermediate levels of UCP-2 expression and insulin secretion (130). This quantitative correlation between UCP-2 and GSIS provides strong evidence of a role for UCP-2 in the regulation of insulin secretion.

1.8 Perspective

Diabetes mellitus and obesity are serious health concerns. The physiologic and economic burden that they place on society is immense. The complex nature of their respective pathogeneses indicates that no one "miracle drug" is likely to provide a solution. Therefore, each small step we take in understanding the overall metabolic processes involved in these disorders represents a valuable contribution to the overall goal.

Identifying UCP-2 as a regulator of insulin secretion could represent an important therapeutic target for the treatment of obesity and type 2 diabetes, which represent two of the biggest (and most rapidly escalating) health concerns facing society today. Oxidative phosphorylation is thought to account for 98% of the ATP produced in the β-cell (61). Previous studies to elucidate the role of ATP in GSIS have disrupted mitochondrial metabolism to show this dependency on mitochondrial ATP. Methods for doing this have

ranged from treatment of cells with chemical uncouplers such as the protonophore carbonylcyanide *m*-chlorophenylhydrazone (CCCP) (142) to disruption of mitochondrial DNA (using ethidium bromide) which encodes for many of the proteins vital to oxidative phosphorylation (143). UCP-2 is thought to affect oxidative phosphorylation by dissipation of the proton gradient (144), similar to that seen with CCCP. However, UCP-2 is naturally expressed in normal β-cells (106;136), making it a better tool to manipulate ATP levels without disrupting other cellular functions. Initial work has shown that increasing UCP-2 expression negatively affects insulin secretion (105;145). Furthermore, studies using UCP-2 knock-out mice have shown that its expression may even have a quantitative correlation to this regulation in insulin secretion (wildtype (+/+) < heterozygous (+/-) < homozygous (-/-) (130). The apparent inducibility of UCP-2 in some models of obesity and type 2 diabetes (130) also makes it a desirable candidate for drug or gene therapy. PPAR-γ agonists such as troglitazone have already been shown to be able to increase UCP-2 expression in pancreatic islets (135) and as more becomes known about the protein, other manipulative agents will likely be developed.

In order to better understand the effects of UCP-2 on insulin secretion, the exact mechanism through which it mediates this regulation must be determined. It has been shown that ATP is reduced when UCP-2 expression is increased (136;137). The next step is to identify which ATP-dependent step(s) are affected by this reduction. The focus of this study is to determine if and how UCP-2 affects the cAMP signaling pathway in glucose-stimulated insulin secretion.

Hypothesis: UCP-2 over-expression reduces the level of cAMP and/or diminishes its ability to potentiate glucose-stimulated insulin secretion.

Objectives:

1. Measure ATP and GSIS in pUCP-2 transfected βTC6-f7 cells.

2. Measure cAMP production in response to glucose and glucose + forskolin in βTC6-f7 cells and intact islets.

3. Measure insulin secretion in response to glucose and glucose + forskolin in βTC6-f7 cells and intact islets.

4. Correlate insulin secretion with cAMP production.

5. Determine efficiency of gene transfer for transient transfection and infection methods.

2. Materials and Methods

2.1 Experimental Design

To study the insulin secretion pathway we employed both a clonal cell line model (βTC6-f7, derived from a transgenic mouse insulinoma) and intact islets isolated from Zucker lean (+/+) rats. Islets isolated from separate rats were used for separate experiments throughout the study (i.e. islets isolated from multiple rats were not pooled prior to experimentation). Induction of UCP-2 over-expression in βTC6-f7 cells was achieved through transient transfection with a plasmid vector containing a copy of the human *ucp-2* cDNA sequence. In intact islets, the spacial arrangement and organization required an infection with an adenovirus construct, which also contained a copy of the human *ucp-2* cDNA sequence. Levels of cAMP and insulin secretion were measured in response to glucose ± forskolin (an adenylyl cyclase activator) in both control and UCP-2 over-expressing cells/islets. To determine the effects of UCP-2 over-expression on the cAMP signaling pathway of GSIS, we looked for changes in cAMP levels and if these changes were reflected by similar changes in GSIS.

2.2 Methodological Rationale

Much of the *in vitro* work focusing on insulin secretion has historically been done using isolated islets from rat and mouse models. These methods are typically quite labor intensive and expensive, with sample sizes often being kept to a minimum for ethical and financial reasons. Over the past decade or so, there has been tremendous growth in the

development and use of insulin secreting clonal cell lines. While cell transformation can often be accompanied by changes in physiologic function, there are a number of insulinoma derived cell lines that have been characterized and validated as appropriate models of insulin secretion (e.g. RIN, HIT, INS-1). A few of the important parameters to be considered when using a insulin secreting cell line are β-cell purity (the percentage of β-cells in relation to other islet cell types which may "contaminate" the cell line), sensitivity to glucose, response to classical and physiological stimuli (e.g. drugs, hormones, nutrients) and, perhaps most importantly, passage number and how it relates to the aforementioned parameters (146). βTC cells originate from transgenic mice which develop heritable β-cell tumors from which a cell line can be derived. Several βTC cell lines exist (βTC1-βTC7) and the original βTC6 line used in this study was engineered by Efrat et al. (1988) (147). Morphological and functional characterization of βTC6 cells shows that they are primarily composed of β-cells and have a left-shifted glucose concentration-response curve (i.e. the cells secrete more insulin at a given glucose concentration) as compared to isolated islets. This sensitivity is retained through passage numbers of 80 or higher. The response to epinephrine and pertussis toxin stimulation is normal, as is G-protein expression and function (148).

Because of the relatively small total islet mass and the complex procedure involved in their isolation, the use of a clonal β-cell line is particularly advantageous for studies that look at second messenger systems and intracellular signaling pathways. Second messengers can be difficult to monitor given their relatively low levels within the cell. Cell culture allows the generation of larger amounts of second messengers and performance of multiple replicates of experimental conditions in a shorter period of time. Using a transient

transfection method to induce the over-expression of UCP-2 may also be more advantageous than the adenovirus infection method used previously in isolated rat islets (105). For example, generating additional plasmid requires only transformation and culture of *E. coli* bacteria (using the original plasmid) followed by the isolation and purification of the plasmid DNA. The larger the transformant culture, the more plasmid you can obtain. The adenovirus is attenuated such that it can not replicate (149) and requires insertion of the UCP-2 gene into a new supply of viral vectors to replenish the stock. These virus vectors must be purchased commercially, adding a significant financial drawback to this method as well. The transfection technique itself is also more favorable to use in that it complexes the plasmid DNA with a lipophilic compound (Lipofectamine^{2000} in our case), which can then passively diffuse across the plasma membrane. Virally-mediated gene transfer can be accompanied by cytotoxicity if conditions are not optimized (150). On the other hand, adenovirus infection methods usually have a greater efficiency of gene transfer and are better suited to islets, which require the virus to penetrate into the β-cell rich core (151). Plasmid transfection is a more passive procedure, which is maximally effective for well dispersed monolayers characteristic of cell cultures (150). All variables considered, studies using clonal cell lines should always be verified, to some extent, in intact native islets.

2.3 Cell Culture

2.3.1 Culture Conditions

Cultures of βTC6-f7 cells were obtained from Dr. Michael Wheeler (Departments of Medicine and Physiology, University of Toronto, Toronto, ON) and were also

purchased from American Type Culture Collection (Manassas, VA). All cell culture work was done in a Forma Scientific Laminar Flow Workstation with all non-sterile materials being autoclaved prior to use. Cells were grown in RPMI-1640 media, pH 7.4, (Life Technologies, Burlington, ON) containing 0.2% sodium bicarbonate, 1% L-glutamine (Sigma, Oakville, ON), 1% penicillin (10 000 units/mL)/streptomycin (10 mg/mL)/amphotericin (25 μg/mL) (Sigma)(from here referred to as RPMI-complete media) and 10% fetal bovine serum (FBS) (Sigma, Oakville ON) at 37° C, 5% CO_2/95% air in a NAPCO CO_2 incubator, model 6300 (NAPCO Scientific Company, Tualatin, OR), with the media replaced every 48 h. Cells were passaged at approximately 75% confluence by trypsin-EDTA (Life Technologies) detachment after removing the media and rinsing once with 0.1 M phosphate buffered saline (PBS; 0.1 M Na_2HPO_4, 0.9% NaCl), pH 7.4. Each plate required approximately 1 mL of trypsin-EDTA, after which 5 mL of RPMI-complete media (10% FBS) was added to the lifted cells. The resulting suspension was diluted with RPMI-complete media (10% FBS) onto new plates. Media was replaced the following day or once cells had adhered.

2.3.2 Cell Storage

βTC6-f7 cells were frozen in freezing media containing 10% sterile dimethyl sulfoxide, 40% FBS and 50% RPMI-complete media (10% FBS). After detachment, cells were aspirated and transferred to a sterile 50 mL conical tube and centrifuged for 4 min at 2400 rpm and 4° C (Beckman J-6M/E centrifuge, TY JS 4.2 rotor; Beckman Instruments Inc., Palo Alto, CA). The supernatant was discarded and the pellet

resuspended in half the total volume of RPMI-complete media (10% FBS). On ice, half the total volume of freezing media was added dropwise while rotating the tube. The resulting suspension was aliquotted into pre-chilled, sterile 1.8 mL Nunc vials on ice. The aliquots were first placed in a -20° C freezer for 1 h, followed by storage at -80° C.

βTC6-f7 cells were thawed by warming vials in a 37° C water bath until partially thawed, then transferring to a flask containing 5 mL of warm (37° C) RPMI-complete media (10% FBS). Media were changed the following day or once cells had adhered.

2.4 Isolation of Rat Islets

All protocols involving animals were approved by the University of Prince Edward Island Animal Care Committee (UPEI-ACC) and conform to guidelines set by the Canadian Council on Animal Care (CCAC) (152). Islets were isolated from adult (> 6 weeks) male and female lean Zucker rats (Charles River Laboratories, Boston, MA and AVC born) by collagenase digestion of the acinar tissue. Rats were anaesthetized with sodium pentobarbital (65 mg/kg) and the abdominal cavity exposed. The main bile duct was ligated at both the distal (by the pylorus) and proximal (before the bifurcation leading to the liver) ends. The rat was then euthanized by detaching the diaphragm, inducing cardio-respiratory arrest. A small incision was made in the bile duct just distal to the proximal ligation point and a polyethylene catheter (PE 50) was carefully inserted into the incision. The pancreas was then fully infused with an ice-cold collagenase (type XI) solution (0.32 mg/mL) (Sigma), dissolved in filter sterilized Hanks' Balanced Salt Solution (HBSS) (Life Technologies) containing 10 mM N-{2-Hydroxyethyl}piperazine-

N-{2-ethanesulfonic acid} (HEPES), 1% L-glutamine, 0.035% sodium bicarbonate (from here referred to as HBSS*) and 0.2% bovine serum albumin (BSA). Once infusion was complete, the pancreas was removed and minced in a siliconized sterile petri dish. The homogenate was then transferred to a siliconized, sterile 50 mL Erlenmeyer flask, the volume brought up to 25 mL with collagenase solution and incubated in a 37° C shaking water bath (~200 rpm) for 20 min. After initial digestion, the homogenate was transferred to a sterile 50 mL conical tube, the volume brought up to 35 mL with HBSS* (0.2% BSA) and centrifuged for 5 min at 1500 rpm and 4° C (Beckman J-6M/E centrifuge, TY JS 4.2 rotor). The supernatant was removed and the pellet was resuspended in 25 mL of collagenase solution, then placed in a 37° C shaker water bath (~200 rpm) for 10 min. The new homogenate was centrifuged again as described above and the pellet suspended in 20-30 mL of HBSS* (0.2% BSA). Undigested tissue was removed by filtration through an 800μm Nitex screen and the filtrate centrifuged again as described previously. The supernatant was discarded and the pellet suspended in 10 mL of a 27% dextran solution (Industrial grade, Sigma) in HBSS* (no BSA). The digested tissue was separated using a dextran step-density gradient by carefully layering 6 mL of 27% dextran below the suspension, then 10 mL of 23% dextran above the suspension and finally 10 mL of 14% dextran above the 23% dextran layer. The gradient was then centrifuged for 15 min at 1500 rpm and 4° C (Beckman J-6M/E centrifuge, TY JS 4.2 rotor). Islets were collected from the 23%/14% interface using a siliconized sterile glass pipette and transferred to a 50 mL conical tube. The volume was brought to 35 mL with HBSS* (0.2% BSA) and was centrifuged for 5 min at 1500 rpm and 4° C (Beckman J-

6M/E centrifuge, TY JS 4.2 rotor). After discarding the supernatant, the pellet was suspended in HBSS* (0.2% BSA) and transferred to a siliconized sterile petri dish. Islets were handpicked into sterile 24 well culture plates and cultured at 37° C, 5% CO_2/95% air in 1 mL of Dulbecco's Modified Eagle's Medium (DMEM) containing 10 mM HEPES, 1% penicillin (10 000 units/mL)/streptomycin (10 mg/mL)/amphotericin (25 μg/mL), 10% calf serum and 8.3 mM glucose (from here referred to as DMEM).

2.5 Isolation of UCP-2 and EGFP Plasmids

2.5.1 Transformation of *E. coli* Bacteria

Plasmids (pcDNA 3.1; Invitrogen, Carlsbad, CA) containing the human uncoupling protein-2 (UCP-2) or enhanced green fluorescent protein (EGFP) cDNA sequences were originally obtained from Dr. Mike Wheeler (Departments of Medicine and Physiology, University of Toronto, Toronto, ON). Generation of additional plasmids was done by transformation of *E. coli* JM 109 competent cells (Promega, Madison WI). The JM 109 cells (10^8 colony forming units/μL) were thawed at room temperature and 100 μL of cells/transformation (one transformation for each plasmid) transferred to a pre-chilled sterile 50 mL conical tube on ice. Plasmid DNA (25 ng) was added to the JM 109 cells and returned to the ice for 10 min. Cells were heat-shocked by immersing them in a stagnant 42° C water bath for 45 s. Tubes were returned to ice for 2 min after which 900 μL of cold, sterile SOC medium (20 mg/mL tryptone, 5 mg/mL yeast extract, 10 mM NaCl, 2.5 mM KCl, 20 mM MgCl and 20 mM glucose), pH 7.0, was added. Cells were then incubated in a 37° C shaking water bath (225 rpm) for 1 h. The transformed cultures

were plated on 2YT medium (Life Technologies) agar plates containing 100 μg/mL kanamycin (Life Technologies) and grown overnight at 37° C. A few colonies were randomly chosen to innoculate starter cultures in 5 mL of 2YT medium broth containing 100 μg/mL kanamycin. These starter cultures were incubated for 8 h in a 37° C shaking water bath (300 rpm), then transferred to 200 mL of 2YT broth containing 100 μg/mL kanamycin. These new cultures were incubated overnight in a 37° C shaking water bath (300 rpm). Cells were collected by centrifugation of the final broth cultures for 5 min at 10 000 rpm and 4° C (Beckman J2-21M/E centrifuge, JA-14 rotor) and stored at -20° C until plasmid purification was undertaken.

2.5.2 Purification of Plasmid DNA

Purification of plasmids (pUCP-2 and pEGFP) was done using a CONCERT™ High Purity Plasmid Maxiprep System (Life Technologies). Purified DNA was digested using an EcoRI restriction endonuclease kit (Promega, Madison, WI). In a 20 μL volume, 2 μL of Buffer H, 2 μL of BSA, 2 μL of EcoRI, 4 μL of DNA and 10 μL of deionized water were combined in a 0.5 mL microcentrifuge tube. Tubes were incubated at 37 ° C for 1 h and the digests subjected to agarose (1%) gel electrophoresis. Qualitative comparison of the purified plasmid digests with a digest of the original plasmid confirmed its identity. Assessment of successful transformation and purification by visualization of the protein product under fluorescence microscopy was also done for the EGFP plasmid.

2.6 Induction of UCP-2 Over-Expression

2.6.1 Transient Transfection of βTC6-f7 Cells

βTC6-f7 cells were plated in sterile 24 well plates at a density of 250 000 cells/well and cultured overnight at 37° C, 5% CO_2/95% air. For EGFP transfections only, cells were grown on 13 mm tissue culture coverslips within the well to allow for microscopic visualization of the EGFP. The following day, transfection reagents were prepared. In a sterile 15 mL conical tube, 0.375 μg of plasmid DNA/transfection was added to 25 μL of serum free OptiMEM I (Life Technologies)/transfection. In a separate tube, lipofectamine^{2000} reagent (4:1, lipofectamine^{2000} : plasmid (v/v)) was added to 25 μL of serum free OptiMEM I/transfection. The two solutions were mixed and incubated for 20 min at room temperature. Control reagents consisted of only lipofectamine^{2000} and serum free OptiMEM, keeping the concentration of lipofectamine^{2000} consistent with that used for the plasmid transfection. Meanwhile, media was removed from the wells and the plated cells rinsed with 0.5 mL of serum free OptiMEM I/well, with this wash fluid being removed just prior to transfection. Following a 20 minute incubation, 0.2 mL of serum free OptiMEM I/transfection was added to the mixture. From the resulting mixture, 0.25 mL was added to each well and cells were incubated at 37° C for 6 h. After 6 h, 0.3 mL/well of RPMI-complete medium (20% FBS) was added and cells were cultured overnight at 37° C. The next day, all media were removed and 1 mL/well of fresh RPMI-complete medium (10% FBS) was added and cells cultured for a further 24 h at 37° C before experiments were conducted. Control wells were treated identically with either transfection reagents containing the EGFP plasmid or no plasmid at all. Transfection of

cells in 6 well plates was achieved using the aforementioned protocol with minor modifications. Cells were plated at a density of 1 000 000 cells/well, with 1.5 μg of DNA/well and 0.1 mL of serum free OptiMEM I/transfection incubated for 20 min at room temperature, followed by the addition of 0.8 mL of serum free OptiMEM I /transfection. Cells were rinsed with 2 mL of serum free OptiMEM I and 1 mL of the transfection mixture was added to each well. After 6 h, 1.2 mL/well of RPMI-complete medium (20% FBS) was added and cells were cultured for 24 h as before. The next day, media were removed and replaced with 4 mL of fresh RPMI-compete media (10% FBS).

2.6.2 Adenovirus Infection of Isolated Islets and βTC6-f7 Cells

Adenovirus constructs containing the human UCP-2 or retinoic acid receptor cDNA sequences (AdUCP-2 and AdRXR respectively), as well as a construct containing both the human UCP-2 and the EGFP cDNA sequences (AdUCP-2/EGFP) were provided by Dr. Michael Wheeler (Departments of Medicine and Physiology, University of Toronto, Toronto, ON). was also provided. The AdUCP-2 was diluted in DMEM or RPMI-complete (10% FBS) such that 0.1 mL of construct gave the multiplicity of infection (MOI) = 10 000 for 200 islets (see appendix B, b.1). The AdRXR construct was diluted such that 0.1 mL gave an MOI of 100 for 200 islets. Isolated islets from lean Zucker rats were handpicked into 24 well plates at 200 islets/well and cultured in 0.8 mL of DMEM at 37° C, 5% CO_2/95% air for 2 h. AdRXR (0.1 mL/well) and AdUCP-2 (0.1 mL/well) were then added and incubated for a further 1 h. Ponasterone A (10 μM/well) (Invitrogen, Carlsbad, CA) and 1 mL/well DMEM were then added and islets were

cultured at 37° C for 48 h. Control islets were uninfected and simply cultured for 48 h in DMEM. βTC6-f7 cells were plated in 24 well plates at a density of 250 000 cells/well as previously described and allowed to adhere overnight. Media was replaced with 0.5 mL of RPMI-complete (10% FBS), 0.25 mL of AdRXR (MOI ~100) and 0.25 mL of AdUCP-2 (MOI ~ 10 000) and incubated for 1 h at 37° C. Ponasterone A (25 μM/well) and 1 mL RPMI-complete (10% FBS) were then added and cells were cultured for 48 h at 37° C. Control cells were uninfected and simply cultured in RPMI-complete media (10% FBS). Previous experiments have shown that infection with AdRXR or AdEGFP alone have no effect on insulin secretion (136), therefore, control islets and cells received no treatment and were simply cultured in DMEM or RPMI-complete media (10% FBS), respectively, for 48 h.

2.7 Assessment of UCP-2 Induction

2.7.1 RNA Isolation

βTC6-f7 cells were plated in 6 well plates and transfected as previously described. After 48 h, media was removed and 1 mL/well of Trizol Reagent (Life Technologies) was added. The Trizol was pipetted back and forth several times to ensure homogenization of the cells and the homogenate was transferred to a diethyl pyrocarbonate (DEPC)-treated 1.5 mL microcentrifuge tube. After incubating for 5 min at room temperature, 0.2 mL of choloroform (Molecular Biology Grade, Sigma) was added to each tube and the tube inverted 20 times for adequate mixing. After 3 min at room temperature, the tubes were centrifuged for 15 min at 12 000 rpm and 4 °C (Beckman Microfuge-12). The aqueous

phase (upper) was collected in a new DEPC-treated 1.5 mL microcentrifuge tube and RNA precipitated with 0.5 mL of isopropyl alcohol (Molecular Biology Grade, Sigma) for 10 min at room temperature. RNA was collected by centrifugation for 10 min at 12 000 rpm and 4 °C. The supernatant was removed and the pellet washed with 1.0 mL of 75% ethanol in DEPC-treated water (0.1% DEPC in deionized water). At this stage, the pellet was either stored overnight at 4 °C or centrifuged for 5 min at 9 000 rpm and 4 °C. The supernatant was again removed and the pellet allowed to air dry in a fume hood. Once dry, the RNA was dissolved in 10-30 µL of DEPC treated water and incubated for 10 min at 55 °C. Isolated RNA was frozen at -80 °C until needed.

2.7.2 Reverse Transcriptase-Polymerase Chain Reaction (RT-PCR)

RNA samples were diluted 1:1000 in DEPC-treated water and concentrations of RNA were determined by measuring absorbance at 260 nM (A_{260}) using a GeneQuant spectrophotometer (Amersham Pharmacia Biotech). The A_{260} was multiplied by a conversion factor of 37 (for single stranded polynucleotides) to obtain a concentration in µg/µL. From these calculations, 2.5 µg of total RNA were loaded on a 1% agarose gel (0.005% ethidium bromide) made with DEPC-treated water. The gel apparatus was soaked overnight in 0.5 M sodium hydroxide and rinsed clean with DEPC-treated water before using. The chamber was filled with 0.5 X Tris-Borate-EDTA (TBE) buffer made up in DEPC treated water and the gel run at 100 V for approximately 30 min. Bands were visualized under ultraviolet light using an Ultra-LUM Electronic DualLight Transilluminator (Ultra-LUM Inc., Paramount, CA) to confirm accuracy of the calculated

RNA concentration and assure purity of RNA isolated. Reverse transcriptase polymerase chain reaction (RT-PCR) amplification of UCP-2 mRNA was done using an RNA PCR kit (Applied Biosystems Roche, Branchburg, NJ) on 2 μg of total RNA or a DEPC-treated water control under the following conditions:

Step 1. room temperature for 10 min

Step 2. 42 °C for 15 min

Step 3. 99 °C for 5 min

Step 4. 5 °C for 5 min

The following primer sequences were obtained from Sigma-Genosys (Woodlands, TX) and used to amplify 2.5 μL, 5 μL, 7.5 μL and 15 μL of the RT product.

5' CTCAGAAAGGTGCCTCCCGA 3' (forward) and
5' ATCGCCTCCCCTGTTGATGTG 3' (reverse)

These primers were designed by comparing the complete DNA sequences for the mouse *ucp-2* and *ucp-3* cDNA sequences and determining an area of significant dissimilarity between the two. They are anticipated to amplify a 240 bp fragment of DNA specific to UCP-2. PCR conditions were:

Step 1.	94 °C for 5 min
Step 2.	94 °C for 1 min (melting)
Step 3.	60 °C for 1 min (annealing)
Step 4.	72 °C for 1.5 min (extension)
Step 5.	Return to Step 2. for 35 cycles
Step 6.	72 °C for 10 min

The PCR product was separated by 1% agarose gel electrophoresis at 100 V and DNA bands visualized under ultraviolet light as before.

2.7.3 Protein Analysis

2.7.3.1 Sodium Dodecyl Sulphate-Polyacrylamide Gel Electrophoresis (SDS-PAGE)

βTC6-f7 cells transfected with pUCP-2, lipofectamine^{2000}-treated control βTC6-f7, AdUCP-2 infected islets and uninfected control islets were collected from wells and centrifuged for 1 min at 13 000 rpm and room temperature (Micromax benchtop microcentrifuge, 851 RCF rotor; International Equipment Company, Needham Heights, MA). Pellets were washed twice with 0.1 M PBS, pH 7.4, then resuspended in 10-20 μL of a Tris-HCl buffer, pH 7.4, containing 1 % Triton X, 1 mM EDTA, 250 mM sucrose, 4 μg/mL aprotinin and 5 μg/mL bestatin and stored at -20 °C. The suspension was subjected to repeated freeze-thawing (> 4 times) and sonication with 10 s pulses at 5 watts (Sonic Dismembrator; Fisher Scientific, Nepean, ON). Total protein concentrations were determined by the Lowry method (153). Up to 50 μg of total protein was loaded onto 10% sodium dodecyl sulfate polyacrylamide minigels and proteins were separated by electrophoresis at 150 V for 1 h using a Mini-PROTEAN 3 Cell and Power Pac 200 system (Bio-Rad, Hercules, CA). Separated proteins were then transferred to nitrocellulose membrane at 40 V for 1 h using a Mini Trans-Blot Electrophoretic Transfer Cell (Bio-Rad) and stored at -20 °C for subsequent immunoblotting.

2.7.3.2 Immunoblotting

Three separate polyclonal anti-UCP-2 antibodies (#907, #908 and #909 rabbit serum samples) were provided as a gift from Dr. Timothy Keiffer (Department of Medicine, University of Alberta) and Dr. Joel Habener (Howard Hughes Medical Institute, Harvard University). All three were directed against a mid-sequence epitope (KQFYTKGSEHASIG) found in the human, mouse and rat UCP-2 amino acid sequences. Generation of the antibodies was done by immunizing New Zealand white rabbits with the peptide fragment conjugated to maleimide activated keyhole limpet hemocyanin. Membranes were blocked for 1 h using a 5% skim milk solution in 0.1 M PBS, pH 7.4 (blocking buffer). The primary anti-UCP-2 antibody was diluted 1:1000 in blocking buffer containing 0.1% polyoxyethylenesorbitan monolaureate (Tween 20) (Sigma) and exposed to the membrane overnight at 4 °C with gentle rocking. The next day, membranes were washed twice with 0.1 M PBS, pH 7.4, containing 0.1% Tween 20 for 15 minutes, then exposed to a 1:15 000 dilution of goat anti-rabbit IgG conjugated with horse radish peroxidase (Gibco BRL) for 1 h at room temperature. Membranes were washed again as before and exposed to enhanced chemiluminescence (ECL) reagents (Amersham Pharmacia Biotech) for 1 min and antibody binding detected using Hyperfilm™ ECL (Amersham Pharmacia Biotech).

2.8 cAMP Formation

2.8.1 βTC6-f7 Cells

Krebs Ringer Buffer containing 0.6 % NaCl, 10 mM HEPES, 0.2% sodium bicarbonate and 0.1% BSA (KRB-HEPES) was prepared and incubated for 30 min at 37° C, 5% CO_2/95% air prior to use. Lipofectamine^{2000}-treated control and pUCP-2 transfected cells were washed with 1 mL/well KRB-HEPES and incubated 30 min. This was repeated once, followed by two 1 mL/well washings and one 2 mL/well washing with no incubation. Cells were then exposed to 2.8 mM and 11 mM glucose in KRB-HEPES, in the presence of 0 μM, 0.1 μM, 1 μM, or 10 μM forskolin (Sigma) in DMSO for 15 min at 37° C (*n.b.* final concentration of DMSO in forskolin treated wells/tubes was 0.25%, v/v in all experiments involving forskolin). The liquid was then removed from the wells and 0.5 mL/well of acid ethanol (70% ethanol, 0.01 % HCl, in water) was added. Cell lysates were frozen at -20° C until assayed.

2.8.2 Isolated Rat Islets

Uninfected control and AdUCP-2 infected islets from separate rats were handpicked into 1.5 mL microcentrifuge tubes at 8 islets/tube. Islets were exposed to 2.8 mM and 11 mM glucose in KRB-HEPES in the presence of 0, 0.1 μM, 1 μM, or 10 μM forskolin in DMSO for 15 min at 37° C, 5% CO_2/95% air. Tubes were then centrifuged for 5 min at 2000 rpm and 20° C (Beckman J-6M/E centrifuge, TY JS 4.2 rotor). Supernatants were removed and 0.5 mL of acid ethanol was added to each pellet. Lysates were frozen at -20° C until assayed.

2.8.3 Quantification of cAMP

Concentrations of total cellular cAMP were determined by radioimmunoassay (RIA) using a standardized kit (Biomedical Technologies Inc., Stoughton, MA), acetylation protocol. A standard curve was generated ranging from 0.05 pM to 5 pM cAMP and dilution of samples (if necessary) was done using a Beckman Accu-Prep™ 222A automatic dispensing system (Beckman Instruments Inc., Palo Alto, CA).

2.9 Insulin Secretion

2.9.1 βTC6-f7 Cells

Lipofectamine^{2000}-treated control and pUCP-2 transfected cells were washed with KRB-HEPES as previously described and exposed to 2.8 mM, 11 mM and 22 mM glucose in KRB-HEPES in the presence of 0 μM, 0.1 μM, 1 μM, or 10 μM forskolin in DMSO for 2 h at 37° C, 5% CO_2/95% air. The media was removed from the wells and placed in clean 1.5 mL microcentrifuge tubes which were then centrifuged for 5 min at 2000 rpm and 20° C (Beckman J-6M/E centrifuge, TY JS 4.2 rotor). Supernatants were collected and labeled as "Releases". To each well, 1 mL of 3% acetic acid was added and wells labeled as "Totals". Releases and Totals were frozen at -20° C until assayed.

2.9.2 Isolated Rat Islets

Uninfected control and AdUCP-2 infected islets were handpicked into 1.5 mL microcentrifuge tubes (3 islets/well) and exposed to 2.8 mM and 11 mM glucose in KRB-HEPES in the presence of 0 μM, 0.1 μM, 1 μM, or 10 μM forskolin in DMSO for 2 h at

37° C, 5% CO_2/95% air. Tubes were then centrifuged for 5 min at 2000 rpm and 20° C (Beckman J-6M/E centrifuge, TY JS 4.2 rotor). Supernatants were collected and labeled as "Releases". To each pellet, 1 mL of 3% acetic acid was added and tubes labeled as "Totals". Releases and Totals were frozen at -20° C until assayed.

2.9.3 Quantification of Insulin

2.9.3.1 Iodination

Concentrations of insulin were determined by RIA using iodine-125 isotope (^{125}I) as the radioactive tracer. To prepare the tracer, pure porcine insulin (Bios Pacific Inc., Emeryville, CA) was dissolved in 0.01 M HCl and diluted in 0.2 M phosphate buffer (0.2 M Na_2HPO_4), pH 7.4, to a concentration of 5 μg/10 μL. Ten μL of this insulin solution was added to ^{125}I (1 mCi) (Amersham Pharmacia Biotech, Baie d'Urfe, QC). To the insulin/tracer solution, 25 μL of chloramine T (4 mg/mL in 0.2 M phosphate buffer) (Fisher Scientific, Nepean, ON) was added and gently mixed. After exactly 10 s, 0.1 mL of sodium metabisulfite solution (2.4 mg/mL in 0.2 M phosphate buffer) was added and allowed to sit for 45 s. Fifty μL of sodium iodide solution (10 mg/mL in 0.2 M phosphate buffer) was then added. This new mixture was then added to 10 mg of microfine silica particulate (QUSO-G32) (Philadelphia Quartz Company, Philadelphia, PA), rinsing the tube with 1.8 mL of 0.04 M phosphate buffer (0.04 M Na_2HPO_4), pH 7.4, to ensure all tracer had been added. The new solution was vortexed and 10 μL of the slurry was placed in a 12 x 75 mm borosilicate culture tube and labeled as "Total Count" (TC). The remainder of the mixture was centrifuged for 5 min at 13 000 rpm and room

temperature (Micromax benchtop microcentrifuge, 851 RCF rotor; International Equipment Company, Needham Heights, MA). The supernatant was removed and the pellet resuspended in 2 mL of deionized water and centrifuged as before. Again the supernatant was removed and the pellet resuspended in 3 mL of acid ethanol and centrifuged as before. The final supernatant was removed and placed in a secure vial, to which 2 mL of acid ethanol and 1.5 mL of deionized water were also added. The pellet was also retained for future calculations (see Appendix B, b.2).

2.9.3.2 Insulin RIA

RIA buffer was prepared as 5% (v/v) charcoal extracted equine serum (Appendix B, b.3) in 0.04 M phosphate buffer (0.04 M Na_2HPO_4), pH 7.4. Insulin standards were prepared by diluting the stock rat insulin standard solution (4800 pM) (Novo, Copenhagen, Denmark) to concentrations ranging from 4800 pM to 150 pM in RIA buffer, with zero (buffer only) and non-specific binding (no insulin antibody) tubes included. Samples were diluted accordingly in RIA buffer to fall within this standard range. All dilutions were done in borosilicate culture tubes using a Beckman Accu-Prep 222A automatic dispensing system to make a total volume of 0.8 mL. Insulin antiserum was raised in guinea pigs as described by Makulu and Wright (1971) (154), lyophilized, reconstituted to its original volume in RIA buffer, then aliquotted and frozen at -20 °C. The reconstituted antiserum was then diluted 1:4000 to give the working antibody solution. To all tubes, excluding total counts (TC) and non-specific binding (NSB) tubes, 0.1 mL of working antibody solution was added (giving a final dilution of 1:40 000 from

the original stock serum). Tubes were vortexed and incubated overnight at 4 °C. The original iodinated tracer solution was diluted with RIA buffer such that 0.1 mL of this "working tracer solution" contained 10 000 CPM (Appendix B, b.2). Working tracer solution (0.1 mL) was added to all tubes, which were covered with aluminum foil, vortexed and incubated overnight at 4 °C. All together, TC tubes contained only 0.1 mL of working tracer solution, NSB tubes contained 0.9 mL RIA buffer + working tracer solution and standards/samples contained 0.8 mL of diluted sample + working tracer solution + working antibody solution. The following day, 0.25 mL of a dextran coated charcoal slurry (Appendix B, b.4) was added to each tube, vortexed and centrifuged for 15 min at 3000 rpm and 4 °C (Beckman J-6M/E centrifuge, TY JS 4.2 rotor). Supernatants were discarded and the tubes inverted for 30 min to allow full decantation. Activity of the pellets was measured as CPM using a Packard RIAStar gamma counter (Packard Instrument Company Inc., Downers Grove, IL) and converted to pM insulin (Appendix B, b.5). Inter-assay and intra-assay variability for this protocol is 14.7% and 11.8%, respectively.

2.10 ATP Formation and Quantification

Lipofectamine^{2000}-treated control, pUCP-2 transfected and AdUCP-2 infected βTC6-f7 cells were washed with KRB-HEPES as before and exposed to 2.8 mM, 11 mM or 22 mM glucose in KRB-HEPES at 37° C, 5% CO_2/95% air for 90 min. Cells were then washed with 0.5 mL/well (24 well plate) 0.1 M PBS, pH 7.4, followed by addition of 0.2 mL/well of Somatic Cell ATP Releasing Reagent (Sigma). Each well was

homogenized by pipetting back and forth several times and allowed to stand 5 min at room temperature. Quantification of ATP was done using an ATP Bioluminescent Kit (Sigma). The ATP Assay Mix (which contains luciferase and luciferin) was diluted 1:300 in the ATP Dilution Buffer and allowed to stand 3 min at room temperature. Diluted ATP Assay Mix (0.1 mL) was then added to separate 1.5 mL microcentrifuge tubes corresponding to each well. After homogenized cells had incubated 5 min in Somatic Cell ATP Releasing Reagent, 0.1 mL of the cell homogenate was added to the corresponding microcentrifuge tube (containing diluted ATP Assay Mix) and vortexed. Luminescence was determined as counts per second using a Wallac MicroBeta TriLux beta counter (Turku, Finland), with a count time of 6 s. Standard ATP solutions were made by dissolving a stock solution of MgATP (Sigma) in Somatic Cell ATP Releasing Reagent and making serial dilutions ranging from 10^{-7} to 10^{-11} M. Protein assays were also done on the cell homogenates using a Protein Assay kit (Sigma Diagnostics, St. Louis, MO) based on the method described by Lowry et al. (1951). (153)

2.11 Statistical Analysis

Means and standard errors from the raw data of all experiments were obtained using a spreadsheet program (Corel Quattro Pro™). These means and standard errors, along with sample sizes, were then entered into a graphical analysis program (Graph Pad Prism™ 3.0). The overall response (cAMP, insulin, ATP, etc.) of the control and UCP-2 over-expressing groups to the stimuli (glucose, forskolin, etc.) was analyzed by a 2-way analysis of variance (ANOVA) to look for interaction between UCP-2 expression and the

given response. To detect specific differences between separate conditions, 1-way ANOVA with bonferroni correction factor was done for responses within each group (e.g. control or UCP-2 over-expressing over the range of forskolin concentrations) and unpaired Students' t-tests were then done between groups at a given treatment (e.g. control vs. UCP-2 over-expressing at a given forskolin/glucose concentration). A $p < 0.05$ was considered significant for all tests, except 1-way ANOVA's, which were corrected for the number of comparisons made.

3. Results

3.1 Isolation of UCP-2 and EGFP Plasmids

The plasmids encoding for the human UCP-2 and EGFP cDNA sequences (pUCP-2 and pEGFP) were originally generated by insertion of each respective sequence into a pcDNA 3.1 plasmid vector (Invitrogen, Carlsbad, CA) at the EcoRI restriction enzyme site (155). The EcoRI plasmid digest product for the purified pUCP-2 is shown in Figure 3.1. Although equal concentrations of DNA were not loaded in each lane, each isolate shows an identical banding pattern when compared to the original UCP-2 plasmid used in the transformation (Lane 4), with the lower band representing the inserted UCP-2 cDNA sequence and the upper band represents the linearized pcDNA 3.1 plasmid. EcoRI digestion of the pEGFP purifications had similar results (not shown) and fluorescence microscopy analysis showed expression of the EGFP product in βTC6-f7 cells transfected with the purified pEGFP (Figure 3.2).

3.2 Validation of Cell Line Model

3.2.1 Induction of UCP-2 Over-expression

Induction of UCP-2 mRNA expression had previously been shown in AdUCP-2 infected rat islets (136) and transfected clonal β-cells by Northern blot analysis using full length ^{32}P human UCP-2 cDNA as a probe (Dr. MB Wheeler, unpublished results). Both methods of UCP-2 over-expression showed a marked increase in UCP-2 mRNA as compared to control cells (Figure 3. 3). However, determination of actual protein is a more reliable and conclusive means by which to demonstrate levels of expression. Hence, immunoblotting

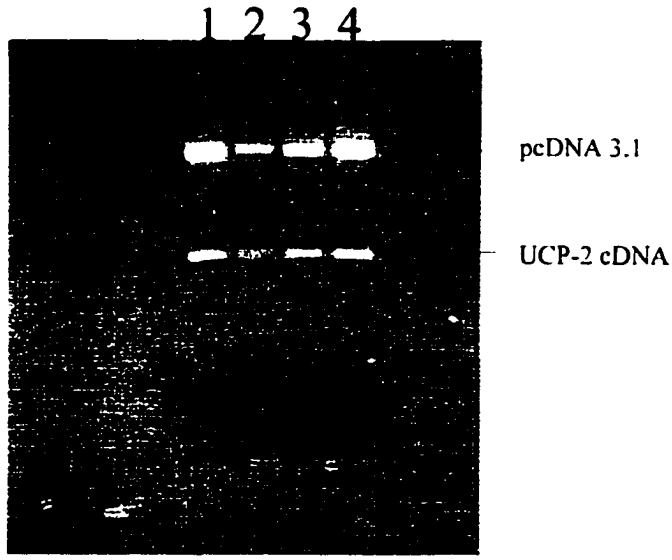

Figure 3.1. EcoRI restriction digest of purified and original UCP-2 pcDNA 3.1 plasmids. Lanes 1, 2 and 3 represent purified plasmid digests, while lane 4 represents the digest of the original pUCP-2 used for the transformation of JM 109 *E. coli* competent cells.

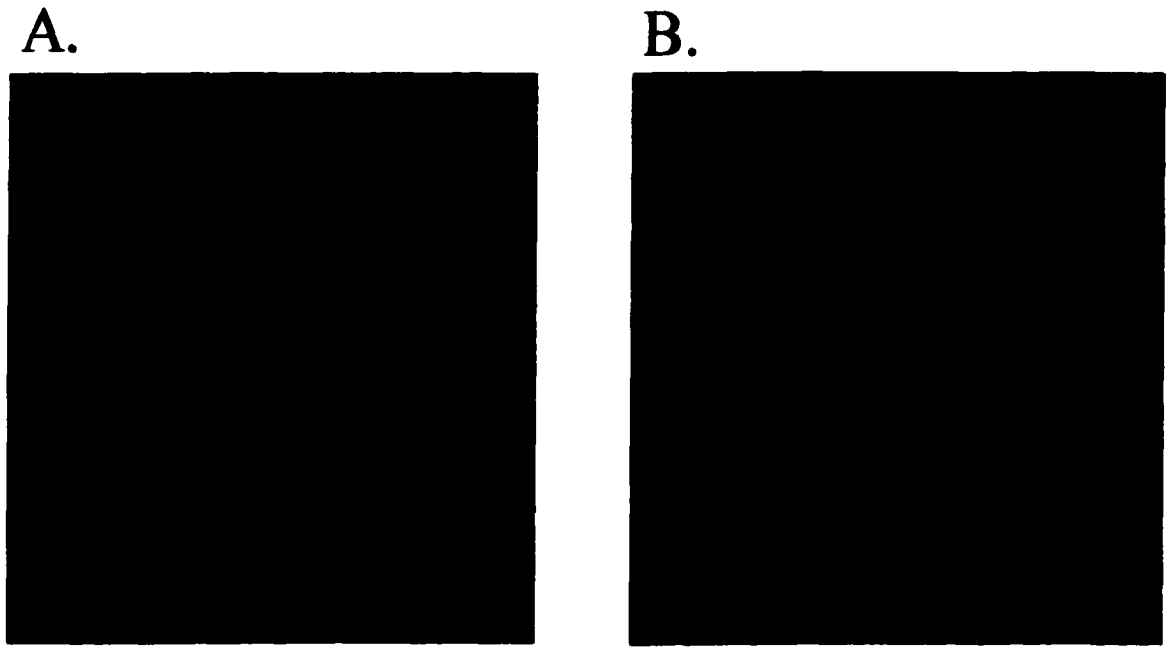

Figure 3.2. Expression of EGFP visualized under fluorescence confocal microscopy following transient transfection of pEGFP into βTC6-f7 cells.

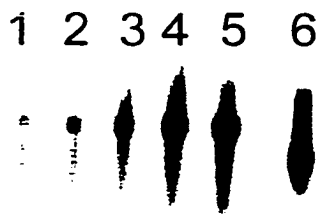

Figure 3.3. Northern blot of UCP-2 mRNA probed with full length ^{32}P labeled human UCP-2 cDNA. Lane 1 represents control RNA, while Lanes 2-5 represent islet RNA infected by AdUCP-2 with increasing amounts of Ponasterone A added (2.5 μM, 5 μM, 10 μM, 20 μM). Lane 6 represents RNA from clonal β-cells transfected with pUCP-2. (Included with permission of Dr. MB Wheeler and JW Joseph)

experiments on the UCP-2 protein were undertaken. Though much work was done to develop a reliable immunoblotting protocol, there were minimal results obtained. An immunoblot of both islets and βTC6-f7 cell homogenates is shown in Figure 3.4. While both over expressing systems (Lanes 1 and 3) showed one band at the anticipated molecular weight (~34 kDa), the actual identity of this protein could not be determined conclusively due to inconsistent results with the antibodies available to us.

Induction of EGFP expression using identical vectors was easily monitored due to the nature of the fluorescent, and hence visible, protein. Strong induction of EGFP was observed in both cells and islets, which supports (but does not confirm) that UCP-2 was also strongly induced (see Figure 3.2, page 86). To assess induction of UCP-2 mRNA, RT-PCR semi-quantitation was also done on isolated total RNA from pUCP-2 transfected and lipofectamine^{2000}-treated control βTC6-f7 cells. The isolation protocol yielded acceptable RNA (A_{260}/A_{280} = 1.5 - 1.6) and 1% agarose gel electrophoresis of the total RNA resulted in two high molecular weight bands corresponding to the 28S and 18S ribosomal subunits (Figure 3.5). PCR amplification of UCP-2 cDNA showed one band in the anticipated molecular weight range (~240-260 bp), which was absent from the DEPC-treated water sample (negative control). Sequencing of the amplified band or amplification of a positive control was not done to conclusively determine the identity of the band, but it was concluded to be that of the UCP-2 cDNA sequence. It was found that amplifying 7.5 μL of the RT product gave optimal results under our conditions. When compared to control βTC6-f7 cells, pUCP-2 transfected βTC6-f7 cells had approximately 2-2.5 fold induction of UCP-2 mRNA. A similar induction was seen in AdUCP-2 infected βTC6-f7 cells (Figure 3.6).

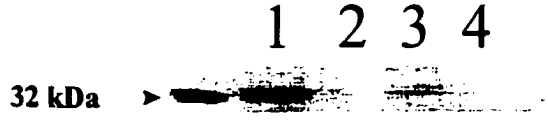

Figure 3.4. Immunoblot of islet and cell homogenates at 25 μg total protein per well. Lane 1 represents protein from AdUCP-2 infected islets; Lane 2, control islets; Lane 3, pUCP-2 transfected clonal β-cells and Lane 4, control clonal β-cells. The 32 kDa molecular weight marker is shown in the left hand lane.

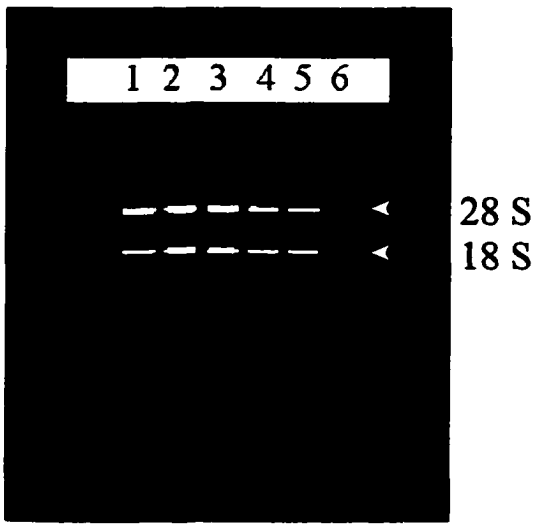

Figure 3.5. Agarose gel (1%) separation of isolated total RNA (2.5 μg per lane) from control and pUCP-2 transfected cells. Lane 1 represents control sample 9; Lane 2, control sample 8; Lane 3 pUCP-2 sample 8; Lane 4, control sample 7; Lane 5, pUCP-2 sample 7; Lane 6, 1 kb RNA standards.

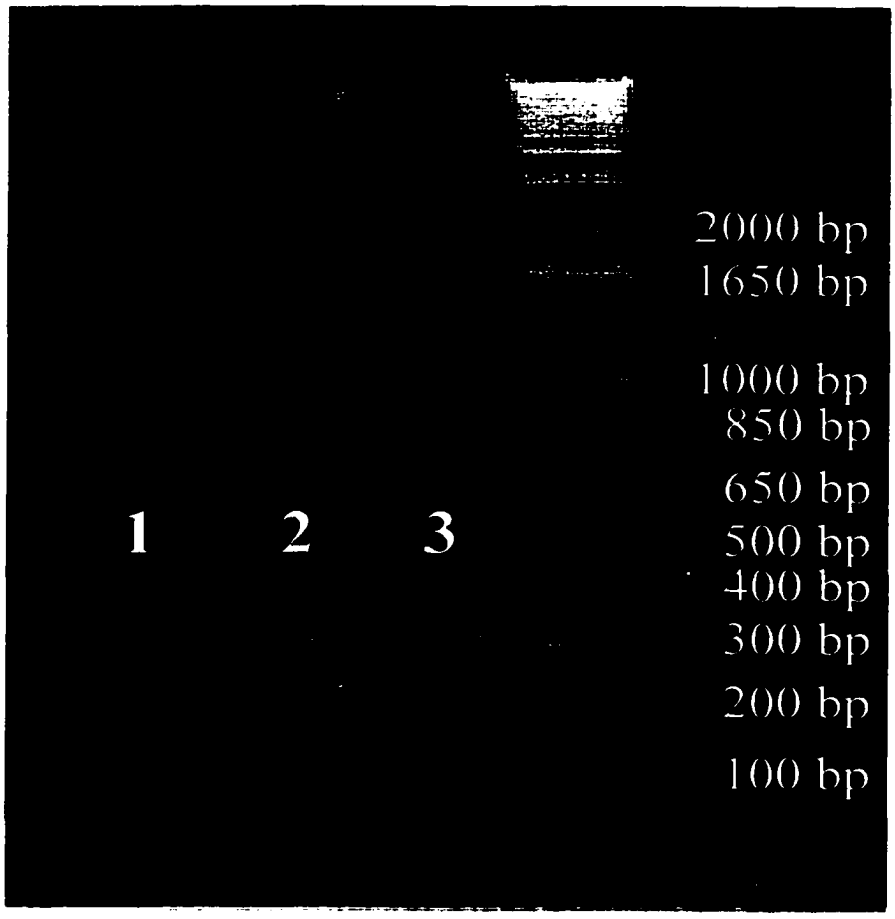

Figure 3.6. Polymerase chain reaction products following amplification of 7.5 μL of product from the reverse transcriptase reaction on RNA isolated from AdUCP-2 infected (1), pUCP-2 transfected (2) and lipofectamine^{2000}-treated control (3) βTC6-f7 cells.

3.2.2 Glucose-Stimulated Insulin Secretion from pUCP-2 Transfected βTC6-f7 Cells

Insulin secretion from pUCP-2 transfected βTC6-f7 cells had not previously been measured in our laboratory. A glucose concentration-response curve was plotted to verify that transfected cells had a decreased insulin response to glucose stimulation as had been seen previously in AdUCP-2 infected islets (105) The glucose concentration-response curve is shown in Figure 3.7. Two-way ANOVA revealed that the level UCP-2 expression had a significant effect on insulin secretion in response to glucose. Lipofectamine^{2000}-treated control βTC6-f7 cells showed a significant increase in insulin secretion at 11 mM and 22 mM glucose as compared to 2.8 mM glucose, as well as an increase at 22 mM glucose as compared to 11 mM glucose. βTC6-f7 cells transfected with pUCP-2 showed a significant increase at 22 mM glucose only as compared to both 2.8 mM and 11 mM glucose. Control cells had significantly higher insulin secretion than pUCP-2 transfected cells ($p < 0.0001$) at both 11 mM and 22 mM glucose.

3.3 cAMP Formation

The availability of cAMP is a key factor in potentiating the insulin response from the β-cell in response to glucose. Since cAMP formation is dependent on a supply of ATP, decreases in ATP (as seen in uncoupling) may also lead to decreases in cAMP formation. Therefore, cAMP levels were measured in β-cell systems which had normal or elevated UCP-2 expression. Forskolin, an adenylyl cyclase activator, was used to elevate cAMP. This would allow us to determine whether cAMP generation (due to limited substrate availability) and/or its potentiating actions were attenuated by UCP-2 over-expression.

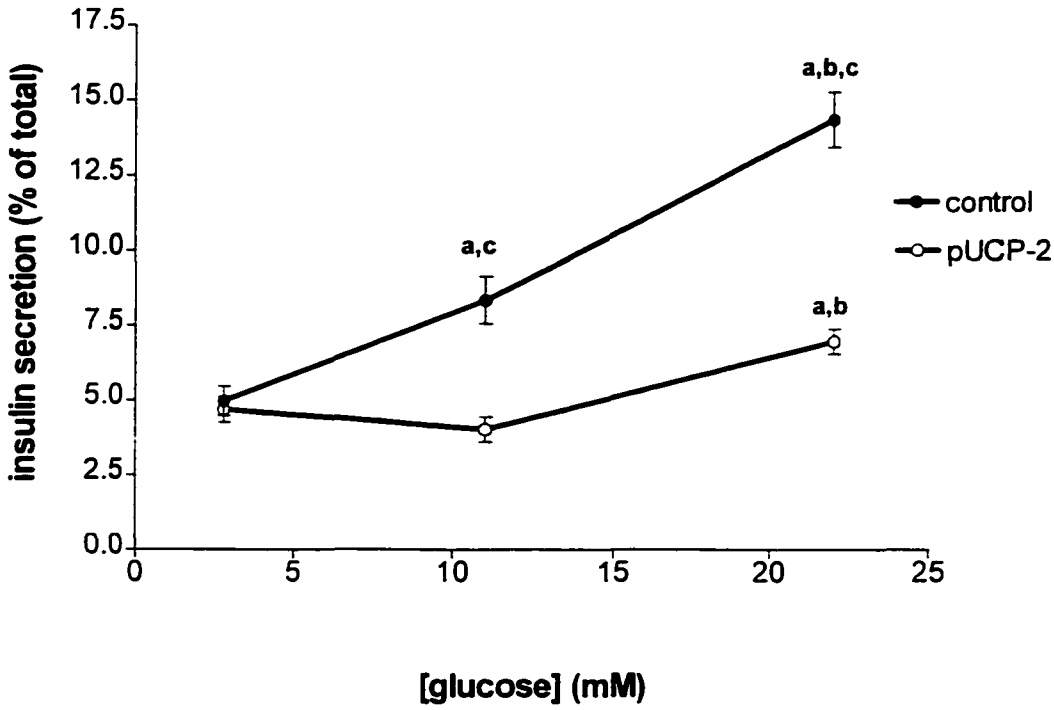

Figure 3.7. Concentration-response of insulin secretion to glucose in control and pUCP-2 transfected βTC6-f7 cells. Control cells were treated with lipofectamine^{2000} only. Data are expressed as means ± SEM for n = 8 or greater with a = $p < 0.05$ compared to 2.8 mM glucose treatment and b = $p < 0.05$ compared to 11 mM glucose treatment using a 2-way ANOVA with bonferroni post-hoc analysis. c = $p < 0.05$ compared to pUCP-2 transfected cells using unpaired Students' t-test.

3.3.1 βTC6-f7 Cells

At 2.8 mM glucose, cells showed no concentration-response to forskolin in either lipofectamine^{2000}-treated control or pUCP-2 transfected cells (Figure 3.8). Two-way ANOVA indicated that the response to forskolin was different between control and pUCP-2 transfected cells. Using an unpaired Student's t-test, it was found that at 10 μM forskolin cAMP was significantly higher in control cells than pUCP-2 transfected cells, but this was not observed at other forskolin concentrations. At 11 mM glucose, control and UCP-2 over-expressing groups did not respond differently to forskolin. A significant concentration-response to forskolin was seen in control cells only between 0.1 μM and 10 μM forskolin (Figure 3.9). However, no significant difference was seen between 0 μM and 10 μM forskolin treatments in control cells was observed. No differences in cAMP were observed between control and pUCP-2 transfected cells at any forskolin concentration used. No concentration-response to glucose was observed in control or pUCP-2 transfected cells exposed 2.8 mM and 11 mM concentrations (Figure 3.10). Total protein content was not significantly different from well to well as indicated by the relatively small SEM of multiple (> 15) wells from separate transfections (#1 CV = 6.1%; #2 CV = 3.0%).

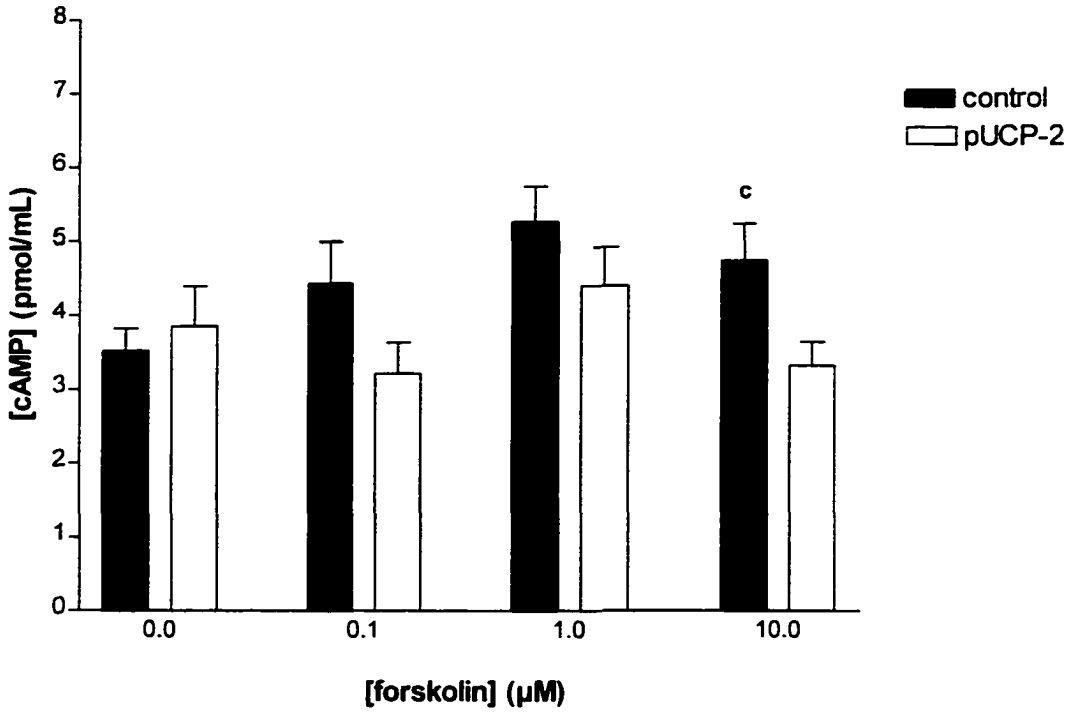

Figure 3.8. Effect of UCP-2 over-expression on cAMP generation in βTC6-f7 cells exposed to 2.8 mM glucose. cAMP was measured in the absence (0) or presence of increasing concentrations of the adenylyl cyclase activator forskolin. Control cells were treated with lipofectamine^{2000} only. Data are expressed as means ± SEM for n = 8 or greater.

c = $p < 0.05$ compared to pUCP-2 transfected cells using unpaired Students' t-test.

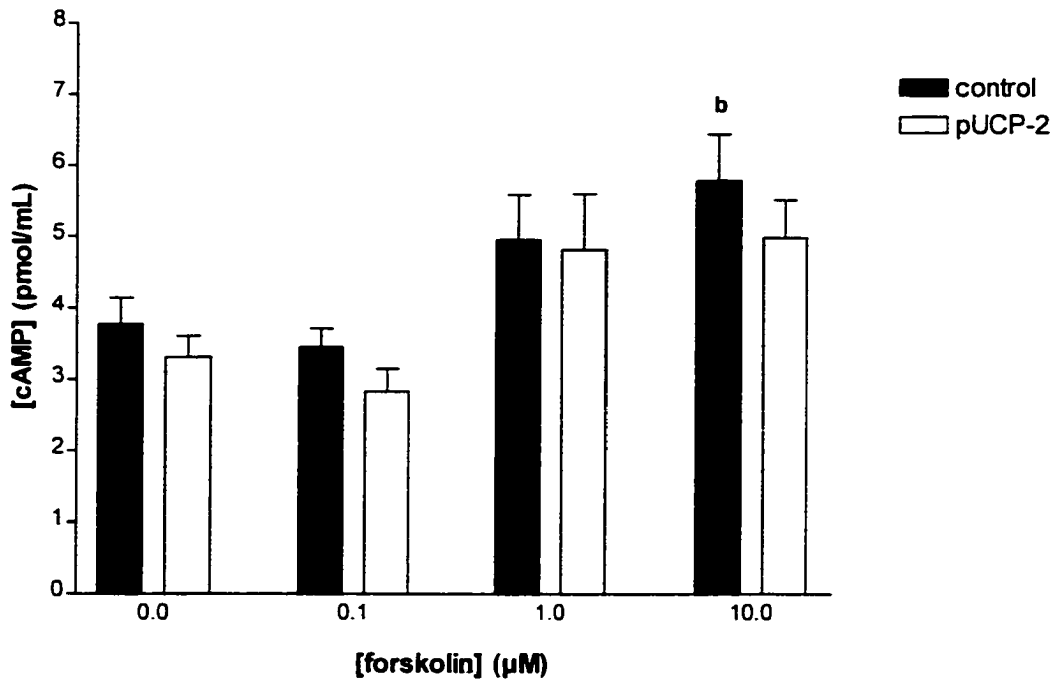

Figure 3.9. Effect of UCP-2 over-expression on cAMP generation in βTC6-f7 cells exposed to 11 mM glucose. cAMP was measured in the absence (0) or presence of increasing concentrations of the adenylyl cyclase activator forskolin. Control cells were treated with lipofectamine^{2000} only. Data are expressed as means ± SEM for n = 8 or greater. b = $p < 0.05$ compared to 0.1 μM forskolin treatment using 2-way ANOVA with bonferroni post-hoc analysis.

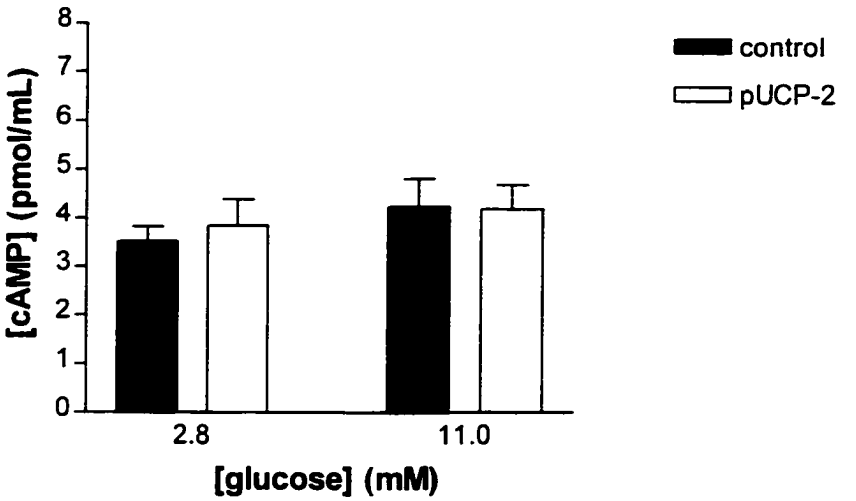

Figure 3.10. Concentration-response of cAMP generation to low (2.8 mM) and high (11 mM) glucose exposure in βTC6-f7 cells. Control cells were treated with lipofectamine^{2000} only. Data are expressed as means ± SEM for n = 8 or greater.

3.3.2 Isolated Rat Islets

At 2.8 mM glucose, islets showed a strong concentration-dependent cAMP response to forskolin in both uninfected control and AdUCP-2 infected islets (Figure 3.11). This response was not found to be different by two-way ANOVA. Both groups had significantly higher cAMP at 1 μM and 10 μM forskolin as compared to no treatment (2.8 and 3.8 fold, respectively), as well as differences between 10 μM and 0.1 μM forskolin treated islets (2.2 fold). At 11 mM glucose, both groups again showed a strong concentration-response to forskolin treatment with differences between 10 μM as compared to both 0.1 μM (2.7 fold higher) and untreated islets (3.2 fold higher) (Figure 3.12). The response between control and AdUCp-2 infected islets was similar. No differences were detected between control and AdUCP-2 infected islets at any forskolin or glucose concentration. As well, no concentration-response to glucose was observed in either group (Figure 3.13).

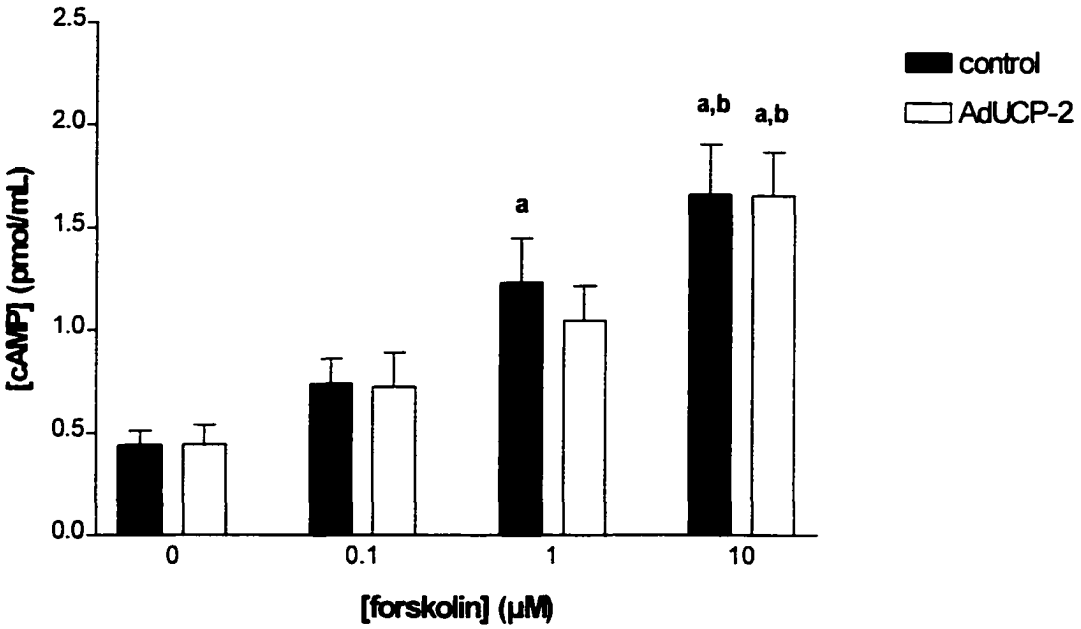

Figure 3.11. Effect of UCP-2 over-expression on cAMP generation in isolated rat islets exposed to 2.8 mM glucose. cAMP was measured in the absence (0) or presence of increasing concentrations of the adenylyl cyclase activator forskolin. Control islets were not infected with any construct. Data are expressed as means ± SEM for n = 8 or greater except for control islets, 1 μM forskolin where n = 7; AdUCP-2 islets, 0.1 μM forskolin and 1 μM forskolin where n = 6 and control islets, 0.1 μM forskolin where n = 5. a = $p < 0.05$ compared to 0 forskolin treatment and b = $p < 0.05$ compared to 0.1 μM forskolin treatment using 2-way ANOVA with bonferroni post-hoc analysis.

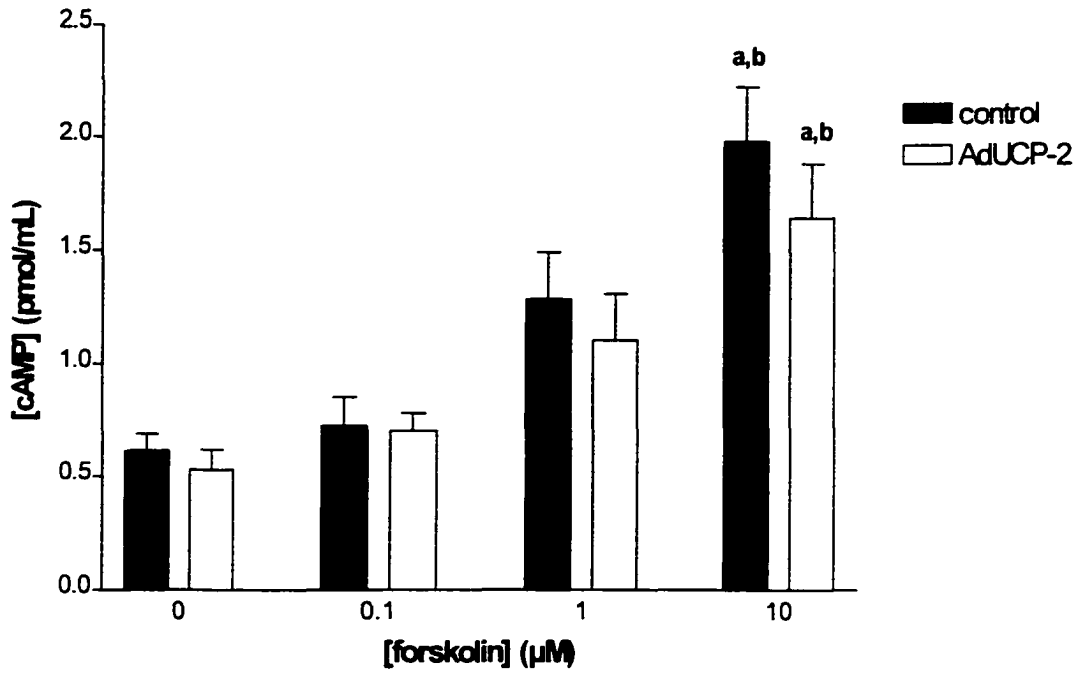

Figure 3.12. Effect of UCP-2 over-expression on cAMP generation in isolated rat islets exposed to 11 mM glucose. cAMP was measured in the absence (0) or presence of increasing concentrations of the adenylyl cyclase activator forskolin. Control islets were not infected with any construct. Data are expressed as means ± SEM for n = 8 or greater except for control islets, 1 μM forskolin where n = 7; control islets 0.1 μM forskolin where n = 6 and AdUCP-2 islets, 0.1 μM forskolin and 1 μM forskolin where n = 5. a = $p < 0.05$ compared to 0 forskolin treatment and b = $p < 0.05$ compared to 0.1 μM forskolin treatment using 2-way ANOVA with bonferroni post-hoc analysis.

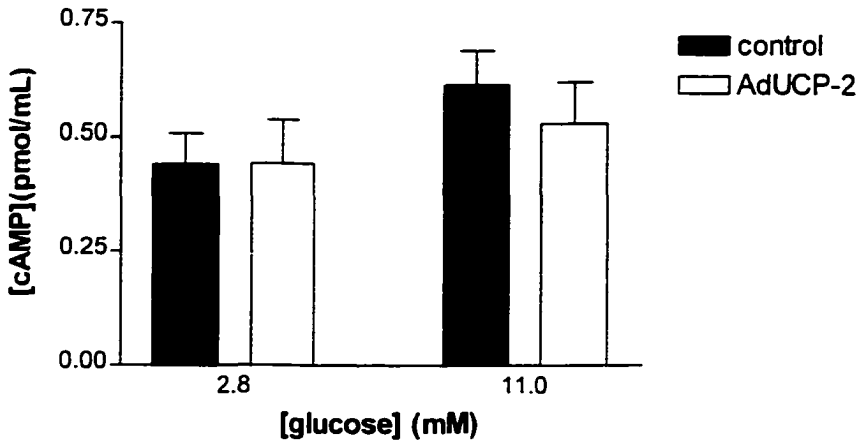

Figure 3.13. Concentration-response of cAMP generation to low (2.8 mM) and high (11 mM) glucose exposure in isolated rat islets. Control islets were not infected with any construct. Data are expressed as means ± SEM for n = 8 rats or greater for all groups except AdUCP-2 islets, 2.8 mM glucose, where n = 7 rats.

3.4 Insulin Secretion

In order to interpret our findings in the cAMP formation experiments, we then measured insulin release in response to forskolin in both βTC6-f7 cells and intact islets. Secretion was measured as percent of total insulin to take into account differences (if any) in cell numbers or insulin content of cells between wells.

3.4.1 βTC6-f7 cells

3.4.1.1 Effects of transfection and DMSO on GSIS

Insulin secretion was determined for EGFP transfected βTC6-f7 cells and DMSO-treated cells to take into account the transfection process and the forskolin solvent, respectively (Figure 3.14). No differences were found between lipofectamine^{2000}-treated control βTC6-f7 cells, lipofectamine^{2000}-treated control βTC6-f7 cells treated with DMSO and pEGFP transfected βTC6-f7 cells at 11 mM glucose and, notably, all three had significantly higher insulin secretion than did pUCP-2 transfected βTC6-f7 cells. Insulin secretion from pUCP-2 transfected βTC6-f7 cells treated with DMSO had similar insulin secretion to untreated pUCP-2 transfected βTC6-f7 cells.

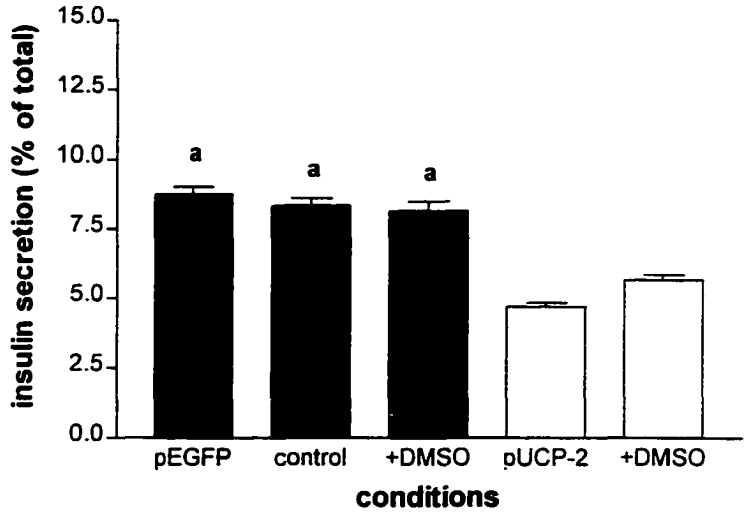

Figure 3.14. Effect of transfection and DMSO treatment (0.25%) on insulin secretion from βTC6-f7 cells exposed to 11 mM glucose. Data are expressed as means ± SEM (n = 12) with a = $p < 0.05$ compared to pUCP-2 transfected βTC6-f7 cells using unpaired Students' t-test.

3.4.1.2 Response to Forskolin

At 2.8 mM glucose, two-way ANOVA indicated that control and pUCP-2 transfected cells had different insulin responses to forskolin. A concentration-dependent insulin response to forskolin was observed in lipofectamine^{2000}-treated control, but not pUCP-2 transfected βTC6-f7 cells (Figure 3.15). A significant difference between control and pUCP-2 transfected βTC6-f7 cells was found at 1 μM forskolin, but not 10 μM forskolin where insulin secretion in pUCP-2 transfected βTC6-f7 cells was similar to that of control cells. At 11 mM glucose, there was also a different insulin response to forskolin in control and pUCP-2 transfected cells. A concentration-response to forskolin observed in both control and pUCP-2 groups, with a maximal response at 1 μM forskolin (Figure 3.16). Significant differences in secretion were found between control and pUCP-2 groups at 0 μM and 0.1 μM forskolin, but not at higher concentrations as secretion in pUCP-2 transfected βTC6-f7 cells was again normalized to that of control βTC6-f7 cells.

3.4.2 Isolated Rat Islets

UCP-2 expression altered the insulin response to forskolin at 11 mM glucose only At 2.8 mM glucose, secretion was modestly increased by forskolin in both uninfected control and AdUCP-2 infected islets (Figure 3.17). However, statistical significance was only observed for infected islets at 1 μM as compared to 0 μM forskolin. Uninfected control islets had higher secretion than AdUCP-2 infected islets at 10 μM forskolin only. At 11 mM glucose, an increase in secretion was seen in AdUCP-2 infected islets only at 10 μM forskolin compared to 0 μM and 0.1 μM forskolin (Figure 3.18).

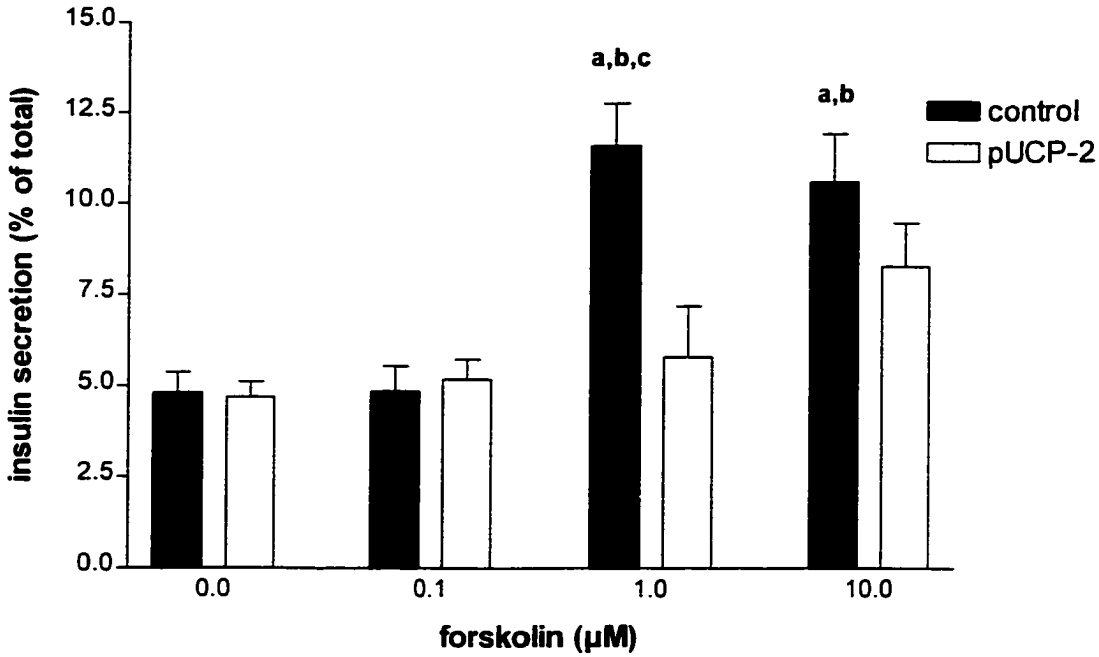

Figure 3.15. Effect of UCP-2 over-expression on forskolin-stimulated insulin secretion from βTC6-f7 cells exposed to 2.8 mM glucose. Secretion was measured in the absence (0) or presence of increasing concentrations of the adenylyl cyclase activator forskolin. Control cells were treated with lipofectamine^{2000} only. Data are expressed as means ± SEM for n = 8 or greater. a = $p < 0.05$ compared to 0 forskolin treatment and b = $p < 0.05$ compared to 0.1 μM forskolin treatment using 2-way ANOVA with bonferroni post-hoc analysis. c = $p < 0.05$ compared to pUCP-2 transfected cells using unpaired Students' t-test.

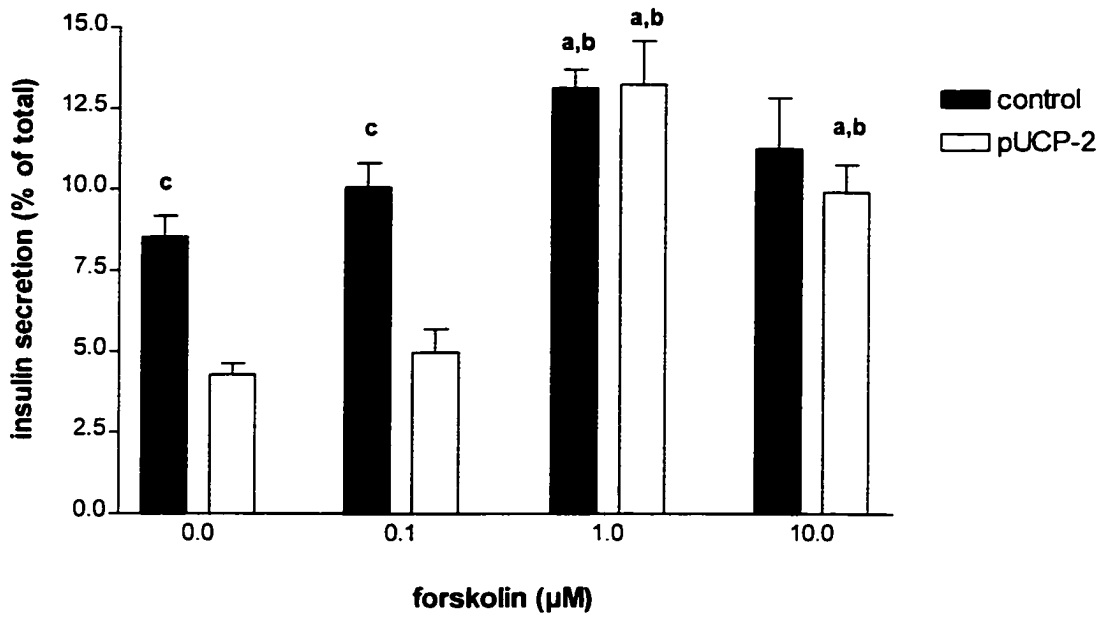

Figure 3.16. Effect of UCP-2 over-expression on forskolin-stimulated insulin secretion from βTC6-f7 cells exposed to 11 mM glucose. Secretion was measured in the absence (0) or presence of increasing concentrations of the adenylyl cyclase activator forskolin. Control cells were treated with lipofectamine^{2000} only. Data are expressed as means ± SEM for n =8 or greater. a = $p < 0.05$ compared to 0 forskolin treatment and b = $p < 0.05$ compared to 0.1 μM forskolin treatment using 2-way ANOVA with bonferroni post-hoc analysis. c = $p < 0.05$ compared to pUCP-2 transfected cells using unpaired Students' t-test.

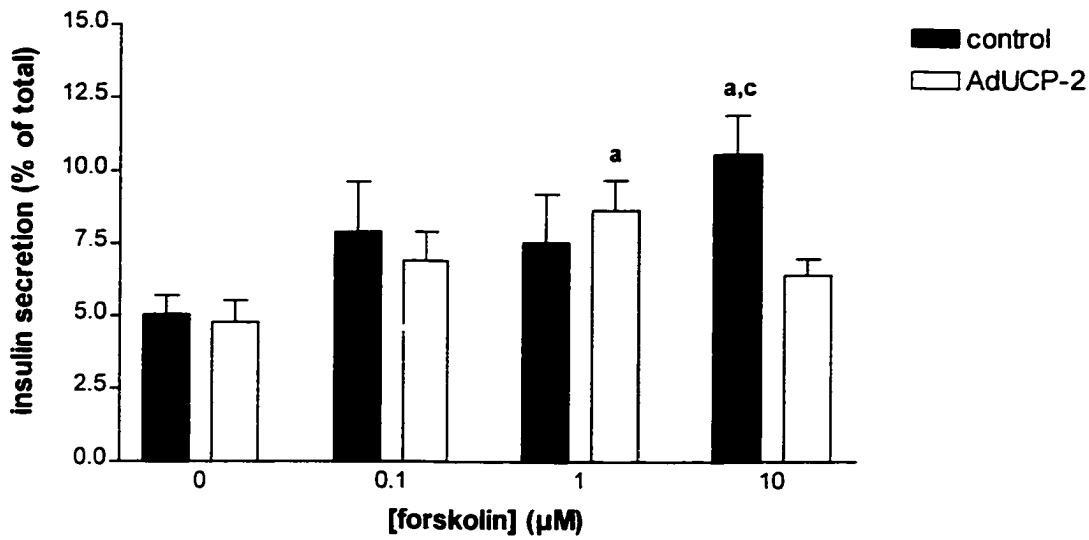

Figure 3.17. Effect of UCP-2 over-expression on forskolin-stimulated insulin secretion from isolated rat islets exposed to 2.8 mM glucose. Secretion was measured in the absence (0) or presence of increasing concentrations of the adenylyl cyclase activator forskolin. Data are expressed as means ± SEM for n = 8 or greater except for control islets, 1 μM forskolin, where n = 6 rats. a = $p < 0.05$ compared to 0 forskolin treatment using 2-way ANOVA with bonferroni post-hoc analysis. c = $p < 0.05$ compared to AdUCP-2 infected islets using unpaired Students' t-test.

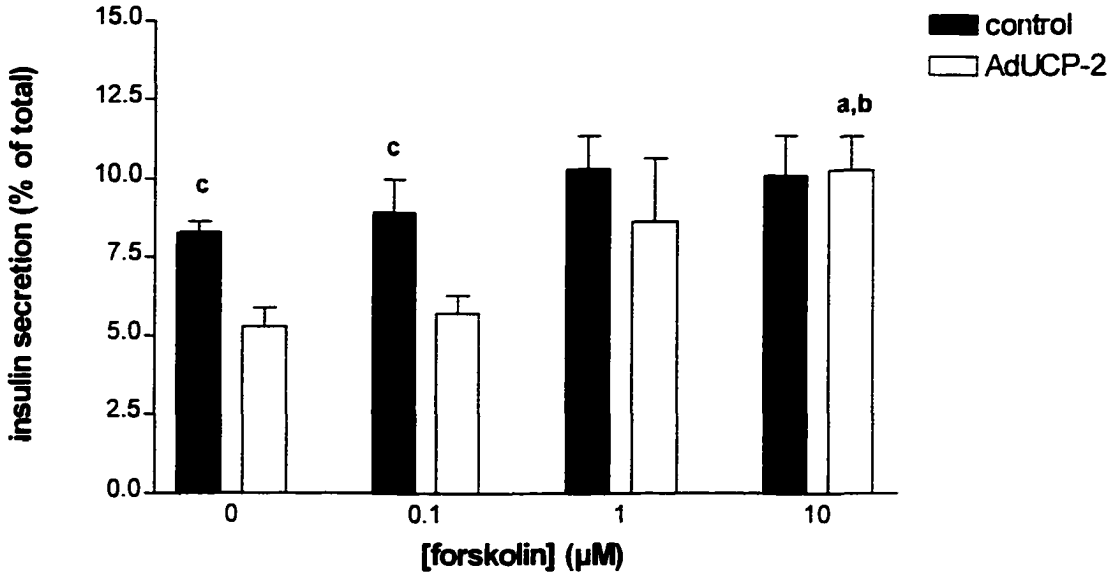

Figure 3.18. Effect of UCP-2 over-expression on forskolin-stimulated insulin secretion from isolated rat islets exposed to 11 mM glucose. Secretion was measured in the absence (0) or presence of increasing concentrations of the adenylyl cyclase activator forskolin. Data are expressed as means ± SEM for n = 8 or greater except for control islets, 0 forskolin and 0.1 μM forskolin where n = 7 rats. a = $p < 0.05$ compared to 0 forskolin treatment and b = $p < 0.05$ compared to 0.1 μM forskolin using 2-way ANOVA with bonferroni post-hoc analysis. c = $p < 0.05$ compared to AdUCP-2 infected islets using unpaired Students' t-test.

In contrast, control islets showed no increase in insulin secretion at any concentration of forskolin. Control islets had higher insulin secretion than AdUCP-2 infected islets at 0 μM and 0.1 μM forskolin, but not at greater forskolin concentrations.

3.5 ATP Formation

ATP levels in lipofectamine^{2000} -treated control and pUCP-2 transfected βTC6-f7 cells were measured to confirm that there was uncoupling taking place as seen previously in AdUCP-2 infected islets (105). ATP was also measured in AdUCP-2 infected βTC6-f7 cells to determine any potential differences in UCP-2 induction using the two different vectors.

The ATP response to glucose was found to be different in control and UCP-2 over-expressing groups using both the plasmid and adenovirus vectors using two-way ANOVA. In transfection experiments, ATP was significantly higher when exposed to 22 mM glucose as compared to 2.8 mM glucose in control cells only (Figure 3.19). pUCP-2 transfected cells had significantly lower ATP (21.8 %; $p < 0.001$) than did control cells exposed to 22 mM glucose only. In infection experiments ATP was significantly higher when exposed to 22 mM glucose as compared to 11 mM glucose (2.8 mM glucose was not done) in control cells only (Figure 3.20). AdUCP-2 infected cells also had significantly lower ATP than did control cells exposed to 11 mM glucose (14.4% of control lower; $p < 0.05$) and 22 mM glucose (38.7% of control lower; $p < 0.0001$). When all three treatment groups (control, pUCP-2 transfected cells and AdUCP-2 infected cells) were compared, control cells had higher ATP levels than both UCP-2 over-expressing cell systems, with pUCP-2 transfected cells having higher ATP levels than AdUCP-2 infected cells (Figure 3.21).

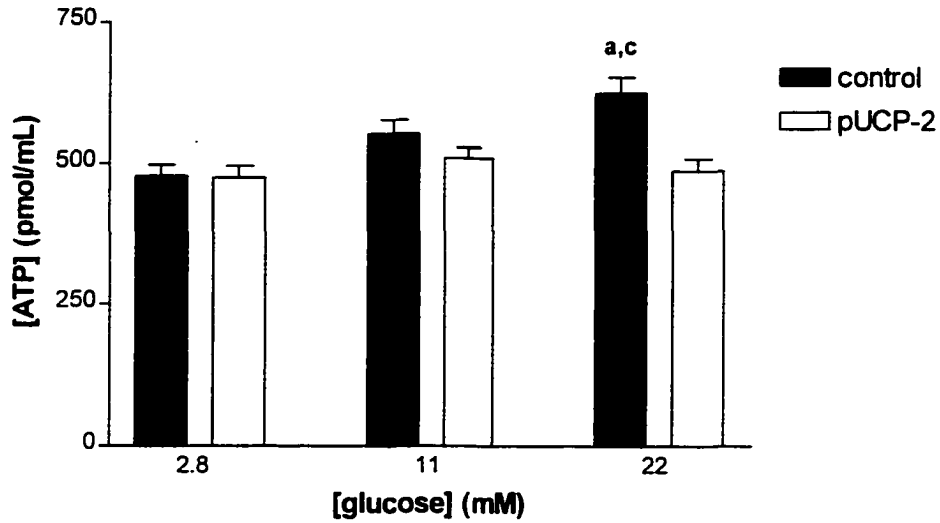

Figure 3.19. Effect of plasmid transfection-induced UCP-2 over-expression on ATP generation in βTC6-f7 cells exposed to increasing concentrations of glucose. Data are expressed as means ± SEM for n = 8 or greater. a = $p < 0.05$ compared to 2.8 mM glucose treatment using 2-way ANOVA with bonferroni post-hoc analysis. c = $p < 0.05$ compared to pUCP-2 transfected cells using unpaired Students' t-test.

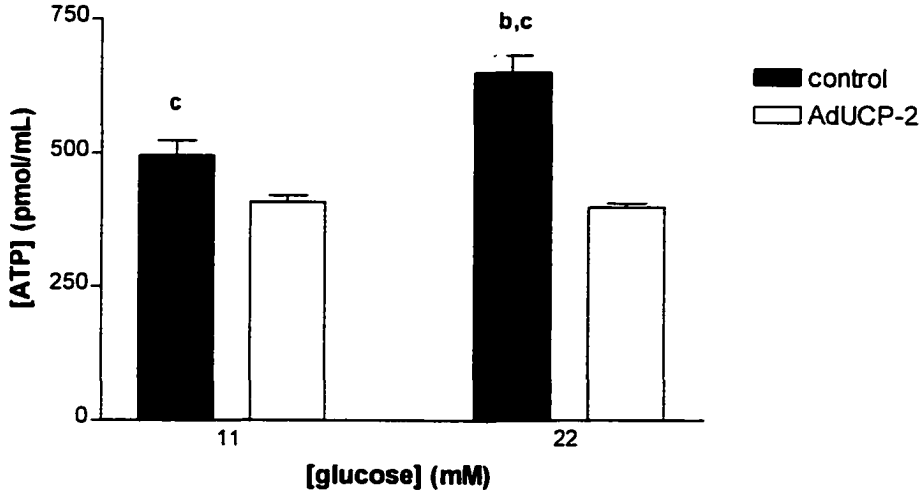

Figure 3.20. Effect of adenovirus infection-induced UCP-2 over-expression on ATP generation in βTC6-f7 cells exposed to increasing concentrations of glucose. Data are expressed as means ± SEM for n = 6 or greater. b = $p < 0.05$ compared to 11 mM glucose treatment using 2-way ANOVA with bonferroni analysis. c = $p < 0.05$ compared to AdUCP-2 infected cells using unpaired Students' t-test.

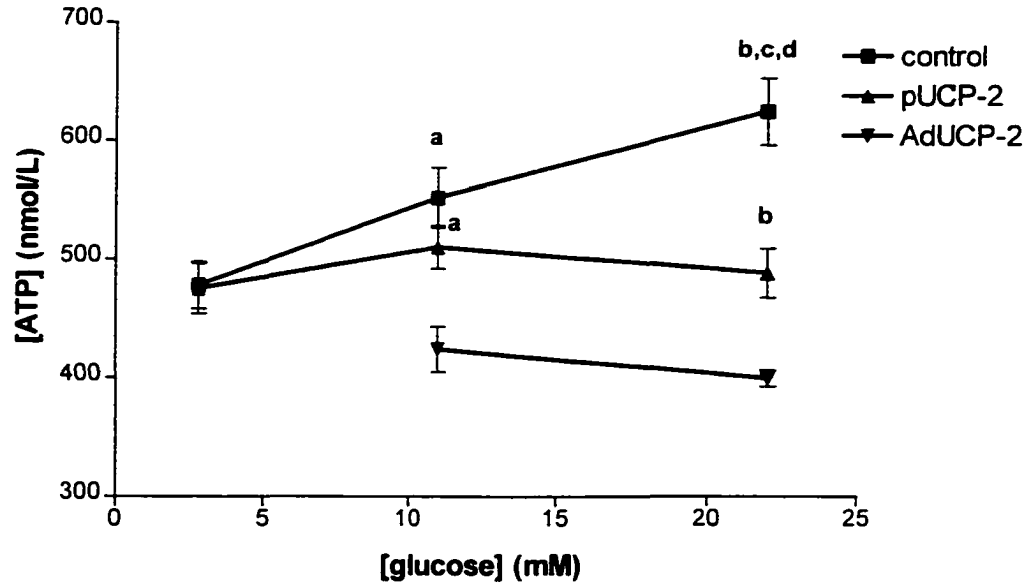

Figure 3.22. Comparison of adenovirus infection- vs. plasmid transfection-induced UCP-2 over-expression on ATP generation upon exposure to increasing concentrations of glucose. Data are expressed as means ± SEM with n = 6 or greater. a = $p < 0.05$ compared to AdUCP-2 infected cells (11 mM glucose), b = $p < 0.05$ compared to AdUCP-2 infected cells (22 mM glucose) and c = $p < 0.05$ compared to pUCP-2 transfected cells (22 mM glucose) using unpaired Students' t-test. d = $p < 0.05$ compared to control cells (11 mM glucose) using 2-way ANOVA with bonferroni post-hoc analysis.

3.6 Comparison of gene transfer efficiency between plasmid and adenovirus vectors

To test transfer efficiency, we used the EGFP plasmid and an AdUCP-2/EGFP adenovirus construct to visualize EGFP expression in the βTC6-f7 cell system. The AdUCP-2/EGFP adenovirus contains both the UCP-2 and EGFP cDNA sequences, with the UCP-2 sequence being upstream and translated first (i.e any EGFP mRNA that is translated will be accompanied by prior translation of UCP-2 mRNA). The EGFP plasmid is identical to the UCP-2 in every manner but the sequence inserted. Thus, EGFP expression can be used as an accurate estimate of UCP-2 expression. Under fluorescent microscopy, only the EGFP expressing cells are visible, while under white light microscopy, all cells are visible. By comparing the fluorescent and white light images of the same field, we were able to qualitatively estimate the transfer efficiency of each vector. In pEGFP transfected cells, the EGFP product was very strongly expressed in altered cells, although the percentages of cells transfected was only ~25% (Figure 3.22). In AdUCP-2/EGFP infected cells, the EGFP product was strongly visible in some altered cells, while only moderately expressed in others. Taken together, the percent of infected cells (regardless of product intensity) was markedly higher (~50-60%) (Figure 3.23). Though not conclusive for UCP-2 expression, the EGFP plasmid vector is identical to its UCP-2 counterpart and provides a good representation of transfection efficiency.

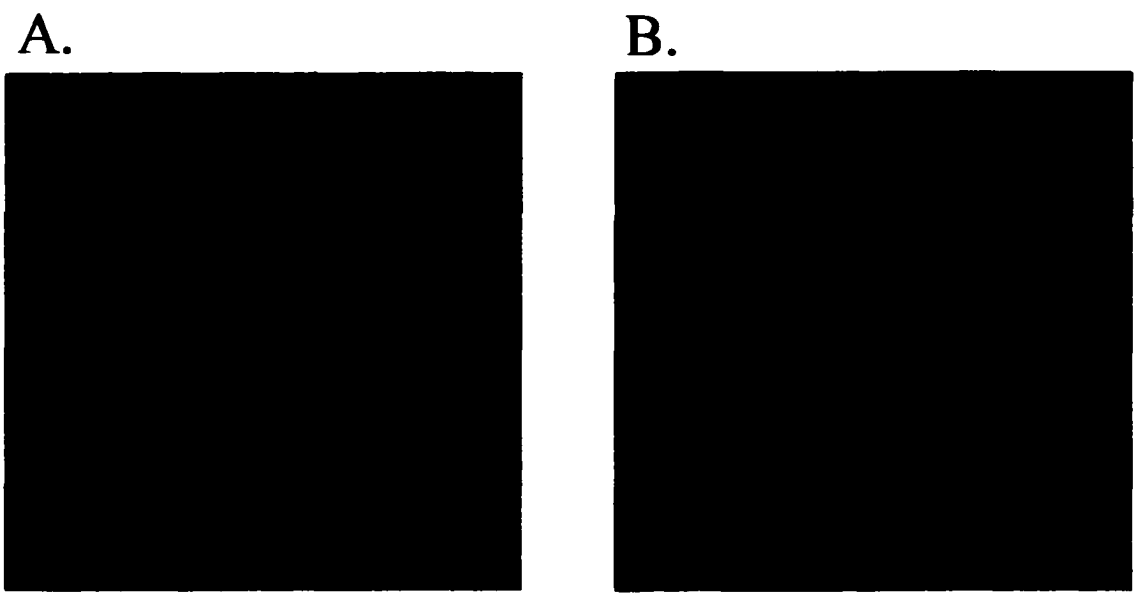

Figure 3.22. βTC6-f7 cells transfected with pEGFP under white light (A) and fluorescence (B) confocal microscopy

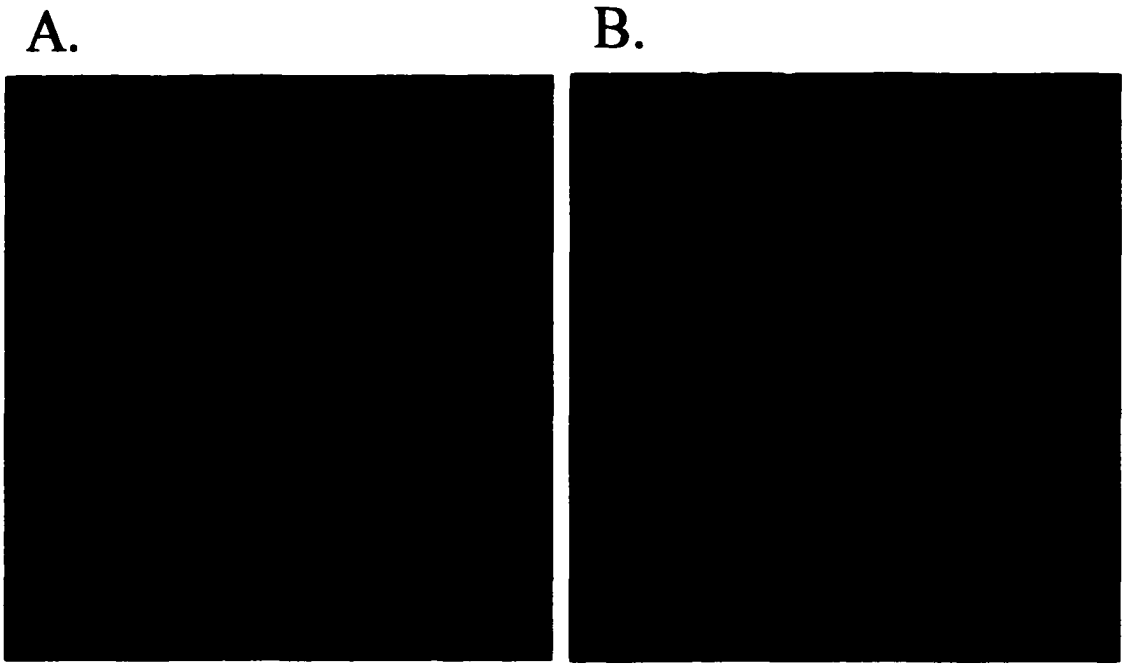

Figure 3.23. βTC6-f7 cells infected with AdUCP-2/EGFP under white light (A) and fluorescence (B) confocal microscopy.

4. Discussion

In most species, blood glucose concentrations typically fluctuate between 4 and 7 mM under normal conditions (156). The secretion and action of insulin is vital to maintaining proper blood glucose concentrations. Glucose concentrations are detected by β-cells and glucose metabolites act at several important sites along the insulin secretory cascade of the β-cell to elicit an appropriate response and maintain normoglycemia. The generation of ATP from glucose metabolism is important at many, but perhaps not all, of these sites. Firstly, ATP donates a phosphate group in the phosphorylation reactions mediated by glucokinase and phosphofructokinase, which enhances glycolytic flux and allows further metabolism of glucose through oxidative phosphorylation. As more ATP is generated, closure of the ATP sensitive potassium channel (K^{+}_{ATP}) causes the membrane depolarization needed to elicit calcium influx (157). Granule trafficking events also depend on ATP to provide energy to the motor protein myosin (52), while many phosphorylation reactions in the secretory cascade are thought to use ATP as a phosphate donor (58). (51) The generation of cAMP from ATP via adenylyl cyclase is key to maintaining adequate insulin secretion (57). Thus, the potential impact of a reduction in ATP on glucose-stimulated insulin secretion (GSIS) is significant.

Before we began studying the cAMP signaling system in insulin secretion, we first validated that the transient transfection of a UCP-2-containing plasmid into βTC6-f7 cells would result in the same abolition of glucose-stimulated insulin secretion as observed using adenoviral-induced over-expression of UCP-2 in islets (105). At a basal (2.8 mM) concentration of glucose, there was no difference seen between pUCP-2 transfected cells and

control cells. More stimulatory concentrations of 11 mM and 22 mM glucose resulted in marked increases in secretion from control cells, while the insulin response from pUCP-2 transfected cells remained virtually unchanged. This corresponds well with results obtained using the adenovirus infection induction of UCP-2 over-expression in isolated rat islets (105). Also, cells transfected with the pEGFP plasmid and treated with DMSO did not differ in terms of insulin response, indicating that the suppressive effects seen with pUCP-2 transfection were specifically due to UCP-2 over-expression. Taken together, this confirms that transient transfection of βTC6-f7 cells with pUCP-2 is a valid model in which to study the effects of UCP-2 on GSIS.

Potentiation of GSIS by cAMP is an important process in which ATP is involved on several levels. Not only does ATP serve as the precursor to cAMP formation, but it is also thought to be an important phosphate donor for PKA mediated phosphorylation reactions which make up a large part of cAMP's effects (59). Augmentation of cAMP through increasing AC activity is a physiologically important action of many insulinotropic hormones such as GLP-1 and GIP. In many cases of type 2 diabetes, the potentiating actions of these incretins are reduced and insufficient insulin is secreted (158). Glucose metabolism, in the absence of any exogenous factor (e.g. forskolin), shows maximal cAMP generation at glucose concentrations between 5 mM (159) and 8 mM (160). Using glucose concentrations of 2.8 mM and 11 mM allowed us to study cAMP generation at intermediate and maximal stimulation. When UCP-2 is over-expressed, the subsequent decrease in ATP was expected to also lead to a decrease levels of cAMP following both glucose and forskolin stimulation.

UCP-2 over-expression did not alter cAMP generation in the presence of glucose

alone in either whole rat islets or clonal β-cells. There was no significant difference in cAMP generation between cells exposed to 2.8 mM and 11 mM glucose in either model. There was also no difference in the amount of cAMP generated by equal concentrations of forskolin at 2.8 mM or 11 mM glucose. Two-way ANOVA also did not reveal any interaction between UCP-2 expression and generation of cAMP in response to glucose or forskolin. This is consistent with results from Bjorkland and Grill (2000), who examined cAMP generation (± forskolin) at 3.3 mM and 11 mM glucose in normal islets (161). We can speculate that enzyme activity, rather than substrate availability, is the limiting factor in cAMP generation in β-cells. While the ATP data from the βTC6-f7 cells do not conclusively show this here, data obtained in isolated rat islets indicates that ATP is significantly reduced (130) with cAMP generation unaffected. Thus, it is conceivable that lower ATP levels (which were reduced almost 40% when UCP-2 was over-expressed (136)) do not affect the cAMP generating capacity of the β-cell. Alternatively, these observations may also be explained by the recently hypothesized concept of compartmentalization of ATP in β-cells (162), as seen in other excitable tissue like cardiac cells (163), certain neurons (164)and oocytes (123). In essence this concept proposes that different ATP-dependent functions in the β-cell rely on separate "pools" of ATP and each may be regulated or respond differently to decreases in their respective pool. A decrease in overall ATP of the β-cell may not significantly affect the ATP pool that cAMP generation depends upon.

The results of our cAMP generation studies in control rat islets were consistent with those from other studies (76;165). Yajima et al. (1999) found a similar concentration-related cAMP response to forskolin at 0 and 11 mM glucose, with maximal stimulation at

approximately 3-5 μM forskolin; the next significant increase was not seen until 100 μM forskolin (76). A forskolin concentration of 10 μM was also shown to elevate cAMP to levels 3-4 fold greater than that induced by GIP (166), assuring that our methods would encompass physiologically anticipated rises in cAMP. In control βTC6-f7 cells, the response to forskolin was modest compared to that observed in whole rat islets. βTC cells are derived from an engineered transgenic mouse insulinoma. Although all isoforms of AC (except AC IX, although it is not present in rat or mouse islets (71)) respond quite well to forskolin (167), cAMP generation has been found to be higher in rat vs. mouse islets given the same forskolin treatment (168). Still, Hinke et al. (2000) were able to stimulate a four-fold increase in cAMP using forskolin (10 μM) in a similar βTC3 clonal cell line, although his incubation time and seeding density of cells were both double that used in our study (166). The explanation of this discrepancy may perhaps lie in the number of cells which are stimulated by forskolin. Being a lipophilic substance, forskolin may diffuse through the plasma membrane of cells. This rate of diffusion would not be expected to differ between islets and clonal β-cells. However, intact islets are linked by gap junctions which allow the transmission of small molecules (7) such as forskolin (MW 410). Thus, forskolin entering one cell of an islet can be transmitted to all others and activate AC throughout. Such gap junctions are absent in clonal β-cells, preventing the rapid sharing of a stimulus like forskolin. If a fixed amount of forskolin molecules are added to the cell culture well, only a certain portion of cells will come in contact with the stimulus. By doubling both the number of cells and exposure time to the stimulus, Hinke's experiments would theoretically increase the probability of forskolin stimulating a cell by 4 times (2 x 2) and thus, show a

greater response.

The bulk of cAMP effects on insulin secretion are thought to be mediated through activation of PKA and phosphorylation of key exocytotic proteins (58;71). If these reactions depend on ATP as a phosphate donor, then a reduction in its availability would represent a limiting factor. One cAMP molecule may activate several PKA molecules, which would go on to phosphorylate multiple protein targets. Given this amplification, the cAMP/PKA downstream pathway would likely require a much larger pool of ATP than that required for cAMP generation. Even though UCP-2 over-expression had no effect on the amount of cAMP generated, its ability to potentiate insulin secretion was predicted to be reduced in UCP-2 over-expressing β-cells.

In isolated rat islets exposed to 2.8 mM glucose, higher concentrations of forskolin (which subsequently increased cAMP levels) were able to induce a modest rise in insulin secretion in both control and AdUCP-2 infected islets. Again, results from similar experiments in normal islets by Bjorkland and Grill (2000) are in agreement with this (161). The potentiating capacity of cAMP at this glucose concentration also did not appear to be affected by UCP-2 over-expression, as no differences were found between control and AdUCP-2 infected islets. As expected, in control islets exposed to 11 mM glucose alone, insulin secretion increased significantly as compared to exposure to 2.8 mM glucose alone. However, secretion was not increased by forskolin treatment in control islets at 11 mM glucose. The Bjorkland and Grill study (2000) did show an increase in insulin secretion at 11 mM glucose with forskolin treatment, but using both a higher forskolin concentration (25 μM compared to 10 μM) in the incubation media (161). AdUCP-2 infected islets again had

virtually no response to glucose, but did show an unexpected pattern of insulin secretion when stimulated by forskolin. At high concentrations of forskolin, GSIS was increased in AdUCP-2 infected to levels comparable to control islets. Had there been no response to forskolin in UCP-2 over-expressing islets, this would have indicated that this pathway of GSIS potentiation was attenuated. However, contrary to our hypothesis, higher concentrations of forskolin (> 0.1 μM) actually increased insulin secretion in UCP-2 over-expressing islets to levels comparable to control cells. Two-way ANOVA revealed that UCP-2 over-expressing islets and control islets responded differently glucose stimulation in the presence of forskolin. Our cAMP studies showed no difference in levels of this messenger and hence, this effect of forskolin is independent of cAMP elevation.

In the βTC6-f7 clonal cell line, forskolin was not able to effectively raise cAMP levels. While the results from the insulin secretion experiments were not able to provide any information on the ability of elevations in cAMP to properly potentiate insulin secretion, they did provide support for the results found in our isolated rat islets experiments. At both 2.8 mM glucose and 11 mM glucose, higher concentrations of forskolin elevated insulin secretion compared to low forskolin or untreated cells. At 2.8 mM glucose and 1 μM forskolin, secretion from control cells was increased significantly compared to both control cells at 0.1 μM forskolin and pUCP-2 transfected cells at 1 μM forskolin. When the forskolin concentration was increased to 10 μM, secretion from control cells remained unchanged (as compared to control cells +1 μM forskolin), but secretion from pUCP-2 transfected cells was increased to levels comparable to control cells. At 11 mM glucose, patterns of insulin secretion were virtually identical to those seen in isolated rat islets. No

response to glucose was seen in pUCP-2 transfected cells, but forskolin concentrations of > 0.1 μM were able to normalize secretion back to that of control cells. As in isolated islets, 2-way ANOVA indicated an interaction between UCP-2 expression and insulin response to glucose with forskolin. Importantly, while GSIS was different between control and pUCP-2 transfected cells treated with glucose alone and cells treated with glucose + forskolin > 0.1 μM, there were no differences in cAMP levels between these groups, further indicating that this stimulatory action of forskolin on GSIS is independent of cAMP.

In search of support of cAMP independent effects of forskolin, a study by Kay-Wagoner and Pallotta (1988) indicated that forskolin had direct effects (i.e. independent of AC activation) on the nicotinic acetyl choline receptor in rat skeletal muscle (169). This class of Ca^{2+} channels underwent desensitization to acetyl choline at a markedly greater rate with prior forskolin treatment and thus inward Ca^{2+} was reduced. While reducing Ca^{2+} current would not stimulate insulin secretion in the β-cell, this study does represent an example of direct modulation of ion channel activity by forskolin. Recall that ion movement (be it K^+ or Ca^{2+}) is a key parameter in GSIS. A second article, described direct forskolin gating of a class of voltage-dependent K^+ channels in neuronal cells which reduced the peak K^+ current (170). This effect was "distinct from those of other agents that raise intracellular cAMP levels" and the study even concluded that it "can lead to misinterpretation of results in experiments in which forskolin is assumed to selectively activate adenylyl cyclase" (170). Further evidence for direct forskolin alterations on K^+ channel activity was also found in human T-lymphocytes (171). Potassium currents and membrane potential are critical parameters in GSIS and may represent the mechanism of forskolin-stimulated insulin

secretion which we observed. Of note, recent work shows that UCP-2 over-expression severely impairs K^+_{ATP} channel closure and secretion can be restored by treatment with the sulphonylurea glybenclamide, which selectively blocks the K^+_{ATP} channel (136). Thus, forskolin effects on K^+ current (via alterations in ion channel activity or ion pumping) could potentially represent a mechanism through which it could directly restore insulin secretion in UCP-2 over-expressing β-cells. Preliminary experiments in our lab using rubidium-86 efflux as a marker of K^+ channel activity indicate that forskolin may indeed significantly reduce potassium current in β-cells (Chan, unpublished observations). A hypothetical representation of the state of K^+ channel activity with increasing forskolin concentration is shown in Figure 4.1.

Uncoupling leads to a decrease in ATP levels. When UCP-2 is over-expressed in β-cells, it is expected that ATP levels are reduced. In pUCP-2 transfected βTC6-f7 cells, ATP was reduced to a greater extent as glucose concentration increased, reaching a 22% reduction at 22 mM glucose. Results from 2-way ANOVA on these data do indicate that there is an interaction between how the cells respond to glucose and the level of UCP-2 expression. However, no significant difference was found in ATP between control and pUCP-2 transfected βTC6-f7 cells at 11 mM glucose, while GSIS remained attenuated. In ATP formation experiments done previously in isolated rat islets infected with AdUCP-2, decreases were greater, reaching 40% reduction at only 8.3 mM glucose (105). The apparent discrepancy may lie simply in the design of the cell line ATP measurements. The seeding density used and proliferation of the clonal βTC6-f7 cells during the transfection protocol leads to approximately 8-10 times higher cell numbers as compared to the studies

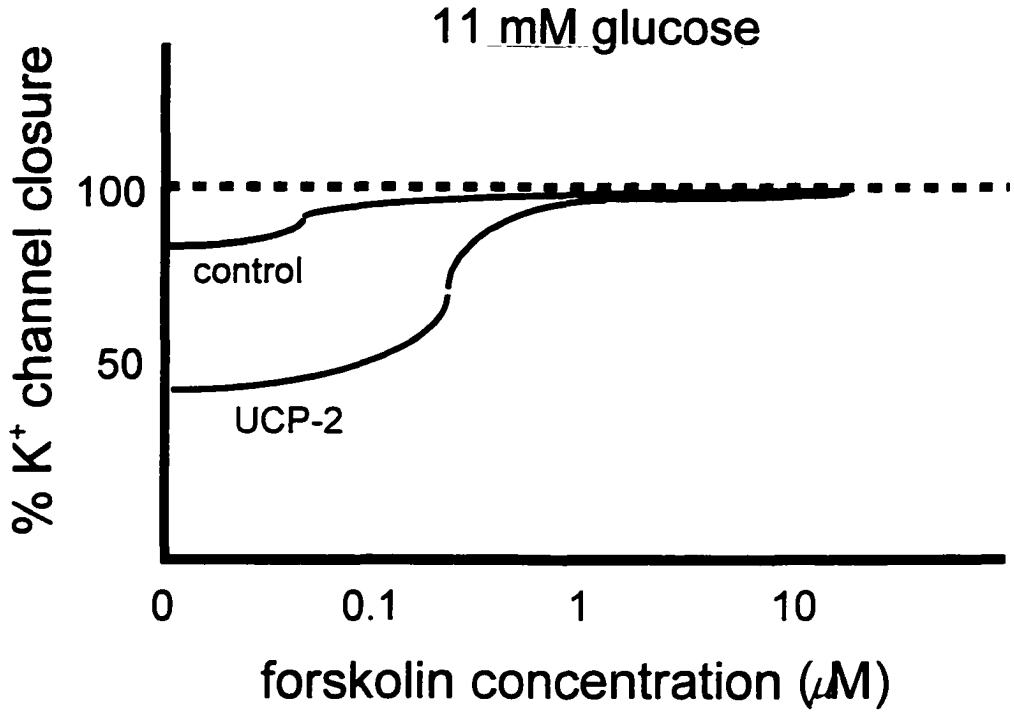

Figure 4.1. Postulated effects of forskolin on K^+ current in β-cells.

on rat islets done previously (105;130). With higher cell numbers, difference in the levels of ATP may not be as apparent and possibly escape detection. Modifications to the ATP protocols for βTC6-f7 cells were not attempted, but may be required in future studies.

An alternative explanation may be that there is a difference in gene transfer efficiency between the two vectors (plasmid vs adenovirus). AdUCP-2 infected βTC6-f7 cells showed a more acute drop in ATP formation as glucose was increased as compared to ATP formation in pUCP-2 transfected cells. A comparison of control, pUCP-2 transfected and AdUCP-2 infected βTC6-f7 cells shows three levels of ATP formation. RT-PCR on total RNA from all three systems showed that pUCP-2 transfected cells and AdUCP-2 infected cells had higher UCP-2 mRNA than control, but similar levels between each other. There may still be differences in the levels of UCP-2 expression (control < pUCP-2 transfected < AdUCP-2 infected).

There may also be a difference in gene transfer efficiency between the transfection and infection methods used. This is a reasonable hypothesis given that virus-mediated gene transfer is often a more efficient method if conditions are optimized (151). When considering the system as a whole, the key factor in the ability of the system to generate ATP is the number of cells affected by the UCP-2 gene transfer. As this number decreases, any effects of the UCP-2 over-expression become masked by the greater number of unaffected cells. Gene transfer efficiency was determined by monitoring EGFP expression using the identical plasmid transfection and adenovirus infection methods as used for UCP-2. An EGFP plasmid was generated in an identical fashion to that used to generate the pUCP-2 plasmid. The *egfp* gene was incorporated into the AdUCP-2 vector, immediately downstream

of the UCP-2 gene sequence (i.e. the *egfp* gene is transcribed after the *ucp-2* gene and UCP-2 expression would be approximately equal to (or even more than) that of EGFP). In this manner, EGFP expression is a reliable estimate of UCP-2 expression in our experiments and similar co-transfection of pEGFP has been used in published accounts as a marker of UCP-2 induction in clonal β-cells (133). Observing cells after transfection or infection indicated that infection resulted in a greater percentage of cells expressing the EGFP protein. Most of the successfully transfected cells showed a very high level of EGFP expression, while successfully infected cells had slight variations in the intensity of fluorescence between individual cells. Thus, even though AdUCP-2 infected cells had a higher percentage of cells infected, the overall content of UCP-2 mRNA for the whole system may not be significantly different from that of pUCP-2 transfected cells (i.e. UCP-2 mRNA is "spread" over a wider range in AdUCP-2 infected cells). It has been shown that even modest increases in UCP-2 expression causes significant attenuations in GSIS (130). Cells showing lower (but still above normal) expression of UCP-2 may still be unresponsive to glucose.

This apparent difference in the efficiency of gene transfer may explain the pattern of ATP formation observed in transfected and infected βTC6-f7 cells. Still, both systems showed similar patterns of GSIS. This again could be support for compartmentalization of ATP in β-cells. While overall ATP content of the cell may not be drastically reduced, certain pool(s) critical to GSIS could be decreased to a greater extent and result in impaired function. In addition, UCP-2 over-expressing cells would be expected to have increased rates of metabolism (98). These cells would take up more glucose from the media without a significant insulin response. This leaves less glucose in the media to stimulate secretion

from normal cells and the overall response of the system is decreased. In essence, "normal" cells are exposed to a lower concentration of glucose and therefore would secrete less insulin.

Quantification of the UCP-2 protein itself represents the most conclusive evidence of over-expression in pUCP-2 transfected cells or AdUCP-2 infected islets. Unfortunately, our efforts to quantify the UCP-2 protein were unsuccessful. Given the relatively short life of UCP-2 in the research world, very few reliable UCP-2 antibodies are commercially available. Though some reports claim to have quantified UCP-2 by immunoblotting, (134;137) reliable and reproducible results have not yet been demonstrated for any of the antibodies available. In addition, UCP-2 is expressed solely in the mitochondria at relatively low levels compared to other cellular proteins. That is to say, 50 μg of total cellular protein separated by SDS-PAGE may not contain a detectable amount of UCP-2. One option to overcome this has been to isolate the mitochondrial fraction of tissues by differential centrifugation for immunoblotting purposes (132). While this is readily achievable for larger tissues such as spleen or white adipose tissue, it is not practical for islet tissue, which makes up only 1-4% of the total pancreatic mass (6). Difficulties in lysing islet or clonal β-cells could also account for the inconsistent immunoblotting results. While most of the classical techniques for disrupting the cell membranes were employed (e.g. Triton-X detergent, repeated freeze-thawing, sonication), they may not have adequately liberated the UCP-2 from its inner mitochondrial entrapment.

5. Conclusions

Transient transfection of βTC6-f7 cells using a UCP-2 containing plasmid vector represents a reliable and convenient model for over-expressing UCP-2 and observing its effects on ATP-dependent signaling pathways in the β-cell. These experiments support the hypothesis that over-expression of UCP-2 leads to diminished GSIS in both isolated rat islets and clonal β-cells. The ability to elevate cAMP is not affected by the UCP-2-induced reduction in ATP. Incubating UCP-2 over-expressing cells or intact islets with forskolin can restore insulin secretion to that of controls, an effect independent of cAMP. This effect may be mediated through alterations in K^+ current of the β-cell, but future work is needed to elucidate the exact mechanism.

Appendix A

a.1 Glycolysis

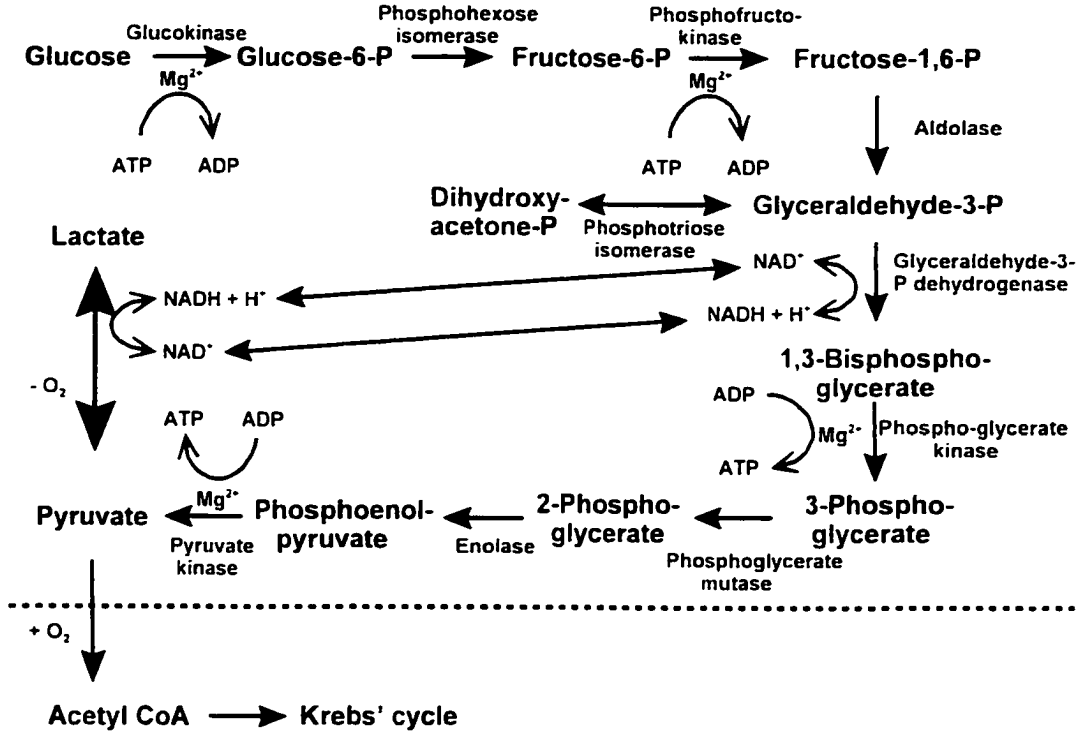

Figure A.1. Enzymes and intermediates of glycolysis.

a.2 The Krebs' Cycle

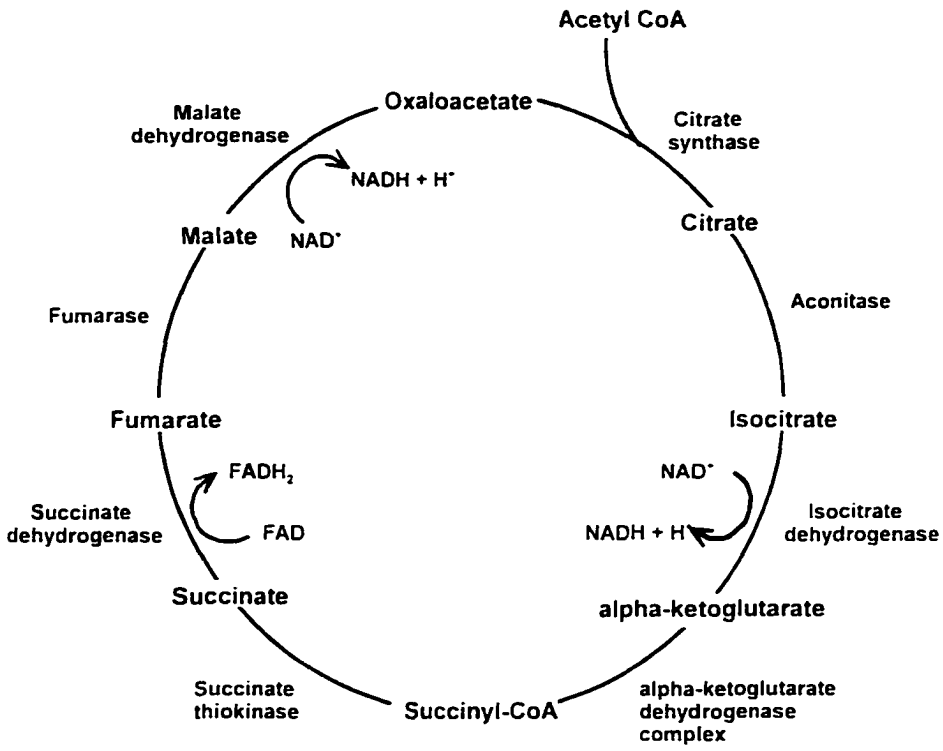

Figure A.2. Enzymes and intermediates of the Krebs' cycle.

a.3 Electron Transport and Oxidative Phosphorylation

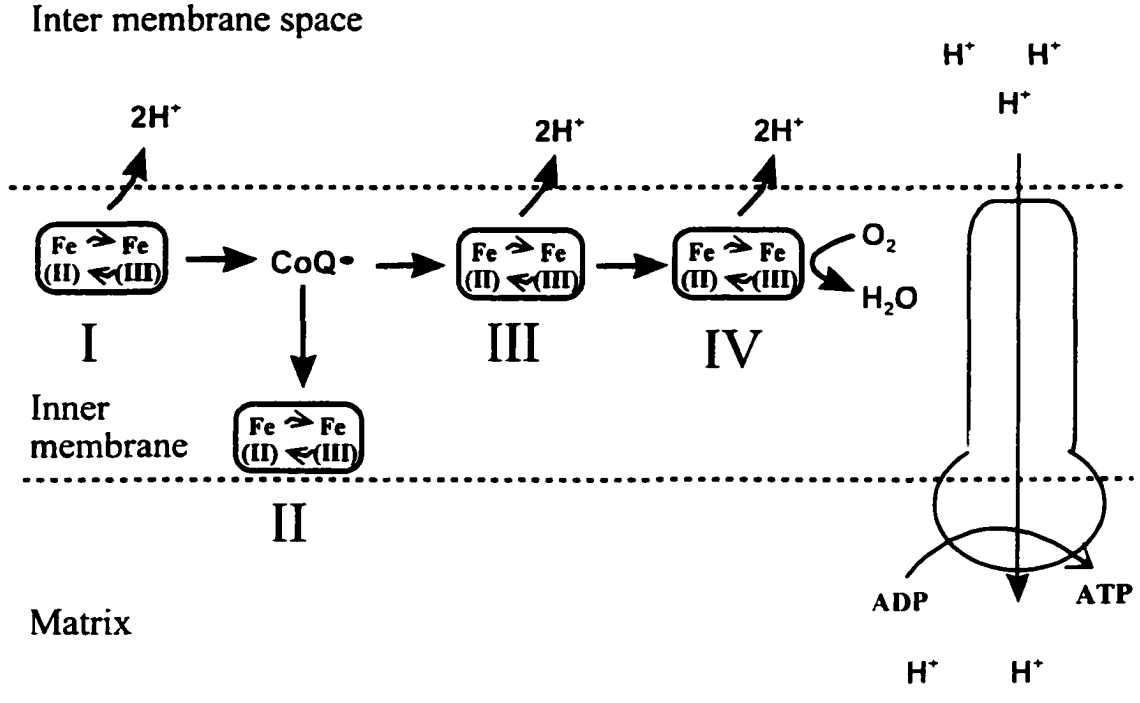

Figure A.3. Representation of electron flow and the chemiosmotic principle involved in oxidative phosphorylation.

Appendix B

b.1 Multiplicity of Infection

The multiplicity of infection (MOI) is determined to optimize the infection efficiency of the adenovirus construct. A_{260} of the virus suspension determines the number of virus particles present. However, this will measure all particles, both active and inactive. To determine the number of active virus particles, the suspension is diluted and a plaque assay is done. The number of plaque forming units (pfu) is used to calculate the MOI as follows:

$$\text{MOI} = \#\ \text{pfu/cell}$$

The amount of virus added to each well during the infection is then based on the number of cells present. For islets, it was assumed that each islet contained 1000 cells (a well of 200 thus containing 200 000 cells) and the amount of virus added is determined by the desired MOI of 10 000. βTC6-f7 were plated at 250 000 cells/well and cultured overnight. Over this culture period, the cells will roughly double. Therefore if there are 500 000 cells/well, we can estimate that using 500 000/200 000 = 2.5 X the amount of virus as used for islets will give approximately the same MOI.

B.2 Percent Incorporation of ^{125}I and Dilution of Radioactive Insulin Tracer

From the iodination procedure described in section 2.6.3.1, there were TC, final supernatant (S) and final pellet (P) collected. Using a Packard RIAStar gamma counter, CPMs were determined and used to calculate the % incorporation of ^{125}I as follows:

$$(\{(S \times 100 \times 6) + P\}/TC) \times 100$$

The dilution of the radioactive insulin (supernatant) to the "working tracer solution" is determined by adding 0.1 mL of radioactive insulin to S(CPM)/10 000 mL of RIA buffer.

b.3 Charcoal Extracted Equine Serum

Equine serum (AVC Teaching Hospital, Charlottetown, PE) was filtered through size 4 Whatman filter paper. Filtered serum was mixed with Norit A decolorizing, neutral charcoal (BDH Chemicals, Toronto, ON) to give a 1% (w/v) Norit A slurry. The slurry was stirred for 1 h, then centrifuged for 30 min at 10 000 rpm and 4 °C (Beckman J2-21M/E centrifuge, JA-14 rotor). The supernatant was filtered again, aliquotted and stored at -20 °C.

b.4 Dextran Coated Charcoal

50 g of Norit A decolorizing, neutral charcoal and 5 g of dextran T-70 (Amersham Pharmacia Biotech) were mixed in 1 L of 0.04 M phosphate buffer, pH 7.4. The mixture was stirred for 30 min and stored at 4 °C.

b.5 Conversion of CPM to pM Insulin

Insulin content was calculated by measuring the amount of radioactive insulin (tracer) in the charcoal pellet. The charcoal particles contain pores which will trap an insulin molecule, but not the larger insulin/antibody complex. When the charcoal is centrifuged out of the solution, it will take with it the unbound insulin molecules. A fixed amount of antibody and radioactive insulin are added to the tubes. The antibody binds the radioactive insulin and the non-radioactive insulin with equal affinities. Therefore, as the amount of non-radioactive insulin (from the sample) increases, the amount of radioactive insulin that will become bound by the antibody will decrease (i.e. the fixed amount of antibody gets used up by the non-radioactive insulin and less binds the radioactive insulin). So as the amount of insulin in the sample increases, the amount of unbound radioactive insulin increases and the CPM of the pellet increases. This is expressed as % CPM of total CPM as:

{(Total count-Sample count) x 100/Total count}- {(Total count-NSB count) x 100/Total count}

The second term takes into account non-specific binding of the radioactive insulin to elements such as RIA buffer proteins, the borosilicate tube, etc. Subtraction of these two percentages gives the % CPM for each sample. This is converted to pM insulin using the % CPM values of the standards.

References

1. Espinal J: Understanding Insulin Action. Chichester, Ellis Horwood Limited, 1989

2. Bliss M: The discovery of insulin: how it really happened. In: Insulin: Its Receptor and Diabetes. Hollenberg MD, Ed. New York, Marcel Dekker Inc., 1985, pp. 7-19

3. Banting FG: The Story of Insulin. Unpublished manuscript from the "Banting Papers", University of Toronto, 1940.

4. Banting FG, Best CH: The internal secretion of the pancreas. *Journal of Laboratory and Clinical Medicine* 7:251-266, 1922

5. Kern HF: Fine structure of the human exocrine pancreas. In: The Exocrine Pancreas: Biology, Pathobiology and Diseases. Vay Liang WG, Gardner JD, Brooks FP, Lebenthal E, DiMagno ER, Scheele GA, Eds. New York, Raven Press, 1986, pp. 9-20

6. Bonner-Weir S: Pancreatic islets: morphology, organization and physiological implications. In: Molecular and Cellular Biology of Diabetes Mellitus: Volume I Insulin Secretion. Draznin B, Melmed S, LeRoith D, Eds. New York, Alan R. Liss Inc., 1989, pp. 1-12

7. Bonner-Weir S: Anatomy of the islets of langerhans. In: The Endocrine Pancreas. Samols E, Ed. New York, Raven Press, 1991, pp. 15-28

8. Patel YC: Somatostatin and its receptor family. *Front.Neuroendocrinol.* 20:157-198, 1999

9. Foch TL, McClearn GE: Genetics, body weight and obesity. In: Obesity. Stunkard AJ, Ed. Toronto, WB Saunders Company, 1980, pp. 48-71

10. Housley MD, Siddle K: Molecular basis of insulin receptor function. In: Diabetes. Leslie RDG, Ed. New York, Churchill Livingstone, 1989, pp. 264-284

11. Ferrannini E: Insulin resistance versus insulin deficiency in non-insulin-dependent diabetes mellitus: problems and prospects. *Endocr.Rev.* 19:477-490, 1998

12. Flatt PR, Bailey CJ: Molecular mechanisms of insulin secretion and insulin action. *J.Biol.Ed.* 25:9-15, 1991

13. Lienhard GE, Slot JW, James DE, Mueckler MM: How cells absorb glucose. *Sci.Am.* 266:86-91, 1992

14. Granner DK: Hormones of the pancreas & gastrointestinal tract. In: Harper's Review of Biochemistry. Martin Jr. DW, Mayes PA, Rodwell VW, Granner DK, Eds. Los Altos, Lange Medical Publications, 1985, pp. 587-609

15. Jefferson LS, Kimball SR: Insulin regulation of protein synthesis. In: Molecular and Cellular Biology of Diabetes Mellitus: Volume 2 Insulin Action. Draznin B, Melmed S, LeRoith D, Eds. New York, Alan R. Liss Inc., 2001, pp. 133-142

16. Drury MI: Diabetes Mellitus. Boston, Blackwell Scientific Publications, 1986

17. Health Canada Diabetes in Canada: National Statistic and Opportunities for Improved Surveillance, Prevention and Control Minister of Public Works and Government Services, Canadian Federal Government, 1999

18. Leslie RDG, Lazarus NR, Vergani D: Aetiology of insulin dependent diabetes. In: Diabetes. Leslie RDG, Ed. New York, Churchill Livingstone, 1989, pp. 59-72

19. Leahy JL: Noninsulin-dependent diabetes mellitus: current concepts of pathogenesis. In: Molecular and Cellular Biology of Diabetes Mellitus: Volume I Insulin Secretion. Draznin B, Melmed S, LeRoith D, Eds. New York, Alan R. Liss Inc., 1989, pp. 149-158

20. Taylor R: Aetilogy of non-insulin dependent diabetes. In: Diabetes. Leslie RDG, Ed. New York, Churchill Livingstone, 1989, pp. 73-91

21. Montague CT, O'Rahilly S: The perils of portliness: causes and consequences of visceral adiposity. *Diabetes* 49:883-888, 2000

22. Clark JB, Palmer CJ, Shaw WN: The diabetic Zucker fatty rat. *Proc.Soc.Exp.Biol.Med.* 173:68-75, 1983

23. Griffen SC, Wang J, German MS: A genetic defect in beta-cell gene expression segregates independently from the fa locus in the ZDF rat. *Diabetes* 50:63-68, 2001

24. Chua SC Jr., Chung WK, Wu-Peng XS, Zhang Y, Liu SM, Tartaglia L, Leibel RL: Phenotypes of mouse diabetes and rat fatty due to mutations in the OB (leptin) receptor. *Science* 271:994-996, 1996

25. Bjorntorp P: The role of adipose tissue in human obesity. In: Obesity. Greenwood M. Ed. New York, Churchill Livingstone, 1983, pp. 17-24

26. DeFronzo RA, Ferrannini E: Insulin resistance. A multifaceted syndrome responsible for NIDDM, obesity, hypertension, dyslipidemia, and atherosclerotic cardiovascular disease. *Diabetes Care* 14:173-194, 1991

27. Greenwood MRC: Genetic and metabolic aspects. In: Obesity. Greenwood MRC, Ed. New York, Churchill Livingstone Inc., 1983, pp. 193-208

28. Kissebah AH, Krakower GR: Regional adiposity and morbidity. *Physiol.Rev.* 74:761-811, 1994

29. Hennes MM, Shrago E, Kissebah AH: Receptor and postreceptor effects of free fatty acids (FFA) on hepatocyte insulin dynamics. *Int.J.Obes.* 14:831-841, 1990

30. Milburn JL Jr., Hirose H, Lee YH, Nagasawa Y, Ogawa A, Ohneda M, BeltrandelRio H, Newgard CB, Johnson JH, Unger RH: Pancreatic beta-cells in obesity. Evidence for induction of functional, morphologic, and metabolic abnormalities by increased long chain fatty acids. *J.Biol.Chem.* 270:1295-1299, 1995

31. Mason TM, Goh T, Tchipashvili V, Sandhu H, Gupta N, Lewis GF, Giacca A: Prolonged elevation of plasma free fatty acids desensitizes the insulin secretory response to glucose in vivo in rats. *Diabetes* 48:524-530, 1999

32. Hotamisligil GS, Spiegelman BM: Tumor necrosis factor alpha: a key component of the obesity-diabetes link. *Diabetes* 43:1271-1278, 1994

33. Kieffer TJ, Heller RS, Habener JF: Leptin receptors expressed on pancreatic beta-cells. *Biochem.Biophys.Res.Commun.* 224:522-527, 1996

34. Gold G: Insulin structure and biosynthesis. In: Molecular and Cellular Biology of Diabetes Mellitus: Volume I Insulin Secretion. Draznin B, Melmed S, LeRoith D, Eds. New York, Alan R. Liss Inc., 1989, pp. 25-35

35. Hutton JC: Insulin secretory granule biogenesis and the proinsulin-processing endopeptidases. *Diabetologia* 37 (Suppl. 2):S48-S56, 1994

36. Nielsen DA, Welsh M, Casadaban MJ, Steiner DF: Control of insulin gene expression in pancreatic beta-cells and in an insulin-producing cell line, RIN-5F cells. I. Effects of glucose and cyclic AMP on the transcription of insulin mRNA. *J.Biol.Chem.* 260:13585-13589, 1985

37. Nagamatsu S, Nakamichi Y, Sawa H: Glucose transporter expression and functional role of hexokinase in insulin biosynthesis in mouse beta TC3 cells. *Am.J.Physiol.* 269:C480-C486, 1995

38. Howell SL, Bird SJ: Biosynthesis and secretion of insulin. In: Diabetes. Leslie RDG, Ed. New York, Churchill Livingstone, 1989, pp. 19-36

39. Welsh M, Nielsen DA, MacKrell AJ, Steiner DF: Control of insulin gene expression in pancreatic beta-cells and in an insulin-producing cell line, RIN-5F cells. II. Regulation of insulin mRNA stability. *J.Biol.Chem.* 260:13590-13594, 1985

40. Boyd AE, III, Rajan AS, Gaines KL: Regulation of insulin secretion by calcium. In: Molecular and Cellular Biology of Diabetes Mellitus: Volume I Insulin Secretion. Draznin B, Melmed S, LeRoith D, Eds. New York, Alan R. Liss Inc., 1989, pp. 93-105

41. Daniel S, Noda M, Straub SG, Sharp GW: Identification of the docked granule pool responsible for the first phase of glucose-stimulated insulin secretion. *Diabetes* 48:1686-1690, 1999

42. Porksen N, Nyholm B, Veldhuis JD, Butler PC, Schmitz O: In humans at least 75% of insulin secretion arises from punctuated insulin secretory bursts. *Am.J.Physiol.* 273:E908-E914, 1997

43. Hales CN: The pathogenesis of NIDDM. *Diabetologia* 37 (Suppl 2):S162-S168, 1994

44. Rothman JE, Orci L: Molecular dissection of the secretory pathway. *Nature* 355:409-415, 1992

45. MacDonald MJ, Kowluru A: Calcium-calmodulin-dependent myosin phosphorylation by pancreatic islets. *Diabetes* 31:566-570, 1982

46. Howell SL, Tyhurst M: The cytoskeleton and insulin secretion. *Diabetes Metab Rev.* 2:107-123, 1986

47. Yu W, Niwa T, Fukasawa T, Hidaka H, Senda T, Sasaki Y, Niki I: Synergism of protein kinase A, protein kinase C, and myosin light-chain kinase in the secretory cascade of the pancreatic beta-cell. *Diabetes* 49:945-952, 2000

48. Easom RA: CaM kinase II: a protein kinase with extraordinary talents germane to insulin exocytosis. *Diabetes* 48:675-684, 1999

49. Hisatomi M, Hidaka H, Niki I: Ca2+/calmodulin and cyclic 3,5' adenosine monophosphate control movement of secretory granules through protein phosphorylation/dephosphorylation in the pancreatic beta-cell. *Endocrinology* 137:4644-4649, 1996

50. Rothman JE: Mechanisms of intracellular protein transport. *Nature* 372:55-63, 1994

51. Gallo-Payet N, Payet MD: Excitation-secretion coupling. In: Cell Physiology Source Book. Sperekalis N, Ed. Toronto, Academic Press, 1998, pp. 632-651

52. Lodish H, Berk A, Zipursky S, Matsudaira P, Baltimore D, Darnell J: Molecular Cell Biology. New York, WH Freeman and Company, 2000

53. Prentki M, Corkey BE: Are the beta-cell signaling molecules malonyl-CoA and cystolic long- chain acyl-CoA implicated in multiple tissue defects of obesity and NIDDM? *Diabetes* 45:273-283, 1996

54. Mayes PA: Metabolism of carbohydrate. In: Harper's Review of Biochemistry. Martin Jr. DW, Mayes PA, Rodwell VW, Granner DK, Eds. Los Altos, Lange Medical Publications, 1985, pp. 166-193

55. Mayes PA: The citric acid cycle: The catabolism of acetyl CoA. In: Harper's Review of Biochemistry. Martin Jr. DW, Mayes PA, Rodwell VW, Granner DK, Eds. Los Altos, Lange Medical Publications, 1985, pp. 158-167

56. Mayes PA: Biologic oxidation. In: Harper's Review of Biochemistry. Martin Jr. DW, Mayes PA, Rodwell VW, Granner DK, Eds. Los Altos, Lange Medical Publications, 1985, pp. 147-157

57. Prentki M, Matschinsky FM: Ca2+, cAMP, and phospholipid-derived messengers in coupling mechanisms of insulin secretion. *Physiol.Rev.* 67:1185-1248, 1987

58. Takahashi N, Kadowaki T, Yazaki Y, Ellis-Davies GC, Miyashita Y, Kasai H: Post-priming actions of ATP on Ca2+-dependent exocytosis in pancreatic beta cells. *Proc.Natl.Acad.Sci.U.S.A.* 96:760-765, 1999

59. Blanpied TA, Augustine GJ: Protein kinase A takes center stage in ATP-dependent insulin secretion. *Proc.Natl.Acad.Sci.U.S.A.* 96:329-331, 1999

60. Patterson GH, Knobel SM, Arkhammar P, Thastrup O, Piston DW: Separation of the glucose-stimulated cytoplasmic and mitochondrial NAD(P)H responses in pancreatic islet beta cells. *Proc.Natl.Acad.Sci.U.S.A.* 97:5203-5207, 2000

61. Erecinska M, Bryla J, Michalik M, Meglasson MD, Nelson D: Energy metabolism in islets of Langerhans. *Biochim.Biophys.Acta* 1101:273-295, 1992

62. Rotig A, Bonnefont JP, Munnich A: Mitochondrial diabetes mellitus. *Diabetes Metab* 22:291-298, 1996

63. Misler S, Pressel DM, Barnett DW: Stimulus transduction in metabolic sensor cells. In: Cell Physiology Source Book. Sperekalis N, Ed. Toronto, Academic Press, 1998, pp. 652-667

64. Nichols CG, Shyng SL, Nestorowicz A, Glaser B, Clement JP, Gonzalez G, Aguilar-Bryan L, Permutt MA, Bryan J: Adenosine diphosphate as an intracellular regulator of insulin secretion. *Science* 272:1785-1787, 1996

65. Komatsu M, Schermerhorn T, Noda M, Straub SG, Aizawa T, Sharp GW: Augmentation of insulin release by glucose in the absence of extracellular Ca2+: new insights into stimulus-secretion coupling. *Diabetes* 46:1928-1938, 1997

66. Niki I: Ca2+ signaling and the insulin secretory cascade in the pancreatic beta-cell. *Jpn.J.Pharmacol.* 80:191-197, 1999

67. Lang J: Molecular mechanisms and regulation of insulin exocytosis as a paradigm of endocrine secretion. *Eur.J.Biochem.* 259:3-17, 1999

68. Berridge MJ, Lipp P, Bootman MD: The versatility and universality of calcium signaling. *Nat.Rev.Mol.Cell Biol.* 1:11-20, 2000

69. Detimary P, Gilon P, Henquin JC: Interplay between cytoplasmic Ca2+ and the ATP/ADP ratio: a feedback control mechanism in mouse pancreatic islets. *Biochem.J.* 333:269-274, 1998

70. Prentki M: New insights into pancreatic beta-cell metabolic signaling in insulin secretion. *Eur.J.Endocrinol.* 134:272-286, 1996

71. Leech CA, Castonguay MA, Habener JF: Expression of adenylyl cyclase subtypes in pancreatic beta-cells. *Biochem.Biophys.Res.Commun.* 254:703-706, 1999

72. Antoni FA: Molecular diversity of cyclic AMP signaling. *Front Neuroendocrinol.* 21:103-132, 2000

73. Chiono M, Mahey R, Tate G, Cooper DM: Capacitative Ca2+ entry exclusively inhibits cAMP synthesis in C6-2B glioma cells. Evidence that physiologically evoked Ca2+ entry regulates Ca(2+)-inhibitable adenylyl cyclase in non-excitable cells. *J.Biol.Chem.* 270:1149-1155, 1995

74. Ammala C, Ashcroft FM, Rorsman P: Calcium-independent potentiation of insulin release by cyclic AMP in single beta-cells. *Nature* 363:356-358, 1993

75. Renstrom E, Eliasson L, Rorsman P: Protein kinase A-dependent and -independent stimulation of exocytosis by cAMP in mouse pancreatic B-cells. *J.Physiol.* 502:105-118, 1997

76. Yajima H, Komatsu M, Schermerhorn T, Aizawa T, Kaneko T, Nagai M, Sharp GW, Hashizume K: cAMP enhances insulin secretion by an action on the ATP-sensitive K+ channel-independent pathway of glucose signaling in rat pancreatic islets. *Diabetes* 48:1006-1012, 1999

77. Yaekura K, Kakei M, Yada T: cAMP-signaling pathway acts in selective synergism with glucose or tolbutamide to increase cytosolic Ca2+ in rat pancreatic beta-cells. *Diabetes* 45:295-301, 1996

78. Gromada J, Dissing S, Bokvist K, Renstrom E, Frokjaer-Jensen J, Wulff BS, Rorsman P: Glucagon-like peptide I increases cytoplasmic calcium in insulin- secreting beta TC3-cells by enhancement of intracellular calcium mobilization. *Diabetes* 44:767-774, 1995

79. Yaekura K, Yada T: [Ca2+]i-reducing action of cAMP in rat pancreatic beta-cells: involvement of thapsigargin-sensitive stores. *Am.J.Physiol.* 274:C513-C521, 1998

80. Ozaki N, Shibasaki T, Kashima Y, Miki T, Takahashi K, Ueno H, Sunaga Y, Yano H, Matsuura Y, Iwanaga T, Takai Y, Seino S: cAMP-GEFII is a direct target of cAMP in regulated exocytosis. *Nat.Cell Biol.* 2:805-811, 2000

81. Turk J, Gross RW, Ramanadham S: Amplification of insulin secretion by lipid messengers. *Diabetes* 42:367-374, 1993

82. Zawalich WS, Zawalich KC: Regulation of insulin secretion by phospholipase C. *Am.J.Physiol.* 271:E409-E416, 1996

83. Corkey BE, Deeney JT, Yaney GC, Tornheim K, Prentki M: The role of long-chain fatty acyl-CoA esters in beta-cell signal transduction. *J.Nutr.* 130:299S-304S, 2000

84. Farfari S, Schulz V, Corkey B, Prentki M: Glucose-regulated anaplerosis and cataplerosis in pancreatic beta-cells: Possible implication of a pyruvate/citrate shuttle in insulin secretion. *Diabetes* 49:718-726, 2000

85. Brun T, Roche E, Assimacopoulos-Jeannet F, Corkey BE, Kim KH, Prentki M: Evidence for an anaplerotic/malonyl-CoA pathway in pancreatic beta-cell nutrient signaling. *Diabetes* 45:190-198, 1996

86. Berne C: The metabolism of lipids in mouse pancreatic islets. The biosynthesis of triacylglycerols and phospholipids. *Biochem.J.* 152:667-673, 1975

87. Limatola C, Schaap D, Moolenaar WH, van Blitterswijk WJ: Phosphatidic acid activation of protein kinase C-zeta overexpressed in COS cells: comparison with other protein kinase C isotypes and other acidic lipids. *Biochem.J.* 304:1001-1008, 1994

88. Schmidt MFG: Fatty acylation of proteins. *Biochim.Biophys.Acta* 988:411-426, 1989

89. Keller H, Wahli W: Peroxisome proliferator-activiated receptors: A link between endocrinology and nutrition. *Trends Endocrinol.Metab.* 4:291-296, 1993

90. Habener JF Drucker DJ, Mojsov S Knepel W, Philippe J: Biosynthesis of glucagon. In: The Endocrine Pancreas. Samols E, Ed. New York, Raven Press, 1991, pp. 53-72

91. Dupre J: Influences of the gut on the endocrine pancreas: An overview of established and potential physiological mechanisms. In: The Endocrine Pancreas. Samols E, Ed. New York, Raven Press, 1991, pp. 253-282

92. Campfield LA, Smith FJ: Neural control of insulin secretion: interaction of norepinephrine and acetylcholine. *Am.J.Physiol.* 244:R629-R634, 1983

93. Holm G: Adrenergic regulation of insulin release. *Acta Med.Scand.(Suppl.)* 672:21-25, 1983

94. Chan CB, MacPhail RM: Functional characterization of alpha-adrenoceptors on pancreatic islets of fa/fa Zucker rats. *Mol.Cell.Endocrinol.* 84:33-37, 1992

95. Porte D Jr., Robertson RP: Control of insulin secretion by catecholamines, stress, and the sympathetic nervous system. *Fed.Proc.* 32:1792-1796, 1973

96. Boyd AE, III: The role of ion channels in insulin secretion. *J.Cell Biochem.* 48:235-241, 1992

97. Fleury C, Sanchis D: The mitochondrial uncoupling protein-2: current status. *Int.J.Biochem.Cell Biol.* 31:1261-1278, 1999

98. Ricquier D, Bouillaud F: The uncoupling protein homologues: UCP1, UCP2, UCP3, StUCP and AtUCP. *Biochem.J.* 345:161-179, 2000

99. Ricquier D, Fleury C, Larose M, Sanchis D, Pecqueur C, Raimbault S, Gelly C, Vacher D, Cassard-Doulcier AM, Levi-Meyrueis C, Champigny O, Miroux B, Bouillaud F: Contributions of studies on uncoupling proteins to research on metabolic diseases. *J.Intern.Med.* 245:637-642, 1999

100. Pecqueur C, Cassard-Doulcier AM, Raimbault S, Miroux B, Fleury C, Gelly C, Bouillaud F, Ricquier D: Functional organization of the human uncoupling protein-2 gene, and juxtaposition to the uncoupling protein-3 gene. *Biochem.Biophys.Res.Commun.* 255:40-46, 1999

101. Jezek P, Engstova H, Zackova M, Vercesi AE, Costa AD, Arruda P, Garlid KD: Fatty acid cycling mechanism and mitochondrial uncoupling proteins. *Biochim.Biophys.Acta* 1365:319-327, 1998

102. Harper ME: Obesity research continues to spring leaks. *Clin.Invest.Med.* 20:239-244, 1997

103. Enerback S, Jacobsson A, Simpson EM, Guerra C, Yamashita H, Harper ME, Kozak LP: Mice lacking mitochondrial uncoupling protein are cold-sensitive but not obese. *Nature* 387:90-94, 1997

104. Boss O, Hagen T, Lowell BB: Uncoupling proteins 2 and 3: potential regulators of mitochondrial energy metabolism. *Diabetes* 49:143-156, 2000

105. Chan CB, MacDonald PE, Saleh MC, Johns DC, Marban E, Wheeler MB: Over-expression of uncoupling protein 2 inhibits glucose-stimulated insulin secretion from rat islets. *Diabetes* 48:1482-1486, 1999

106. Zhou YT, Shimabukuro M, Koyama K, Lee Y, Wang MY, Trieu F, Newgard CB, Unger RH: Induction by leptin of uncoupling protein-2 and enzymes of fatty acid oxidation. *Proc.Natl.Acad.Sci.U.S.A.* 94:6386-6390, 1997

107. Nedergaard J, Cannon B: [3H]GDP binding and thermogenin amount in brown adipose tissue mitochondria from cold-exposed rats. *Am.J.Physiol.* 248:C365-C371, 1985

108. Fleury C, Neverova M, Collins S, Raimbault S, Champigny O, Levi-Meyrueis C, Bouillaud F, Seldin MF, Surwit RS, Ricquier D, Warden CH: Uncoupling protein-2: a novel gene linked to obesity and hyperinsulinemia. *Nat.Genet.* 15:269-272, 1997

109. Gimeno RE, Dembski M, Weng X, Deng N, Shyjan AW, Gimeno CJ, Iris F, Ellis SJ, Woolf EA, Tartaglia LA: Cloning and characterization of an uncoupling protein homolog: a potential molecular mediator of human thermogenesis. *Diabetes* 46:900-906, 1997

110. Gong DW, He Y, Karas M, Reitman M: Uncoupling protein-3 is a mediator of thermogenesis regulated by thyroid hormone, beta3-adrenergic agonists, and leptin. *J.Biol.Chem.* 272:24129-24132, 1997

111. Sivitz WI, Fink BD, Donohoue PA: Fasting and leptin modulate adipose and muscle uncoupling protein: divergent effects between messenger ribonucleic acid and protein expression. *Endocrinology* 140:1511-1519, 1999

112. Boss O, Muzzin P, Giacobino JP: The uncoupling proteins, a review. *Eur.J.Endocrinol.* 139:1-9, 1998

113. Kaisaki PJ, Woon PY, Wallis RH, Monaco AP, Lathrop M, Gauguier D: Localization of tub and uncoupling proteins (UCP) 2 and 3 to a region of rat chromosome 1 linked to glucose intolerance and adiposity in the Goto-Kakizaki (GK) type 2 diabetic rat. *Mamm.Genome* 9:910-912, 1998

114. Tu N, Chen H, Winnikes U, Reinert I, Marmann G, Pirke KM, Lentes KU: Molecular cloning and functional characterization of the promoter region of the human uncoupling protein-2 gene. *Biochem.Biophys.Res.Commun.* 265:326-334, 1999

115. Astrup A, Toubro S, Dalgaard LT, Urhammer SA, Sorensen TI, Pedersen O: Impact of the v/v 55 polymorphism of the uncoupling protein 2 gene on 24-h energy expenditure and substrate oxidation. *Int.J.Obes.Relat Metab Disord.* 23:1030-1034, 1999

116. Urhammer SA, Dalgaard LT, Sorensen TI, Moller AM, Andersen T, Tybjaerg-Hansen A, Hansen T, Clausen JO, Vestergaard H, Pedersen O: Mutational analysis of the coding region of the uncoupling protein 2 gene in obese NIDDM patients: impact of a common amino acid polymorphism on juvenile and maturity onset forms of obesity and insulin resistance. *Diabetologia* 40:1227-1230, 1997

117. Cassell PG, Neverova M, Janmohamed S, Uwakwe N, Qureshi A, McCarthy MI, Saker PJ, Albon L, Kopelman P, Noonan K, Easlick J, Ramachandran A, Snehalatha C, Pecqueur C, Ricquier D, Warden C, Hitman GA: An uncoupling protein 2 gene variant is associated with a raised body mass index but not Type II diabetes. *Diabetologia* 42:688-692, 1999

118. Walder K, Norman RA, Hanson RL, Schrauwen P, Neverova M, Jenkinson CP, Easlick J, Warden CH, Pecqueur C, Raimbault S, Ricquier D, Silver MH, Shuldiner AR, Solanes G, Lowell BB, Chung WK, Leibel RL, Pratley R, Ravussin E: Association between uncoupling protein polymorphisms (UCP2-UCP3) and energy metabolism/obesity in Pima Indians. *Hum.Mol.Genet.* 7:1431-1435, 1998

119. Bao S, Kennedy A, Wojciechowski B, Wallace P, Ganaway E, Garvey WT: Expression of mRNAs encoding uncoupling proteins in human skeletal muscle: effects of obesity and diabetes. *Diabetes* 47:1935-1940, 1998

120. Samec S, Seydoux J, Dulloo AG: Post-starvation gene expression of skeletal muscle uncoupling protein 2 and uncoupling protein 3 in response to dietary fat levels and fatty acid composition: a link with insulin resistance. *Diabetes* 48:436-441, 1999

121. Vidal H, Langin D, Andreelli F, Millet L, Larrouy D, Laville M: Lack of skeletal muscle uncoupling protein 2 and 3 mRNA induction during fasting in type-2 diabetic subjects. *Am.J.Physiol.* 277:E830-E837, 1999

122. Nordfors L, Hoffstedt J, Nyberg B, Thorne A, Arner P, Schalling M, Lonnqvist F: Reduced gene expression of UCP2 but not UCP3 in skeletal muscle of human obese subjects. *Diabetologia* 41:935-939, 1998

123. Miller DS, Horowitz SB: Intracellular compartmentalization of adenosine triphosphate. *J.Biol.Chem.* 261:13911-13915, 1986

124. Rieusset J, Auwerx J, Vidal H: Regulation of gene expression by activation of the peroxisome proliferator-activated receptor gamma with rosiglitazone (BRL 49653) in human adipocytes. *Biochem.Biophys.Res.Commun.* 265:265-271, 1999

125. Memon RA, Hotamisligil GS, Wiesbrock SM, Uysal KT, Faggioni R, Moser AH, Feingold KR, Grunfeld C: Upregulation of uncoupling protein 2 mRNA in genetic obesity: lack of an essential role for leptin, hyperphagia, increased tissue lipid content, and TNF-alpha. *Biochim.Biophys.Acta* 1484:41-50, 2000

126. Chavin KD, Yang S, Lin HZ, Chatham J, Chacko VP, Hoek JB, Walajtys-Rode E, Rashid A, Chen CH, Huang CC, Wu TC, Lane MD, Diehl AM: Obesity induces expression of uncoupling protein-2 in hepatocytes and promotes liver ATP depletion. *J.Biol.Chem.* 274:5692-5700, 1999

127. Rashid A, Wu TC, Huang CC, Chen CH, Lin HZ, Yang SQ, Lee FY, Diehl AM: Mitochondrial proteins that regulate apoptosis and necrosis are induced in mouse fatty liver. *Hepatology* 29:1131-1138, 1999

128. Arsenijevic D, Onuma H, Pecqueur C, Raimbault S, Manning BS, Miroux B, Couplan E, Alves-Guerra MC, Goubern M, Surwit R, Bouillaud F, Richard D, Collins S, Ricquier D: Disruption of the uncoupling protein-2 gene in mice reveals a role in immunity and reactive oxygen species production. *Nat.Genet.* 26:435-439, 2000

129. Faggioni R, Shigenaga J, Moser A, Feingold KR, Grunfeld C: Induction of UCP2 gene expression by LPS: a potential mechanism for increased thermogenesis during infection. *Biochem.Biophys.Res.Commun.* 244:75-78, 1998

130. Zhang C, Baffy G, Perret P, Krauss S, Peroni O, Grujic D, Hagen T, Vidal-Puig A, Boss O, Zheng X, Wheeler M, Shulman G, Chan C, Lowell B: Uncoupling protein-2 negatively regulates insulin secretion and is a major link between obesity, beta-cell dysfunction and type 2 diabetes. *Cell* 105:745-755, 2001

131. Vidal-Puig AJ, Grujic D, Zhang CY, Hagen T, Boss O, Ido Y, Szczepanik A, Wade J, Mootha V, Cortright R, Muoio DM, Lowell BB: Energy metabolism in uncoupling protein 3 gene knockout mice. *J.Biol.Chem.* 275:16258-16266, 2000

132. Pecqueur C, Alves-Guerra MC, Gelly C, Levi-Meyrueis C, Couplan E, Collins S, Ricquier D, Bouillaud F, Miroux B: Uncoupling protein-2: in vivo distribution, induction upon oxidative stress, and evidence for translational regulation. *J.Biol.Chem.* 276:8705-8712, 2001

133. Li LX, Skorpen F, Egeberg K, Jorgensen IH, Grill V: Uncoupling protein-2 participates in cellular defense against oxidative stress in clonal beta-cells. *Biochem.Biophys.Res.Commun.* 282:273-277, 2001

134. Lameloise N, Muzzin P, Prentki M, Assimacopoulos-Jeannet F: Uncoupling protein 2: a possible link between fatty acid excess and impaired glucose-induced insulin secretion? *Diabetes* 50:803-809, 2001

135. Shimabukuro M, Zhou YT, Lee Y, Unger RH: Induction of uncoupling protein-2 mRNA by troglitazone in the pancreatic islets of Zucker diabetic fatty rats. *Biochem.Biophys.Res.Commun.* 237:359-361, 1997

136. Chan CB, De Leo D, Joseph JW, McQuaid TS, Ha XF, Xu F, Tsushima RG, Pennefather PS, Salapatek AM, Wheeler MB: Increased uncoupling protein-2 levels in beta-cells are associated with impaired glucose-stimulated insulin secretion: mechanism of action. *Diabetes* 50:1302-1310, 2001

137. Wang MY, Shimabukuro M, Lee Y, Trinh KY, Chen JL, Newgard CB, Unger RH: Adenovirus-mediated overexpression of uncoupling protein-2 in pancreatic islets of Zucker diabetic rats increases oxidative activity and improves beta-cell function. *Diabetes* 48:1020-1025, 1999

138. Freake HC: Uncoupling proteins: beyond brown adipose tissue. *Nutr.Rev.* 56:185-189, 1998

139. Wang H, Antinozzi PA, Hagenfeldt KA, Maechler P, Wollheim CB: Molecular targets of a human HNF1 alpha mutation responsible for pancreatic beta-cell dysfunction. *EMBO J.* 19:4257-4264, 2000

140. Wang H, Maechler P, Antinozzi PA, Hagenfeldt KA, Wollheim CB: Hepatocyte nuclear factor 4alpha regulates the expression of pancreatic beta-cell genes implicated in glucose metabolism and nutrient-induced insulin secretion. *J.Biol.Chem.* 275:35953-35959, 2000

141. Yamagata K, Furuta H, Oda N, Kaisaki PJ, Menzel S, Cox NJ, Fajans SS, Signorini S, Stoffel M, Bell GI: Mutations in the hepatocyte nuclear factor-4alpha gene in maturity-onset diabetes of the young (MODY1). *Nature* 384:458-460, 1996

142. Rustenbeck I, Herrmann C, Grimmsmann T: Energetic requirement of insulin secretion distal to calcium influx. *Diabetes* 46:1305-1311, 1997

143. Kennedy ED, Maechler P, Wollheim CB: Effects of depletion of mitochondrial DNA in metabolism secretion coupling in INS-1 cells. *Diabetes* 47:374-380, 1998

144. Echtay KS, Winkler E, Frischmuth K, Klingenberg M: Uncoupling proteins 2 and 3 are highly active H(+) transporters and highly nucleotide sensitive when activated by coenzyme Q (ubiquinone). *Proc.Natl.Acad.Sci.U.S.A* 98:1416-1421, 2001

145. Hong Y, Fink BD, Dillon JS, Sivitz WI: Effects of adenoviral overexpression of uncoupling protein-2 and -3 on mitochondrial respiration in insulinoma cells. *Endocrinology* 142:249-256, 2001

146. Poitout V, Olson LK, Robertson RP: Insulin-secreting cell lines: classification, characteristics and potential applications. *Diabetes Metab* 22:7-14, 1996

147. Efrat S, Linde S, Kofod H, Spector D, Delannoy M, Grant S, Hanahan D, Baekkeskov S: Beta-cell lines derived from transgenic mice expressing a hybrid insulin gene-oncogene. *Proc.Natl.Acad.Sci.U.S.A* 85:9037-9041, 1988

148. Poitout V, Stout LE, Armstrong MB, Walseth TF, Sorenson RL, Robertson RP: Morphological and functional characterization of beta TC-6 cells--an insulin-secreting cell line derived from transgenic mice. *Diabetes* 44:306-313, 1995

149. Hardy S, Kitamura M, Harris-Stansil T, Dai Y, Phipps ML: Construction of adenovirus vectors through Cre-lox recombination. *J.Virol.* 71:1842-1849, 1996

150. Colosimo A, Goncz KK, Holmes AR, Kunzelmann K, Novelli G, Malone RW, Bennett MJ, Gruenert DC: Transfer and expression of foreign genes in mammalian cells. *Biotechniques* 29:324 314-22, 2000

151. Stone D, David A, Bolognani F, Lowenstein PR, Castro MG: Viral vectors for gene delivery and gene therapy within the endocrine system. *J.Endocrinol.* 164:103-118, 2000

152. Guide to the Care and Use of Experimental Animals Olfert ED, Cross BM, and McWilliam AA Canadian Council on Animal Care, 1993

153. Lowry OH, Roseburg NJ, Farr AL, Randall RJ: Protein measurement with the Folin phenol reagent. *J.Biol.Chem.* 193:265-275, 1951

154. Makulu DR, Wright P: Immune response to insulin in guinea pigs. *Metabolism* 20:770-781, 1971

155. Salapatek AM, MacDonald PE, Gaisano HY, Wheeler MB: Mutations to the third cytoplasmic domain of the glucagon-like peptide 1 (GLP-1) receptor can functionally uncouple GLP-1-stimulated insulin secretion in HIT-T15 cells. *Mol.Endocrinol.* 13:1305-1317, 1999

156. Cryer PE: Regulation of glucose metabolism in man. *J.Intern.Med.(Suppl.)* 735:31-39, 1991

157. Ashcroft FM, Proks P, Smith PA, Ammala C, Bokvist K, Rorsman P: Stimulus-secretion coupling in pancreatic beta cells. *J.Cell Biochem.* 55 Suppl:54-65, 1994

158. Nauck MA, Heimesaat MM, Orskov C, Holst JJ, Ebert R, Creutzfeldt W: Preserved incretin activity of glucagon-like peptide 1 [7-36 amide] but not of synthetic human gastric inhibitory polypeptide in patients with type-2 diabetes mellitus. *J.Clin.Invest.* 91:301-307, 1993

159. Cawthorn EG, Chan CB: Effect of pertussis toxin on islet insulin secretion in obese (fa/fa) Zucker rats. *Mol.Cell.Endocrinol.* 75:197-204, 1991

160. Dachicourt N, Serradas P, Giroix MH, Gangnerau MN, Portha B: Decreased glucose-induced cAMP and insulin release in islets of diabetic rats: reversal by IBMX, glucagon, GIP. *Am.J.Physiol.* 271:E725-E732, 1996

161. Bjorklund A, Grill VE: Relief from glucose-induced over-stimulation sensitizes the adenylate cyclase-cAMP system of rat pancreatic islets. *J.Endocrinol.* 166:537-544, 2000

162. Kennedy HJ, Pouli AE, Ainscow EK, Jouaville LS, Rizzuto R, Rutter GA: Glucose generates sub-plasma membrane ATP microdomains in single islet beta-cells. Potential role for strategically located mitochondria. *J.Biol.Chem.* 274:13281-13291, 1999

163. Tsuchiya K, Horie M, Watanuki M, Albrecht CA, Obayashi K, Fujiwara H, Sasayama S: Functional compartmentalization of ATP is involved in angiotensin II- mediated closure of cardiac ATP-sensitive K+ channels. *Circulation* 96:3129-3135, 1997

164. Solsona C, Salto C, Ymbern A: Effects of potassium depolarization on intracellular compartmentalization of ATP in cholinergic synaptosomes isolated from Torpedo electric organ. *Biochim.Biophys.Acta* 1095:57-62, 1991

165. Chan SL, Mourtada M, Morgan NG: Characterization of a KATP channel-independent pathway involved in potentiation of insulin secretion by efaroxan. *Diabetes* 50:340-347, 2001

166. Hinke SA, Pauly RP, Ehses J, Kerridge P, Demuth HU, McIntosh CH, Pederson RA: Role of glucose in chronic desensitization of isolated rat islets and mouse insulinoma (betaTC-3) cells to glucose-dependent insulinotropic polypeptide. *J.Endocrinol.* 165:281-291, 2000

167. Defer N, Best-Belpomme M, Hanoune J: Tissue specificity and physiological relevance of various isoforms of adenylyl cyclase. *Am.J.Physiol.Renal.Physiol.* 279:F400-F416, 2000

168. Ma YH, Wang J, Rodd GG, Bolaffi JL, Grodsky GM: Differences in insulin secretion between the rat and mouse: role of cAMP. *Eur.J.Endocrinol.* 132:370-376, 1995

169. Wagoner PK, Pallotta BS: Modulation of acetylcholine receptor desensitization by forskolin is independent of cAMP. *Science* 240:1655-1657, 1988

170. Hoshi T, Garber SS, Aldrich RW: Effect of forskolin on voltage-gated K+ channels is independent of adenylate cyclase activation. *Science* 240:1652-1655, 1988

171. Krause D, Lee SC, Deutsch C: Forskolin effects on the voltage-gated K+ conductance of human T cells. *Pflugers Arch.* 412:133-140, 1988